THE
LONDON, EDINBURGH, AND DUBLIN
PHILOSOPHICAL MAGAZINE
AND
JOURNAL OF SCIENCE.

[SEVENTH SERIES.]

*DECEMBER* 1931.

## CIII. *Thermionic Emission and Electrical Conductivity of Oxide Cathodes.*

*By* A. L. REIMANN, *B.Sc., Ph.D., and* L. R. G. TRELOAR, *B.Sc.** (*Communication from the Staff of the Research Laboratories of the General Electric Co., Ltd., Wembley, England.*)

ABSTRACT.

EXPERIMENTS are described which form a continuation of the work initiated and discussed by Reimann and Murgoci. A more accurate method has been employed for measuring conduction phenomena in oxide cathodes, and new information has been obtained on

(1) The variation of the conductivity of the coating and of the thermionic emission with temperature,

(2) the relation between the conduction current and electrode potential difference at various temperatures.

(3) the relation between the thermionic current and anode potential at various temperatures.

The theoretical position is discussed in the light of this new knowledge together with the results of recent work by other observers.

It is concluded that the weight of experimental evidence is still in favour of the theory of the mechanism of these cathodes according to which the current, thermionically

* Communicated by C. C. Paterson, Director.

emitted at the surface of the core metal, is carried almost exclusively by barium * ions through the coating, at the outer surface of which it is re-emitted thermionically.

## Introduction.

IN recent papers by Becker [1, 2], Reimann and Murgoci [3] and Lowry [4], theories of the mechanism of oxide cathodes have been proposed which differ from one another in certain important respects. It is our purpose, after giving the results of some new observations on conduction and emission phenomena in these cathodes, to discuss

Fig. 1.

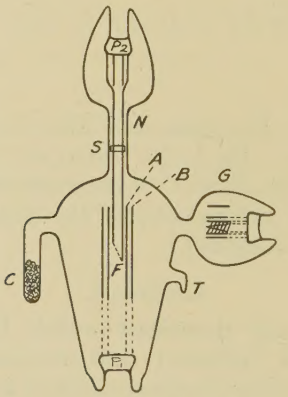


the theoretical position in the light of the whole of the evidence now available.

## Part I. Experimental.

### (1) *Description of Apparatus.*

In order to avoid the difficulties of determining the temperature of a short filament heated by a current, and to simplify the conduction and emission measurements, the filaments were heated in a suitably designed furnace. This consisted of two concentric cylinders, made from nickel sheet of 0·2 mm. thickness, 60 mm. long, and 12 and 20 mm., respectively, in diameter, (A and B, fig. 1),

* We shall, for the sake of brevity, write barium where we mean barium and/or strontium and/or calcium.

mounted on a pinch $P_1$ and sealed into a glass bulb. In the annular space between these two cylinders were arranged three loops of tungsten filament which were supported from wires in the pinch. By heating the tungsten filament, the temperature of the inner cylinder could be raised to any value up to 1100° K.

Measurements were made on two oxide coated nickel filaments, of 0·044 mm. diameter, and 15 mm. long, having 5 mm. of their central portions twisted together. The filaments were re-coated after twisting, and mounted in the centre of the furnace (F, fig. 1) by means of four 0·6 mm. nichrome wires attached to the pinch $P_2$. These wires were passed through a steatite plug S in order to increase the rigidity of the filament system, and the filaments could be removed from the furnace by cutting the glass neck N. The inner cylinder was used as the anode when thermionic emission currents were being taken. The filament coating consisted of equal proportions of barium and strontium oxides. The tube was also provided with a side tube C, containing out-gassed charcoal, which was immersed in liquid air during operation, an ionization gauge G, which was provided with magnesium getter so that any residual gas in the tube could be "cleaned up" by running the gauge, and an exhausting tube T. All measurements were made with the tube sealed off from the pump.

(2) *Temperature Calibration of Furnace.*

The temperature of the furnace was calibrated in terms of the wattage supplied to the heating filment by measuring (*a*) the E. M. F. developed in a chromel-alumel thermocouple and (*b*) the resistance of a closely spiralled tungsten filament. These were introduced through the neck of the tube (N). Care was taken to avoid errors due to the cooling of the leads, and the maximum difference between temperatures as measured by these two methods was 15° C. The experiments do not require a high degree of accuracy in the temperature determinations.

(3) *Preparation of Tube.*

After the coated filaments had been introduced, the tube was pumped and baked at 400° C. for 30 minutes, during which time, also, the charcoal was out-gassed.

The electrodes of the ionization gauge were bombarded, and the magnesium was " dispersed " on to the bulb. The furnace was now heated for 20 minutes, the inner tube being at 1100° K, in order to remove gas from the metal parts. Next, the filaments were " formed " for 30 minutes. The furnace was then heated again for a few minutes to remove gas collected on it from the coated filaments, the gauge was re-bombarded, and the filaments were re-formed for a short time. After sealing off the tube was now ready for use.

(4) *Variation of Conductivity and Thermionic Emission with Temperature.*

The current conducted between the two filaments under a P. D. of 0·1 volt was taken as a measure of the conductivity of the coating. The justification for this will be considered later. The emission was taken with 90 volts on the anode and with the filaments connected in parallel. The circuit was arranged so that at any temperature the conduction and emission currents could be read alternately by a change of switches. The emission and conduction currents therefore relate to the same filaments in as nearly as possible the same state, the probability of errors arising from gradual changes in the activity of the filaments being thus diminished.

The curves of fig. 2 are typical of the results obtained. At temperatures below about 700° K, it was not generally found possible to repeat readings with consistency, and the conduction current appeared to be subject to disturbances due to mechanical vibration of the tube. The curves may be represented by the formulæ $c = \alpha\epsilon^{-\beta/T}$ and $i = A\epsilon^{-B/T}$ for the conductivity and emission respectively. The values of $\beta/B$ obtained varied from 0·78 to 0·89. The corresponding values of thermionic work function varied between 1·02 and 1·23 volts, though there was no correlation between this and $\beta/B$. These differences must be regarded as due to real variations in the condition of the oxide coating.

(5) *Relation between Conduction Current and Voltage.*

A comprehensive study was made of the relation between the conduction current and the applied voltage at various temperatures. The curves obtained fall naturally into three groups.

Fig. 2.

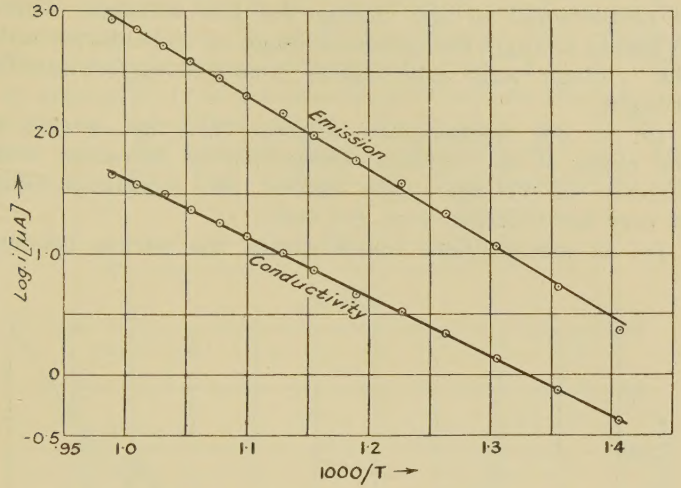


Variation of Emission and Conductivity with Temperature.

Fig. 3.

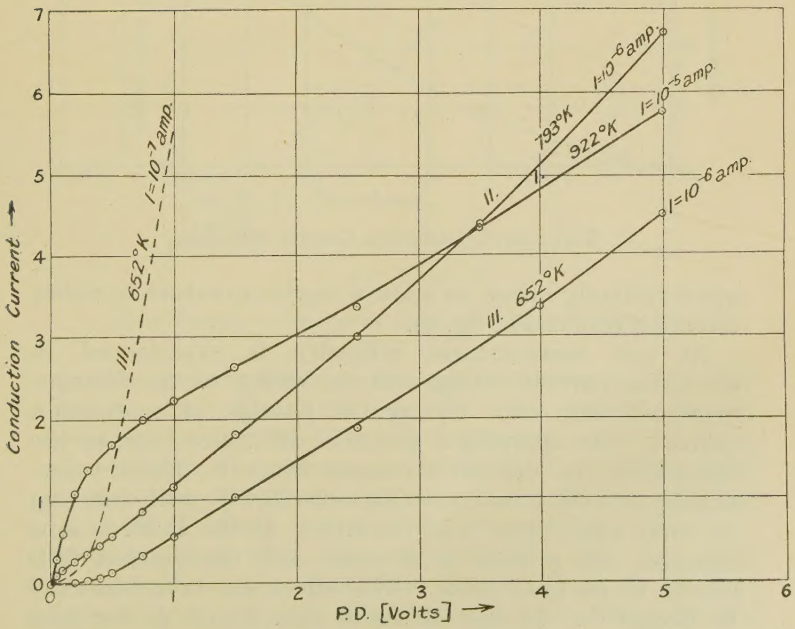


Variation of Conduction Current with P.D.

(*a*) At high temperatures (Curve I., fig. 3) the current is proportional to the voltage for low voltages, whilst at higher voltages the current-voltage curve bends towards the voltage axis and again becomes approximately straight.

(*b*) At low temperatures (Curves III., figs. 3 and 4) the slope of the current-voltage curves increases with increase of voltage. The curves are rectilinear only at very low voltages (*e. g.*, 0·1 volt).

(*c*) At intermediate temperatures the curves become

Fig. 4.

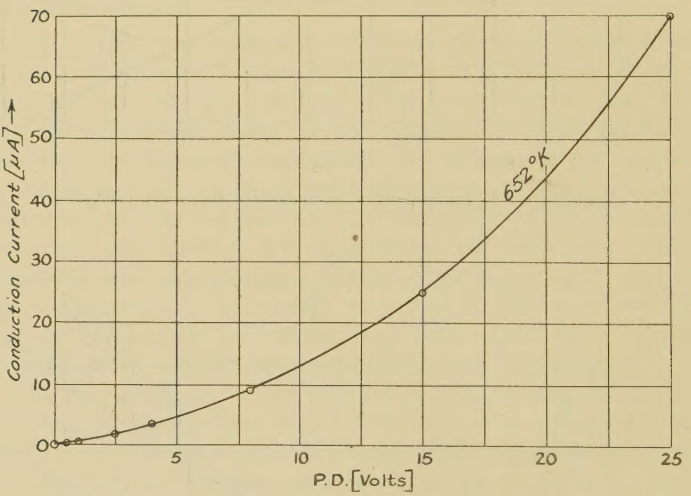


Variation of Conduction Current with P.D.

approximately linear, or show a slight curvature in either direction (Curve II., fig. 3).

At low temperatures difficulty is experienced in obtaining current-voltage curves, owing to the changes produced with time during the passage of conduction current. On applying a potential difference between the electrodes, the current increases from its initial value, rapidly at first, then more and more slowly, until reaching its final value some minutes later. If the P. D. is now reduced, the process is reversed and the current falls slowly to its final value. This effect has been observed by Becker [2]. In the curves of figs. 3 and 4, the final values are used.

By reading the current at definite intervals of time after changing the P. D., an attempt was made to find, by extrapolation, its value immediately after changing. The result of such an attempt is depicted in fig. 5. With an applied P. D. of 0·5 volt, the final current was $2{\cdot}5\times10^{-8}$ amperes, as shown at A. On raising the P. D. to 1·0 volt, the current finally obtained was $8{\cdot}8\times10^{-8}$ amperes (B). The voltage was then lowered to 0·5,

Fig. 5.

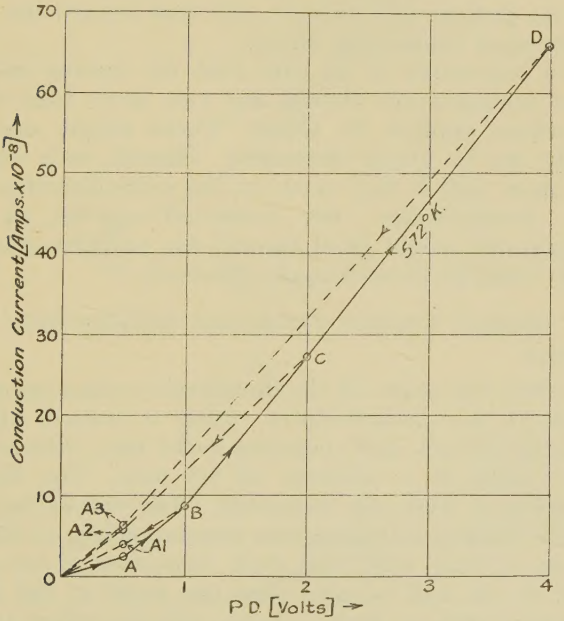


Time changes in Conduction Current-Voltage Relationship.

and the current reading obtained immediately after this change was $3{\cdot}9\times10^{-8}$ amperes ($A_1$). After passing a steady current of $27{\cdot}1\times10^{-8}$ amperes, under a P. D. of 2·0 volts, the current on lowering the voltage again to 0·5 was $5{\cdot}8\times10^{-8}$ amperes ($A_2$), and on lowering the voltage from 4·0 to 0·5, the current was $6{\cdot}1\times10^{-8}$ amperes ($A_3$). The experiments are not very accurate, but they show that the curvature of the low-temperature current-voltage curves is due at least largely to changes produced in the oxide by the passage of current

and it is probable that if the currents could be measured instantaneously, the current-voltage relationship would be found to be linear.

However such time changes as these may affect the shape of the current-voltage curves, they are not likely to affect the slope of the tangent at the origin, which (by taking readings at a voltage below that at which the curvature becomes noticeable) we have taken as a measure of conductivity. This follows at once from the fact that the observed time changes are associated with the passage of a current, and that toward the origin this becomes vanishingly small.

It is impossible to be sure that the curves taken at higher temperatures should not also have time-change corrections applied to them. These might occur so rapidly as to evade detection. Should such changes take place, and if they occur in the same direction as at lower temperatures, the corrected curves at high temperatures would bend toward the voltage axis more rapidly than do those actually observed.

(6) *Relation between Thermionic Current and Anode Potential.*

A study was made of the thermionic voltage-saturation curves at low temperatures, using a coated filament of length 36 mm. and diameter 0·044 mm. between two nickel plates at a distance of 0·5 mm. The filament temperatures were not measured. The curves for three different filament temperatures (corresponding to filament voltages of 0·30, 0·35, and 0·55, respectively) are shown in fig. 6. It will be seen that the slope of the curves increases rapidly at high voltages, and this effect appears to be greatest at low temperatures. The low-voltage portions of two of these curves are shown on a larger scale in fig. 7. (The currents in the case of the lowest-temperature curve were below the range of the galvanometer used.) These show the ordinary kind of thermionic saturation.

Comparing these curves with the conduction current curves, we notice certain qualitative resemblances :

(1) At higher temperatures there is an initial bend toward the voltage axis. As the temperature is lowered, this becomes less marked, finally—if still existent—escaping detection altogether.

Fig. 6.

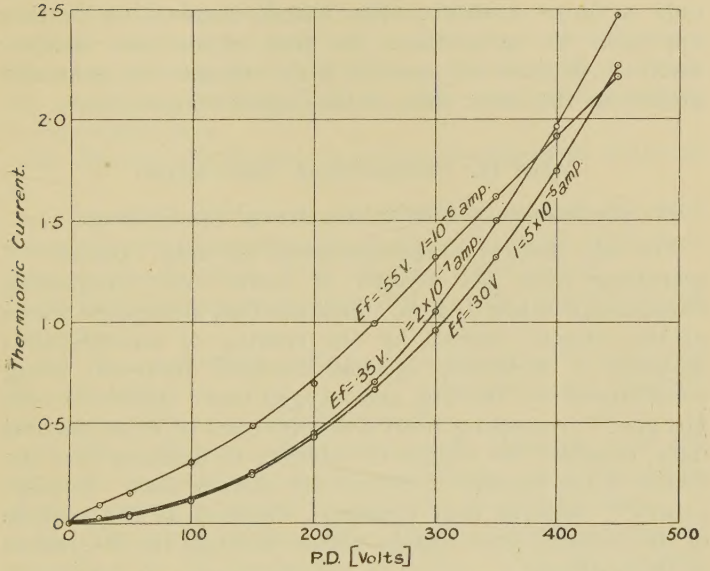


Variation of Thermionic Current with Anode Potential.

Fig. 7.

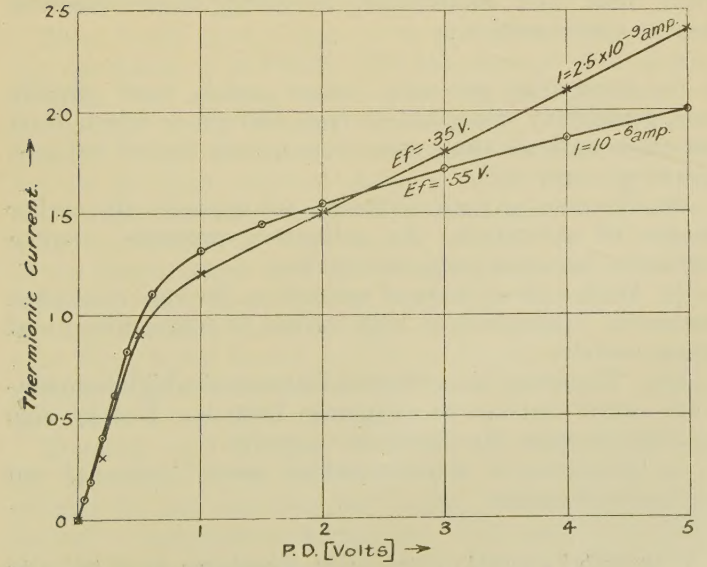


Variation of Thermionic Current with Anode Potential.

(2) This bend toward the voltage axis continues for only a finite distance, after which there is no further approach to saturation. In this region the relative rates of increase of current with voltage are generally greater at the lower than at the higher temperatures.

## Part II. Theoretical Discussion.

(1) *Mechanism of Conduction through the Coating.*

For this, three rival theories are in the field. Becker[1, 2] reasoning from the results of some very interesting experiments made by him, concludes that almost the whole of the current carried by the coating of an activated filament is electronic, a small fraction, however, being contributed by barium and oxygen ions. Reimann and Murgoci[3], reasoning from a different set of experimental data, consider the weight of evidence to indicate that the whole of the current is carried by barium ions. Finally, Lowry[4] believes that electrons, emitted at the surface of the metallic core, simply diffuse through the interstices of the coating.

In order to appraise the relative merits of these theories, let us first draw up a list of the main relevant experimental facts now well established, including those observed by the above writers :—

(*a*) Activation generally occurs much more rapidly and completely when an electron current is drawn from an oxide cathode than when it is merely heated without drawing a current *.

(*b*) Vigorous oxygen evolution accompanies the earlier stages of activation. As activation proceeds, oxygen evolution becomes progressively less.

(*c*) With a given state of activation, the rate of oxygen evolution is greatest at high values of temperature and space current.

(*d*) " Flashing " an activated filament at a high temperature causes barium to evaporate from it. It may also greatly decrease the thermionic activity.

(*e*) Exposure to electronegative gases " poisons " an activated filament.

* Although Lowry did not find this, it nevertheless seems to be the experience of the majority of writers on this subject.

(*f*)Polarization has been observed in the coatings of oxide cathodes, indicating electrolysis.

(*g*) If electrons are sent into an inactive coated filament from an external source, barium appears at the surface, but only at roughly 1/200th the rate corresponding to Faraday's law.

(*h*) Barium, distilled on to an inactive filament, activates it.

(*i*) Spectroscopic examination of the cores of activated filaments whose coatings have been dissolved off reveals the presence in them of the alkaline earth metals.

(*j*) Both barium and oxygen diffuse very readily through the coating.

(*k*) The conductivity of the coating varies with temperature according to a law $c = \alpha\epsilon^{-\beta T}$ (Reimann and Murgoci) or $c = \alpha_1\epsilon^{-\beta_1/T} + \alpha_2\epsilon^{-\beta_2/T}$ (Becker [2]).

(*l*) The "flicker" effect with oxide cathodes is of the order to be expected on the assumption that the whole of the current is carried through the coating by ions.

(*m*) The conductivity of the coating varies enormously according to its thermionic activity. The two exhibit a very marked parallelism.

(*n*) The maximum activity of an oxide cathode depends to an important extent on the nature of the core material.

From items (*a*)–(*g*) and (*i*) in the above list of data the conclusion is inevitable that the passage of a current through the coating electrolyses it, the products of electrolysis being barium and oxygen. Furthermore, from (*b*), (*d*), (*e*) and (*h*) it is evident that it is to uncombined barium in some physical state or other that the high thermionic emission obtainable from an activated cathode must be attributed. This cannot be stable in bulk form at the temperatures at which these cathodes are normally operated, and must almost certainly, therefore, exist in the form of an adsorbed film of monatomic thickness, such films being known to have a relatively low vapour pressure. Thus far, all writers on this subject appear now to be in complete agreement.

Reimann and Murgoci believed not only some, but all the current to be carried by ions. One of their main reasons for this was that the conductivity of the coating showed a temperature dependence which was of the type exhibited by all solid electrolytes whose conductivity-temperature relation had been determined. Becker[2]

has, however, pointed out that there are also electronic conductors, notably $Cu_2O$ and CuO, whose conductivity, according to the work of Vogt[5] and Horton[6] respectively, varies with temperature in the same kind of way, and whose existence opens up the possibility that the alkaline earth oxides also, in spite of their conductivity-temperature variation, conduct mainly electronically. It must, then, be conceded that the probability, based on these general considerations, of the alkaline earth oxides conducting purely electrolytically is less strong than Reimann and Murgoci believed it to be.

A further argument advanced by Reimann and Murgoci was that since the alkaline earth oxides were dielectrics and no dielectric was known to conduct otherwise than electrolytically, it was highly probable that the alkaline earth oxides, also, were electrolytic conductors. Becker, however, quotes a list of "dielectrics," of widely varying insulating properties, which are classed by Smekal[7, 8] as electronic conductors. We now consider that for the purposes of this discussion it would be in the interests of clear thinking to abandon the purely relative classification of materials into dielectrics and non-dielectrics, and with it the arguments based thereon, for in the absence of any *absolute* definition there will never be general agreement as to the class to which border-line cases should be assigned.

A logical consequence of purely electrolytic conduction, when considered in conjunction with the great length of life of oxide cathodes, would be, as Reimann and Murgoci have shown, a continuous circulation of the material electrolysed, whose rate is in beautiful quantitative agreement with the order of magnitude of the "flicker" effect observed by Johnson[9] and discussed by Schottky[10].

Becker's model also necessitates a circulation, as he himself recognises, for he states that "by far the largest part, about 0·998, of the barium which is produced by electrolysis must diffuse into the oxide and must recombine with oxygen to form barium oxide." This circulation is, however, only about 1/200th as vigorous as that of the purely electrolytic model. The observed magnitude of the "flicker" effect thus constitutes quantitative evidence favouring pure, as against only partial, electrolysis.

On the other hand, Becker's observations of the rate at which barium appears at the surface of a coated filament when electrons are sent into it appear at first sight definitely to demand that almost the whole of the current is carried by electrons, and only an insignificant fraction by ions. It would appear, however, that in drawing this conclusion Becker has overlooked the effects of diffusion. Whether the electrolytic current is carried by barium ions only, as pictured by Reimann and Murgoci, or barium and oxygen ions, as Becker supposes, the important thing that must be taken into account here is that if the liberated material diffuses, the possibility is given for recombination to occur, side by side with electrolysis. Becker has shown that oxygen diffuses through the coating with great ease. As regards barium, a circulation has had to be postulated by Becker as well as by Reimann and Murgoci. Might not this circulation easily account for the whole of Becker's observed disparity between the electrical equivalent of the free material found and the quantity of electricity passed ?

It is interesting to note that the theory of barium circulation—whether that required by complete or only partial electrolysis—suggests a quite natural explanation of the items (*b*) and (*c*) in our list of experimentally established facts. First let us take (*b*). As barium appears at the electrolytic cathode (the inside of the coating), oxygen must be left behind at the anode (the outside). If there is little or no covering of barium at the anode surface, and the temperature is high enough, some of this oxygen will evaporate before it has had time, by its own diffusion and that of the barium, to recombine with the latter. As activation (building up of a film of barium) proceeds, oxygen left behind at the anode has less and less chance of escaping in this way and thus the oxygen yield falls off.

Next let us take item (*c*). The greater the current drawn from the filament, the more vigorous will be the circulation of barium and the greater will become the disparity between the surface concentration of barium on the inside and outside of the filament coating. When the outside of the coating is sufficiently depleted of barium in this manner it becomes possible for oxygen to be liberated. Diffusion is probably much less violently temperature-dependent than emission. Consequently it is

at high temperatures and when strong currents are drawn that the oxygen yield is greatest.

There remains for consideration Lowry's[4] picture of electron diffusion through the interstices of the coating. From observations of the important influence of the material of the core in determining thermionic activity, Lowry and Reimann and Murgoci independently of one another inferred that the seat of the observed emission might well be the surface of the core, rather than that of the coating. On this view it must be supposed either that the coating electrically conducts the current collected by it from the core (with which it is in the main not in true contact), re-emitting it from its outer surface, or else that the electrons emitted by the core simply diffuse through the spaces between the crystals of the coating. Reimann and Murgoci chose the former alternative for their picture, Lowry the latter.

Lowry's proposed mechanism has the advantage of extreme simplicity, and by means of it he is able to suggest explanations for the life-failure and poor saturation of oxide cathodes, the former being brought about by the gradual closing up of the pores of the coating consequent upon crystal growth. It is our general experience, however, that both the life at any given temperature and such peculiarities of behaviour as poor saturation of the emission, as well as its magnitude, are influenced to a very considerable extent by the material of the core. It therefore seems unlikely that such things as crystal size and growth in the coating can alone be held accountable for these phenomena. Reimann and Murgoci also proposed that crystal growth in the coating might be the cause of life-failure. In view of the facts just stated, however, we no longer regard this as probable.

A difficulty of the electron-diffusion theory lies in the observed violence with which the conductivity varies with temperature. One would naturally expect a current carried by electrons diffusing through the spaces between the crystals of a coating to depend as little on the temperature as do ordinary space charge limited thermionic currents. Furthermore, no explanations have been advanced on the electron-diffusion theory for such important phenomena as (*a*), (*b*), (*c*), (*f*), (*l*), and (*m*). These are accounted for quite naturally by the electrolytic theory.

(2) *The Seat of the Emission.*

We have just stated one of the reasons which lead one to infer that it is the surface of the core (contaminated with barium or with oxygen and barium as an adsorbed film) which is the seat of the emission that is actually measured. Reimann and Murgoci believed to have corroborative evidence for this conclusion in the signs of saturation of the conduction current observed by them, these occurring at values which were of the same order as the saturated thermionic current at the same temperature. This phenomenon was interpreted as meaning that a thermionic limit had been reached to the current that could be passed through the coating. From certain calorimetric measurements of Davisson and Germer, it was reasoned that the limitation must occur at the surface of the core.

It now appears from our measurements, and also from a recent observation of Becker[2], that at a sufficiently low temperature this incipient saturation of the conduction current does not occur, the current-voltage relationship being something like linear. At first we thought this to constitute a serious objection to the idea of thermionic limitation of the conduction current. It ceases to do so, however, in view of our subsequent observations of the quite parallel behaviour of the emission current, to which as we have seen, there appears to be no limit at low temperatures. Although it is not clear what is the explanation of this*, from the *fact* it must follow that for the conduction current also no saturation is to be expected at low temperatures. From geometrical considerations it is evident that as the temperature is lowered the conduction current must cease to saturate before the emission current, as we have observed it to do. In the twisted wire arrangement used for measuring conduction currents, the coating must be imagined as being separated by finite gaps from the metallic electrodes. In these gaps, which are small in comparison with the thickness of the coating, quite considerable fields can exist before the potential drops across them contribute any important

* It seems just possible that an important part of the potential difference between the cathode core and the anode might occur in the space between the core and the coating. If so, the fields would be of about the right order for autoelectronic emission to become appreciable.

fraction of the total potential drop, by far the greater part being in the coating. But when the thermionic saturation has become sufficiently poor, and even before it has vanished altogether, such strong fields will give rise to thermionic currents across the gaps far in excess of those at which the rate of increase of thermionic current with voltage begins to fall off. And so long as we may neglect the potential drops across the gaps at the two electrodes, the current-voltage relationship will be that characteristic of the conductivity of the coating. Thus if the conductivity is ohmic, it will be a linear relationship.

The picture of thermionic limitation at the surface of the core is not inconsistent with items (*g*) and (*h*) in our list of observational data. It must be remembered that barium diffuses through the coating very rapidly, and that although the coating is not, in the main, in true contact with the core, there must be scattered points where such contact does occur (else how could the core support the coating ?). By surface flow across such points there might well be a constant interchange of adsorbed barium between the core and the coating. Such interchange, if sufficiently rapid, would make it impossible to increase the barium covering of the one without at the same time increasing that of the other.

It cannot be claimed that there is yet sufficient experimental material for the theory of exclusively electrolytic conduction, barium circulation and thermionic limitation at the surface of the core to have been established beyond a doubt. It does seem, however, that the main phenomena exhibited by these cathodes can, where at all, be accounted for more naturally by this theory than by either of the alternatives here discussed.

## *References.*

(1) J. A. Becker, Phys. Rev. xxxiv. p. 1323 (1929).
(2) J. A. Becker, Trans. Am. Electrochem. Soc. lix. p. 381 (1931).
(3) A. L. Reimann and R. Murgoci, Phil. Mag. ix. p. 440 (1930).
(4) E. F. Lowry, Phys. Rev. xxxv. 1367 (1930).
(5) W. Vogt, Ann. d. Phys. vii. p. 183 (1930).
(6) F. Horton, Phil. Mag. xi. p. 505 (1906).
(7) A. Smekal, *Zs. f. techn. Phys.* viii. p. 561 (1927).
(8) A. Smekal, *Zs. f. Electrochemie,* xxxiv. p. 472 (1928).
(9) J. B. Johnson, Phys. Rev. xxvi. p. 71 (1925).
(10) W. Schottky, Phys. Rev. xxviii. p. 74 (1926).

CIV. *The Structure of Ferromagnetic Ferric Oxide.* *By* J. Thewlis, *M.Sc., Physics Department, National Physical Laboratory, Teddington, Middlesex* †.

[Plate XXI.]

## I. Introduction.

THE polymorphism of $Fe_2O_3$ has been known for a long time, being first noted by Robbins ‡ in 1859. There are several marked differences in the properties of the two forms. One modification, hæmatite, is paramagnetic, whereas the other is ferromagnetic. The ferromagnetic oxide is in addition much more active chemically than hæmatite.

It is not surprising to find, therefore, that the two forms of $Fe_2O_3$ differ also in crystal structure. Actually, hæmatite is trigonal and ferromagnetic $Fe_2O_3$ is cubic.

Welo and Baudisch § prepared ferromagnetic $Fe_2O_3$ by oxidation of magnetite, $Fe_3O_4$, and found on examination by X-rays that the chemical change had apparently not been accompanied by any change in structure. The powder photograph of ferromagnetic $Fe_2O_3$ appeared to be identical with that of $Fe_3O_4$ ||. They pointed out that the unit cube of $Fe_3O_4$ contained eight molecules and could therefore be written $Fe_{24}O_{32}$, and that the corresponding composition for $Fe_2O_3$ was $Fe_{21}O_{36}$. Consequently, room for four additional oxygen atoms had to be found in the unit cube of $Fe_3O_4$. They suggested two ways of inserting these atoms, assuming the "radius" of the iron atom to be about 1·2 Å. and that of the oxygen atom to be about 0·65 Å. in accordance with the figures proposed by W. L. Bragg in 1920 ¶. All subsequent work ††, however, has shown that these figures require amendment, and that in fact the anion is large and the cation small. It will be shown later that in the light of this knowledge the positions suggested by Welo and Baudisch are improbable.

† Communicated by Dr. G. W. C. Kaye, O.B.E.

‡ Chem. News, i. p. 11 (1859).

§ Phil. Mag. l. p. 399 (1925).

|| This was repeated by Lilian H. Twenhofel, Econ. Geol. xxii. p. 180 (1927).

¶ Phil. Mag. xl. p. 169 (1920).

†† J. Wasastjerna, Soc. Scient. Fenn. Comm. i. p. 38 (1923). W. L. Bragg, Phil. Mag. ii. p. 258 (1926). L. Pauling, Journ. Am. Chem. Soc. xlix. p. 765 (1927). V. M. Goldschmidt, Geochem. Verteil. der Elemente, pt. vii., Oslo, 1926; Trans. Faraday Soc. xxv. p. 252 (1929).

## II. Experimental.

Ferromagnetic $Fe_2O_3$ was prepared (in connection with other work) by heating a ferromonohydrate $Fe_2O_3 . H_2O$ at 400° C. for two hours. The composition of the oxide was checked by chemical analysis.

X-ray powder photographs were taken of this oxide † and of magnetite, using an iron target and a circular camera of 5 cm. radius. The photographs were then photometered on a Moll self-recording photometer. The photographs are

Fig. 2 (*a*).

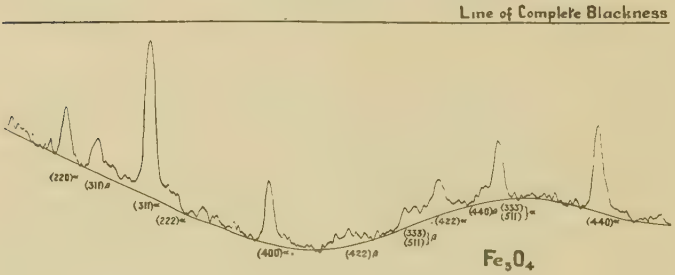


Fig. 2 (*b*).

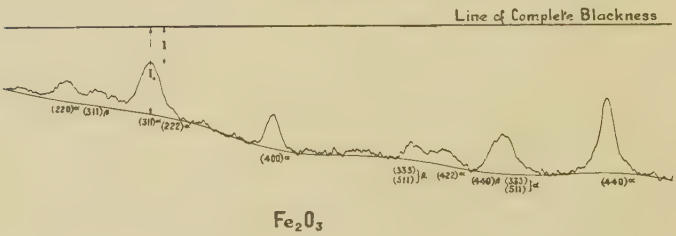


reproduced in Pl. XXI. (figs. 1 (*a*) & 1 (*b*)) and the photometer records in figs. 2 (*a*) & 2 (*b*).

Table I. gives the intensities of the lines, the (311) reflexion having been put at 100 in each case. In the calculation of the intensities from the photometer records the following expression was used :—

$$\text{Intensity} \propto \log \frac{I_0}{I}.$$

† This is referred to below as $\gamma - Fe_2O_3$ by analogy with $\gamma - Al_2O_3$.

$I_0$ and I are explained in fig. 2 (*b*), the (311) line of $Fe_2O_3$ being chosen as an example †.

The lines occur at the same places on the two films and the intensities are also very similar. There is, however, a definite increase in the intensities of the (400) and (440) reflexions as we go from $Fe_3O_4$ to $\gamma-Fe_2O_3$.

## III. Possible Atomic Positions.

Comparison of the powder photographs of $Fe_3O_4$ and $\gamma-Fe_2O_3$ shows that the two structures must be remarkably similar. The unit of $\gamma-Fe_2O_3$ is the same size as that of $Fe_3O_4$ and it follows that the iron atoms, which are more

Table I.

| Line (*hkl*). | Intensity in $Fe_3O_4$. | Intensity in $\gamma-Fe_2O_3$. |
|---|---|---|
| 111 | Not observed. | Not observed. |
| 220 | 30 | 32 |
| 311 | 100 | 100 |
| 222 | 6 | 7 |
| 400 | 26 | 35 |
| 331 | Not observed. | Not observed. |
| 422 | 15 | 13 |
| 333 } 511 } | 30 | 31 |
| 440 | 45 | 79 |

efficient scatterers of X-rays than the oxygen atoms, must be in practically identical positions in the two substances. Welo and Baudisch suggested that thirty-two oxygen atoms in the unit cube of $\gamma-Fe_2O_3$ occupy the same positions as in $Fe_3O_4$, and that four additional oxygen atoms are inserted. Whilst this appears extremely probable, it seems just possible, in view of the low reflecting power of oxygen compared with that of iron, that not all the thirty-two oxygen positions in $Fe_3O_4$ are repeated in $\gamma-Fe_2O_3$, but that certain atoms are rearranged, thirty-six oxygen atoms finally being included in the unit cube. This possibility has been borne in mind in

† Strictly speaking, account ought to be taken of the area under the curve corresponding to the line whose intensity is being measured. If the lines are of the same breadth, however, the value of log $I_0/I$ at a peak may be taken as proportional to the intensity of the corresponding line.

the following discussion regarding possible oxygen positions in $\gamma - Fe_2O_3$.

The space group of $Fe_3O_4$ is $O_h^7$, but since this space group cannot in any way accommodate thirty-six oxygen atoms † it cannot be the space group of $\gamma - Fe_2O_3$. If the only difference between the structures were that due to the addition of four oxygen atoms, any lines of $\gamma - Fe_2O_3$ not satisfying the space group conditions of $O_h^7$ would be due to the extra oxygens alone and would be so weak on the powder photograph as to escape detection. The fact that the observed lines of $\gamma - Fe_2O_3$ satisfy the same conditions as those of $Fe_3O_4$ thus furnishes no clue to the space group of $\gamma - Fe_2O_3$.

A step towards the determination of the space group can be made however if it is remembered that only those space groups are possible which can accommodate thirty-six oxygen atoms in the unit cell and at the same time allow twenty-four iron atoms to occupy the same positions as in $Fe_3O_4$. Six such space groups are found, namely, $O^6$, $T_d^2$, $T_d^1$, $T^4$, $T^2$, and $T^1$.

The next step is to determine all spatially possible atomic arrangements which satisfy the requirements of these six space groups and conform to the conditions set out above. Minimum permissible iron-oxygen and oxygen-oxygen distances must first be decided upon.

The smallest iron-oxygen distance in $Fe_3O_4$ is the $Fe^{++}-O$ distance, the value being 1·88 Å. (assuming the atomic positions given by Claassen ‡). In $\gamma - Fe_2O_3$ all the iron atoms are trivalent, so that a somewhat smaller distance than 1·88 Å. might be possible for the least iron-oxygen distance.

According to Goldschmidt § the "radius" of $Fe^{++}$ is 0·78 Å. and that of $Fe^{+++}$ is 0·63 Å. for co-ordination number 4, hence the smallest iron-oxygen distance in $\gamma - Fe_2O_3$ could be 0·15 Å. less than in $Fe_3O_4$, *i. e.*, it might be as low as about 1·7 Å.

The least oxygen-oxygen distance to be expected is not so obvious. If it is assumed that in $Fe_3O_4$ the $Fe^{++}$ atom has a "radius" of 0·78 Å. the oxygen atom would have a "radius" of 1·1 Å. so that the oxygen-oxygen distance might possibly

† See Wyckoff, 'The Analytical Expression of the Results of the Theory of Space Groups,' Washington, 1922.

‡ Proc. Phys. Soc. xxxviii. p. 482 (1926).

§ *Loc. cit.* The "radius" of $Fe^{++}$ is 0·83 Å. and that of $Fe^{+++}$ is 0·67 Å. for co-ordination number 6. These must be reduced by 6 per cent. for co-ordination number 4, *i. e.*, that of $Fe^{++}$ in $Fe_3O_4$.

be as low as 2·2 Å., in any case it is not likely to be much lower.

With the above considerations in mind all the arrangements were examined which allowed twenty-four iron atoms and thirty-six oxygen atoms in the unit cube (the iron atoms occupying the same positions as in $Fe_3O_4$). Those arrangements which were found to be spatially possible are set out below. The notations used are those given by Mark † and Wyckoff ‡ and for convenience the $Fe_3O_4$ arrangement has been given in full. The oxygen positions marked by an asterisk are those which also occur in $Fe_3O_4$.

$Fe_3O_4$ *arrangement.*

*Space group* $O_h^7$.

*Iron atoms*:

Divalent.

8 atoms at $\left\{ \begin{matrix} 8\mathrm{T} \\ 8f \end{matrix} \right.$ . $\begin{matrix} (118)az(\mathrm{M}) \\ (\mathrm{W}) \end{matrix} \left. \right\}$, *i. e.*, at

| | | | | | |
|---|---|---|---|---|---|
| 0·000 | 0·500 | 0·500 | 0·500 | 0·000 | 0·500 |
| 0·500 | 0·500 | 0·000 | 0·000 | 0·000 | 0·000 |
| 0·250 | 0·750 | 0·750 | 0·750 | 0·250 | 0·750 |
| 0·750 | 0·750 | 0·250 | 0·250 | 0·250 | 0·250 |

Trivalent.

16 atoms at $\left\{ \begin{matrix} 16\mathrm{D}_{3d}(137)fz(\mathrm{M}) \\ 16c \qquad\qquad\quad (\mathrm{W}) \end{matrix} \right.$, *i. e.*, at

| | | | | | |
|---|---|---|---|---|---|
| 0·125 | 0·375 | 0·875 | 0·875 | 0·125 | 0·375 |
| 0·375 | 0·875 | 0·125 | 0·375 | 0·625 | 0·375 |
| 0·125 | 0·625 | 0·125 | 0·125 | 0·125 | 0·625 |
| 0·625 | 0·125 | 0·125 | 0·625 | 0·625 | 0·625 |
| 0·875 | 0·375 | 0·125 | 0·125 | 0·875 | 0·375 |
| 0·375 | 0·125 | 0·875 | 0·625 | 0·375 | 0·375 |
| 0·875 | 0·625 | 0·875 | 0·875 | 0·875 | 0·625 |
| 0·625 | 0·875 | 0·875 | 0·375 | 0·375 | 0·625 |

† 'Die Verwendung der Röntgenstrahlen in Chemie und Technik,' Table 52, Leipzig, 1926.

‡ *Loc. cit.*

*Oxygen atoms*:

32 atoms at $\left\{\begin{matrix}32C_{3v}(M)\\32b\ \ (W)\end{matrix}\right\}$ with $u=0{\cdot}379$, *i.e.*, at

| | | | | | |
|---|---|---|---|---|---|
| 0·379 | 0·379 | 0·379 | 0·879 | 0·879 | 0·379 |
| 0·879 | 0·379 | 0·879 | 0·379 | 0·879 | 0·879 |
| 0·379 | 0·621 | 0·621 | 0·879 | 0·121 | 0·621 |
| 0·879 | 0·621 | 0·121 | 0·379 | 0·121 | 0·121 |
| 0·621 | 0·379 | 0·621 | 0·121 | 0·879 | 0·621 |
| 0·121 | 0·379 | 0·121 | 0·621 | 0·879 | 0·121 |
| 0·621 | 0·621 | 0·379 | 0·121 | 0·121 | 0·379 |
| 0·121 | 0·621 | 0·879 | 0·621 | 0·121 | 0·879 |
| 0·871 | 0·871 | 0·871 | 0·371 | 0·371 | 0·871 |
| 0·371 | 0·871 | 0·371 | 0·871 | 0·371 | 0·371 |
| 0·871 | 0·629 | 0·629 | 0·371 | 0·129 | 0·629 |
| 0·371 | 0·629 | 0·129 | 0·871 | 0·129 | 0·129 |
| 0·629 | 0·871 | 0·629 | 0·129 | 0·371 | 0·629 |
| 0·129 | 0·871 | 0·129 | 0·629 | 0·371 | 0·129 |
| 0·629 | 0·629 | 0·871 | 0·129 | 0·129 | 0·871 |
| 0·129 | 0·629 | 0·371 | 0·629 | 0·129 | 0·371 |

(M) Denotes Mark's notation.
(W) Denotes Wyckoff's notation.

## $\gamma-Fe_2O_3$ *arrangements.*

*Arrangement* (1). *Space group* $O^6$.

*Iron atoms*:

4 atoms at $\left\{\begin{matrix}4D_3(136)(M)\\4h\ \ \ \ \ \ \ (W)\end{matrix}\right\}$.

8 atoms at $\left\{\begin{matrix}8C_3(M)\\8j\ (W)\end{matrix}\right\}$ with $u=0{\cdot}0$.

12 atoms at $\left\{\begin{matrix}12C_2(M)\\12q\ (W)\end{matrix}\right\}$ with $u=0{\cdot}875$.

*Oxygen atoms*:

24 atoms* at $\left\{\begin{matrix}24C_1(M)\\\text{See note † below}\end{matrix}\right\}$ with $x=0{\cdot}371$, $y=0{\cdot}129$, and $z=0{\cdot}629$.

† This arrangement is peculiar to this space group and Wyckoff does not include it in his special notation.

8 atoms* at $\left\{\begin{matrix}8C_3(M)\\8j\ (W)\end{matrix}\right\}$ with $u=0\,871$.

4 atoms at $\left\{\begin{matrix}4D_3(133)(M)\\4g\qquad(W)\end{matrix}\right\}$.

*Arrangement* (2). *Space group* $O^6$.

*Iron atoms*:

As in arrangement (1).

*Oxygen atoms*:

24 atoms* as in arrangement (1).

12 atoms at $\left\{\begin{matrix}12C_2(M)\\12q\ (W)\end{matrix}\right\}$ with $u$ about 0·625.

*Arrangement* (3). *Space group* $T_d^2$.

*Iron atoms*:

4 atoms at $\left\{\begin{matrix}4T_d(33)bz(M)\\4b\qquad(W)\end{matrix}\right\}$.

4 atoms at $\left\{\begin{matrix}4T_d(77)bz(M)\\4d\qquad(W)\end{matrix}\right\}$.

16 atoms at $\left\{\begin{matrix}16C_{3v}(M)\\16a\ (W)\end{matrix}\right\}$ with $u=0{\cdot}625$.

*Oxygen atoms*:

16 atoms at $\left\{\begin{matrix}16C_{3v}(M)\\16a\ (W)\end{matrix}\right\}$ with $u=0{\cdot}125$ †.

16 atoms* at $\left\{\begin{matrix}16C_{3v}(M)\\16a\ (W)\end{matrix}\right\}$ with $u=0{\cdot}871$.

4 atoms at $\left\{\begin{matrix}4T_d(40)bz(M)\\4c\qquad(W)\end{matrix}\right\}$.

*Arrangement* (4). *Space group* $T_d^2$.

*Iron atoms*:

As in arrangement (3).

† The value of this parameter must be very nearly 0·125 and this actual value has been chosen because it places an oxygen atom midway between two iron atoms.

*Oxygen atoms*:

16 atoms at $\left\{\begin{matrix}16C_{3v}(M)\\16a\ \ (W)\end{matrix}\right\}$ with $u=0{\cdot}125$ †.

16 atoms* at $\left\{\begin{matrix}16C_{3v}\ (M)\\16a\ \ (W)\end{matrix}\right\}$ with $u=0{\cdot}379$.

4 atoms at $\left\{\begin{matrix}4T_d(90)bz(M)\\4e\qquad\ (W)\end{matrix}\right\}$.

*Arrangement* (5). *Space group* $T_d^1$.

*Iron Atoms*:

1 atom at $\left\{\begin{matrix}1T(1)(M)\\1a\ \ (W)\end{matrix}\right\}$.

3 atoms at $\left\{\begin{matrix}3V_d(103)(M)\\3a\qquad\ (W)\end{matrix}\right\}$.

4 atoms at $\left\{\begin{matrix}4C_{3v}(M)\\4a\ \ (W)\end{matrix}\right\}$ with $u=0{\cdot}250$.

4 atoms at $\left\{\begin{matrix}4C_{3v}(M)\\4a\ \ (W)\end{matrix}\right\}$ with $u=0{\cdot}625$.

12 atoms at $\left\{\begin{matrix}12C_2(M)\\12g\ (W)\end{matrix}\right\}$ with $u=0{\cdot}250$, $v=0{\cdot}625$.

*Oxygen atoms*:

4 atoms* at $\left\{\begin{matrix}4C_{3v}(M)\\4a\ \ (W)\end{matrix}\right\}$ with $u=0{\cdot}379$.

4 atoms* at $\left\{\begin{matrix}4C_{3v}(M)\\4a\ \ (W)\end{matrix}\right\}$ with $u=0{\cdot}871$.

4 atoms at $\left\{\begin{matrix}4C_{3v}(M)\\4a\ \ (W)\end{matrix}\right\}$ with $u=0{\cdot}125$ †.

12 atoms* at $\left\{\begin{matrix}12_2C(M)\\12g(W)\end{matrix}\right\}$ with $u=0{\cdot}121$, $v=0{\cdot}379$.

12 atoms* at $\left\{\begin{matrix}12C_2(M)\\12g(W)\end{matrix}\right\}$ with $u=0{\cdot}629$, $v=0{\cdot}871$.

† See note ‡, p. 1095.

*Arrangement* (6). *Space group* $T^4$.

*Iron atoms*:

4 atoms at $\left\{\begin{matrix}4C_3(M)\\4f(W)\end{matrix}\right\}$ with $u=0$.

4 atoms at $\left\{\begin{matrix}4C_3(M)\\4f(W)\end{matrix}\right\}$ with $u=0{\cdot}250$.

4 atoms at $\left\{\begin{matrix}4C_3(M)\\4f(W)\end{matrix}\right\}$ with $u=0{\cdot}625$.

12 atoms at $12C_1$ (M)† with $x=0{\cdot}625$, $y=0{\cdot}125$, and $z=0{\cdot}125$.

*Oxygen atoms*:

12 atoms* at $12C_1$(M)† with $x=0{\cdot}371$, $y=0{\cdot}129$, $z=0{\cdot}629$.

12 atoms at $12C_1$(M)† with $x=0{\cdot}121$, $y\equiv0{\cdot}879$, $z=0{\cdot}621$.

4 atoms at $\left\{\begin{matrix}4C_3(M)\\4f(W)\end{matrix}\right\}$ with $u=0{\cdot}379$.

4 atoms* at $\left\{\begin{matrix}4C_3(M)\\4f(W)\end{matrix}\right\}$ with $u=0{\cdot}871$.

4 atoms at $\left\{\begin{matrix}4C_3(M)\\4f(W)\end{matrix}\right\}$ with $u=0{\cdot}125$‡.

The arrangements arising from the space group $T^2$ are the same as those from $T_d^2$, *i. e.* arrangements (3) and (4). $T^1$ gives the same atomic positions as $T_d^1$ (arrangement (5)).

The arrangements suggested by Welo and Baudisch are not included in the above list since they give an oxygen-oxygen distance of about 1·8 Å. and are therefore improbable. They belong to space group $T_d^2$ and are set out below.

*Arrangement of Welo and Baudisch.*

*Iron atoms*:

As in $T_d^2$ arrangements (3) and (4).

*Oxygen atoms*:

16 atoms* at $\left\{\begin{matrix}6C_{3v}(M)\\16a\ (W)\end{matrix}\right\}$ with $u=0{\cdot}379$

† See note †, p. 1094.
‡ See note ‡, p. 1095.

16 atoms* at $\left\{ \begin{matrix} 16C_{3v}(\mathrm{M}) \\ 16a \quad (\mathrm{W}) \end{matrix} \right\}$ with $u=0{\cdot}871$.

4 atoms at either $(a)$ $\left\{ \begin{matrix} 4T_d(40)bz(\mathrm{M}) \\ 4c \qquad\quad (\mathrm{W}) \end{matrix} \right\}$.

or $(b)$ $\left\{ \begin{matrix} 4T_d(90)bz(\mathrm{M}) \\ 4e \qquad\quad (\mathrm{W}) \end{matrix} \right\}$.

In Table II. the calculated intensities for the above arrangements are compared with the observed intensities. The observed and calculated intensities for $Fe_3O_4$ are also included in the table. Claassen's† atomic positions for $Fe_3O_4$ have been assumed and his values for the "F" curves of iron and oxygen have been used. The following expression has been employed in calculating the intensities :—

$$\mathrm{I}(hkl) \propto \frac{\mathrm{N}\,\mathrm{S}^2}{\sin^2\theta},$$

where $\mathrm{I}(hkl)$ is the required intensity, N the number of co-operating planes, S the structure-amplitude, and $\theta$ the glancing angle of reflexion for the plane $(hkl)$.

Reflexions omitted from the above table are those which are absent in $Fe_3O_4$ owing to space group conditions. Their calculated intensities are found to be very small for all the arrangements considered above.

It will be noticed that arrangements (2), (3), and (4) give intensities which are inconsistent with the observed facts. The most outstanding inconsistency is given by the (222) reflexion. In each case the calculated value is much too high. Attempts to obtain agreement by altering the parameters of the atoms in these arrangements met with no appreciable success.

In the arrangements suggested by Welo and Baudisch there is also a definite lack of parallelism between the observed and calculated $Fe_3O_4$–$Fe_2O_3$ intensity changes. The three planes for which this shows up are the (111), (220), and (400) planes. The calculated intensity for the (111) reflexion can be lowered by adjustment of oxygen parameters but the other discrepancies cannot be removed.

On the other hand the intensities calculated for arrangements (1), (5), and (6) do show a parallelism. Thus the final choice has to be made between these arrangements.

The atomic positions set out above are the same for

† *Loc. cit.*

## Table II.

| Line (*hkl*). | Intensity in $Fe_3O_4$. | | Intensity in $\gamma$–$Fe_2O_3$. | | | | | | | | |
|---|---|---|---|---|---|---|---|---|---|---|---|
| | Obs. | Calc. | Obs. | Calculated. | | | | | | | |
| | | | | Arr. (1). | Arr. (2). | Arr. (3). | Arr. (4). | Arr. (5). | Arr. (6). | W. & B. (*a*) | W. & B. (*b*) |
| 111 | Abs. | 5 | Abs. | 3 | 4 | 8 | 8 | 3 | 3 | 19 | 19 |
| 220 | 30 | 30 | 32 | 31 | 37 | 57 | 57 | 31 | 31 | 43 | 43 |
| 311 | 100 | 100 | 100 | 100 | 100 | 100 | 100 | 100 | 100 | 100 | 100 |
| 222 | 6 | 7 | 7 | 11 | 32 | 65 | 65 | 11 | 11 | 9 | 9 |
| 400 | 26 | 20 | 35 | 25 | 31 | 38 | 38 | 25 | 25 | 20 | 20 |
| 331 | Abs. | 1 | Abs. | 1 | 0 | 1 | 1 | 1 | 1 | 2 | 2 |
| 422 | 15 | 11 | 13 | 12 | 14 | 25 | 25 | 12 | 12 | 15 | 15 |
| 333<br>511 | 30 | 35 | 31 | 36 | 38 | 40 | 40 | 36 | 36 | 37 | 37 |
| 440 | 45 | 53 | 79 | 62 | 74 | 87 | 87 | 62 | 62 | 64 | 64 |

arrangements (1) and (6), so the choice lies between arrangements (1) and (5).

## IV. Choice of Oxygen Arrangement.

Since arrangements (1) and (5) give the same calculated intensities for the planes considered it is obviously impossible to differentiate between them on the basis of X-ray measurements. A study of the features of co-ordination of the two structures, however, makes it possible to say which is the more probable. Pauling †, partly from the empirical study of known crystal structures and partly from energy considerations, has summarized the rules which hold for ionic compounds. In the present case two of these rules can be applied with useful results. These are Pauling's rules II. and V. and are given below:—

> Rule II.—In a stable co-ordination structure the electric charge of each anion tends to compensate the strength of the electrostatic valence bonds reaching to it from the cations at the centres of the polyhedra of which it forms a corner.
>
> Rule V.—(The rule of parsimony). The number of essentially different kinds of constituents in a crystal tends to be small. (Pauling remarks that crystallographic non-equivalence does not imply essential difference from the standpoint of the co-ordination theory.)

These rules are very much bound up in each other and cannot conveniently be discussed separately. As W. L. Bragg ‡ points out it is not quite clear whether rule V. has any further significance than that of being a consequence of the balancing of electrostatic valency.

In order to appreciate the application of these rules to the $\gamma-Fe_2O_3$ arrangements under consideration it will be convenient to consider first the $Fe_3O_4$ structure. In $Fe_3O_4$ there are two kinds of iron atom, viz., $Fe^{++}$ and $Fe^{+++}$, and one kind of oxygen atom. Each $Fe^{++}$ atom is in the middle of a tetrahedron of oxygen atoms and each $Fe^{+++}$ atom is in the middle of an octahedron of oxygen atoms. Each oxygen atom is at the corner of three octahedra and one tetrahedron of oxygen atoms. Since $Fe^{++}$ is divalent and lies between

† Sommerfeld—Festschrift, Leipzig, 1928; Journ. Am. Chem. Soc. li. p. 1010 (1929).

‡ "The Structure of Silicates," *Zeits. f. Krist.* lxxiv. p. 237 (1930).

four oxygen atoms a bond between $Fe^{++}$ and oxygen has the value 2/4. Similarly, a bond between $Fe^{+++}$ and oxygen has the value 3/6. The strength of the bonds reaching an oxygen atom is then : $2/4+3/6+3/6+3/6=2$, thus compensating the charge of the oxygen atom as required by rule II.

In arrangement (1) of $\gamma-Fe_2O_3$ under consideration there are two kinds of iron atom and two kinds of oxygen atom.

TABLE III.

| Structure. | Number of kinds of iron atom. | Description. | Number of kinds of oxygen atom. | Description. | Strength of bonds reaching oxygen atoms. |
|---|---|---|---|---|---|
| $Fe_3O_4$ | 2 | (*a*) 16 in group, each atom between 6 oxygens.<br>(*b*) 8 in group, each atom between 4 oxygens. | 1 | 32 in group, each atom at corner of 1 4-fold and 3 6-fold groups. | 3/6+3/6 +3/6+2/4 =2·0. |
| $\gamma-Fe_2O_3$ Arrangement (1). | 2 | (*a*) 16 in group, each atom between 6 oxygens.<br>(*b*) 8 in group, each atom between 5 oxygens. | 2 | (*a*) 32 in group, each atom at corner of 1 5-fold and 3 6-fold groups.<br>(*b*) 4 in group, each atom at corner of 2 5-fold-groups. | 3/6+3/6 +3/6+3/5 =2·1.<br>3/5+3/5 =1·2. |
| $\gamma-Fe_2O_3$ Arrangement (5). | 4 | (*a*) 3 in group, each atom between 4 oxygens.<br>(*b*) 4 in group, each atom between 5 oxygens.<br>(*c*) 12 in group, each atom between 6 oxygens.<br>(*d*) 1 in group, this atom is between 8 oxygens. | 4 | (*a*) 16 in group, each atom at corner of 1 5-fold and 3 6-fold groups.<br>(*b*) 12 in group, each atom at corner of 1 4-fold and 3 6-fold groups.<br>(*c*) 4 in group, each atom at corner of 1 8-fold and 3 6-fold groups.<br>(*d*) 4 in group, each atom at corner of 1 5-fold and 1 8-fold group. | 3/6+3/6 +3/6+3/5 =2·1.<br>3/6+3/6 +3/6+3/4 =2·25.<br>3/6+3/6 +3/6+3/8 =1·875.<br>3/5+3/8 =0·975. |

In arrangement (5) there are four kinds of iron atom and four kinds of oxygen atom. Details are given in Table III.

A study of this table shows that arrangement (1) satisfies both Pauling's rules better than arrangement (5), in particular it will be noticed that the number of different constituents in the latter arrangement is twice as great as in the former. Accordingly arrangement (1) has been assumed to give the correct structure for $\gamma-Fe_2O_3$. The co-ordinates given for the oxygen atoms are, of course, not exact. The

values were chosen so as to make thirty-two oxygen atoms in $\gamma-Fe_2O_3$ occupy the same positions as in $Fe_3O_4$, and any small deviation from them has very little effect on the calculated intensities of reflexion. Consequently, although these atoms must have very nearly the same positions in $\gamma-Fe_2O_3$ as in $Fe_3O_4$, they have been assumed to have exactly the same positions only for want of evidence to the contrary.

The structure of $\gamma-Fe_2O_3$ is thus the same as that of $Fe_3O_4$ with oxygen atoms added to the unit cell in the following positions †:—

| | | | | | |
|---|---|---|---|---|---|
| 0·125 | 0·125 | 0·125 | 0·625 | 0·375 | 0·875 |
| 0·875 | 0·625 | 0·375 | 0·375 | 0·875 | 0·625 |

Fig. 3.

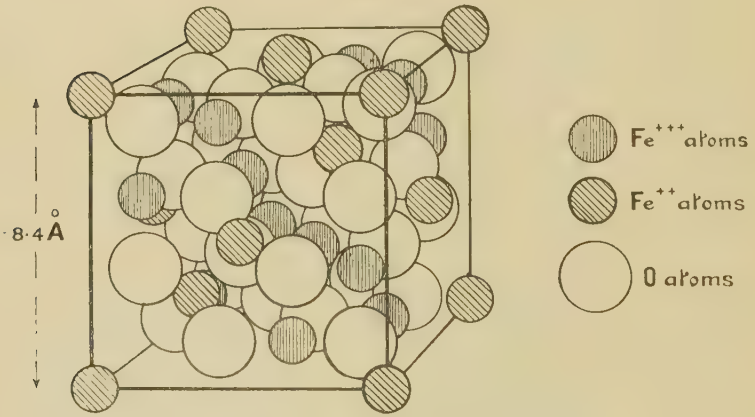


The unit cube of $Fe_3O_4$.

Diagrams of the structures of $Fe_3O_4$ and $\gamma-Fe_2O_3$ are given in figs. 3 and 4.

† In arrangement (1) the four extra oxygens are at $\left\{\begin{matrix}4D_3(133)(M)\\4g\quad\quad(W)\end{matrix}\right\}$. This gives the positions

| | | | | | |
|---|---|---|---|---|---|
| 0·125 | 0·125 | 0·125 | 0·625 | 0·375 | 0·875 |
| 0·875 | 0·625 | 0·375 | 0·375 | 0·875 | 0·625 |

for these atoms.

In arrangement (6) the four extra oxygens are at $\left\{\begin{matrix}4C_3(M)\\4f(W)\end{matrix}\right\}$ with $u=0{\cdot}125$. The positions are:

$$uuu\,;\ u+\tfrac{1}{2},\ \tfrac{1}{2}-u,\ \bar{u}\,;\ \bar{u},\ u+\tfrac{1}{2},\ \tfrac{1}{2}-u\,;\ \tfrac{1}{2}-u,\ \bar{u},\ u+\tfrac{1}{2}.$$

The space group of the above $\gamma-Fe_2O_3$ structure is $O^6$ or $T^4$. Since, however, $O^6$ is enantiomorphous with $O^7$, another structure is possible, belonging to the latter space group †. The two structures are related to one another in the same way as an object and its mirror image, and are indistinguishable by X-ray methods.

## V. Discussion of the Structure.

### (a) *Co-ordination.*

A striking feature of the structure is that certain iron atoms (those occupying the $Fe^{++}$ positions of $Fe_3O_4$) are placed between five oxygen atoms. An arrangement of this kind is most unusual and has to the author's knowledge only

Fig. 4.

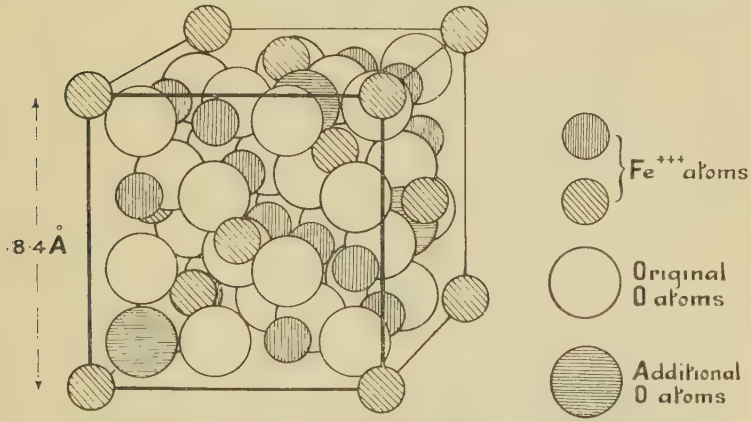


The unit cube of $\gamma-Fe_2O_3$.

once previously been noted, namely, in the case of andalusite ‡ where an aluminium atom was found to occur between five oxygen atoms. The structure may, with regard to its co-ordination properties, be regarded as intermediate between $Fe_3O_4$ and $\alpha-Fe_2O_3$. The five-fold oxygen groups of $\gamma-Fe_2O_3$ can be considered as intermediate between the four-fold groups of $Fe_3O_4$ and the six-fold groups of $\alpha-Fe_2O_3$ §.

† The same remark applies to the $Fe_3O_4$ structure which also possesses the symmetry of space group $O^6$, but in this case the $O^7$ structure is identical with the $O^6$ structure.

‡ W. H. Taylor, *Zeits. f. Krist.* lxxi. p. 205 (1929).

§ In $\alpha-Fe_2O_3$ each iron atom lies between six oxygens.

(b) *Interatomic Distances.*

On the assumption that thirty-two oxygen atoms in $\gamma-Fe_2O_3$ occupy exactly the same positions as in $Fe_3O_4$ the smallest oxygen-oxygen distance works out to be 2·14 Å. (*i. e.*, a "radius" of 1·07 Å.). If the oxygen positions are altered so as to increase this distance the calculated intensities of reflexion begin to agree less satisfactorily with the observed by the time the distance has increased to 2·4 Å. It would therefore appear that the smallest oxygen "radius" is about 1·1 Å. This is somewhat smaller than Goldschmidt's figure of 1·32 Å. †. A list of interatomic distances is given in Table IV. (assuming $Fe_3O_4$ positions for thirty-two oxygen atoms).

The distance to be expected from Goldschmidt's figures are 2·64 Å. for the oxygen-oxygen distance and 1·99 Å. for the iron-oxygen distance.

TABLE IV.

| Interatomic Distances in Å. | |
|---|---|
| Oxygen-Oxygen. | Iron o Oxygen. |
| 2·14<br>3 06 | 1·82<br>1·88 } for co-ordination number 5. |
| — | 2·07 for co-ordination number 6. |

(c) *Ferromagnetism.*

According to Heisenberg's theory ‡ one of the conditions necessary for ferromagnetism to occur in a crystal is that each atom must have at least eight nearest neighbours. Sachse § has applied this test to $Fe_3O_4$, $\alpha-Fe_2O_3$, and $\gamma-Fe_2O_3$ (assuming the oxygen positions suggested by Welo and Baudisch) ‖ and finds that the condition is satisfied by $Fe_3O_4$ and $\gamma-Fe_2O_3$ but not by $\alpha-Fe_2O_3$. The condition is also satisfied by the structure proposed in the present paper. Table V. gives a list of neighbours at various distances for

† *Loc. cit.*

‡ *Zeits. f. Phys.* xlix. p. 619 (1928); 'Probleme der modernen Physik,' p. 114, Leipzig, 1928.

§ *Zeits. f. Phys. Chemie*, B. 9, p. 83 (1930).

‖ The arrangement chosen was that corresponding to (*b*) of the present paper.

this structure. The "nearest neighbour" atoms are denoted by an asterisk.

## Summary.

The probable crystal structure of ferromagnetic $Fe_2O_3$ has been determined from considerations of intensity, atomic dimensions, and rules of co-ordination.

X-ray powder photographs of $Fe_3O_4$ and ferromagnetic $Fe_2O_3$ were taken and the intensities of reflexion estimated by a photometric method. From considerations of symmetry and atomic size certain arrangements were found to be possible. Of these, two only satisfied intensity requirements. Since these two arrangements gave the same calculated intensities no distinction could be made between them on

Table V.

| Neighbours of | Distance. | | | | | | |
|---|---|---|---|---|---|---|---|
| | 1·82 Å. | 1·88 Å. | 2·07 Å. | 2·14 Å. | 2·97 Å. | 3·06 Å. | 3·48 Å. |
| FeA | $1O_\beta$* | $4O_\alpha$* | — | — | — | — | $12{\cdot}0_\alpha$ 12FeB* |
| FeB | — | — | $6O_\alpha$* | — | 6Fe*B | — | 6FeA* |
| O | — | 1FeA* | 3FeB* | $1O_\beta$* | — | $12O_\alpha$* | 3FeA |
| O | 2FeA | — | — | $6O_\alpha$* | — | — | — |

FeA=Iron atom occupying same position as Fe++ atom in $Fe_3O_4$.
FeB=Iron atom occupying same position as Fe+++ atom in $Fe_3O_4$.
$O_\alpha$ =Original oxygen atom (*i. e.*, as in $Fe_3O_4$).
$O_\beta$ =Additional oxygen atom.

the basis of X-ray measurements. By the application of Pauling's rules of co-ordination, however, it was possible to decide which arrangement was the more probable.

The structure of ferromagnetic $Fe_2O_3$ is found to be cubic, the side of the unit cube being 8·4 Å. as in $Fe_3O_4$ and the space group $O^6$ (or $O^7$) or $T^4$. Iron and oxygen atoms occupy the same positions as in the unit cube of $Fe_3O_4$ and there are four additional oxygen atoms.

A feature of the structure is the placing of certain iron atoms between five oxygens and in a sense the arrangement can be considered as intermediate between magnetite and hæmatite.

The structure satisfies the requirements of Heisenberg's theory of ferromagnetism regarding the number of nearest neighbours.

The author is indebted to Mr. R. D. Williams, M.Sc., of the Research Association of British Paint, Colour, and Varnish Manufacturers, who prepared the $Fe_2O_3$ and carried out the chemical analysis, and to Dr. G. Shearer for his interest in the work.

---

CV. *Hyperfine-structure of Spectrum Lines of Lead Arc in the Visible and the Ultra-Violet Regions.* *By* Wali Mohammad, *M.A. (Punjab), B.A. (Cantab.), Ph.D. (Göttingen), Professor of Physics, Lucknow University, and* Prem Nath Sharma, *M.Sc., Research Fellow, Lucknow University* *.

THE following paper is an extension of the authors' work on the Fine-structure of Spectrum Lines. Previous to this the fine-structure of cadmium [1] and thallium [2] lines has been investigated by one of the authors, and that of zinc [3] and silver [4] lines by both the authors.

Gehrcke and Von Baeyer [5], Janicki [6], Lunelund [7], Nutting [8], and Wali Mohammad [9] have worked on the same element, but their attention has been confined only to the visible region. There is no information available on the fine-structure of lead lines in the ultra-violet region, and the present paper deals for the first time with this matter.

### *Experimental Procedure.*

The apparatus used was the same as was described in the previous papers [1, 2, 3, 4]. A specially constructed arc lamp in vacuum was employed as the source of light. Pure lead metal stick was used as the anode. The oxy-cathode in the lamp was heated to incandescence by a current of from 15 to 20 amperes and a voltage of 220 applied between the anode and the cathode. The melting-point of lead is nearly 325° C., and the thermionic current varied between 0·5 to 1·5 amp. The light of the lead-arc was faintly bluish.

The spectrograph used was Hilger's 3-metre type with interchangeable optical systems. This gives a very good dispersion in the regions investigated. Ilford S. R. Panchromatic and Wellington Spectrum and Anti-screen

* Communicated by the Authors.

plates were used for photographing the spectrum and the Lummer fringes. Two Lummer-Gehrcke plates of quartz were available for use, one was 195 mm. long and 3·65 mm. thick, and the other was 130 mm. long and 4·597 mm. thick. The time of exposure was generally about ten minutes except in the case of faint lines, when it had to be made longer.

*Wave-length Calculation.*

Von Baeyer's formula has been employed for calculating $\Delta\lambda_{max.}$ in A.Us., the distance between the two successive orders of the fringe-system of a line,

$$\Delta\lambda_{max.} = \frac{n\lambda^2}{n^2\lambda - 4t^2\mu\frac{d\mu}{d\lambda}},$$

where "$n$" the order of the fringe-system is given by

$$n\lambda = 2t\sqrt{\mu^2 - 1}.$$

The position and the wave-length of the satellite were found in the previous cases [1, 2, 3, 4].

*Measurement on Lead Lines.*

The following lines, in agreement with Janicki [6], Lunelund [7], and Wali Mohammad [9], are found simple :—

1 ..... 5005·62 (4 *r*).
2 ..... 4340·65 (2).
3 ..... 4168·21 (3R) $P_2 - 3d_2$.
4 ..... 4002·30 (3R) $P_2 - 3d_1$.

5. λ 4057·97 (6R) $p_2 - 2s$.

This line has been investigated by Janicki [6], Lunelund [7], and Wali Mohammad [9]. It has been found to possess two satellites. The authors' results are given side by side with those of Janicki, Lunelund, and Wali Mohammad :—

| Janicki. | Lunelund. | Wali Mohammad. | Authors. |
|---|---|---|---|
| — | −0·092 (2)? | — | — |
| −0·041 (3) | −0·041 (2) | −0·041 (5) | +0·0400 (4) |
| 0·000 (10) | 0·000 (10) | 0·000 (10) | 0·000 (10) |
| +0·033 (2) | +0·034 (3) | +0·032 (5) | +0·034 (5) |

The agreement between the authors' results and those of previous investigators is fairly marked.

6. λ 4019·77 (3R) $P_2-3d_3$.

Janicki, Wali Mohammad, and Luneland found this line to be simple. The authors also find that this line is simple.

The following three lines have also been found to be simple :—

7 ..... 3740·40 (5R).
8 ..... 3683·60 (6R).
9 ..... 3671·65 (3R).

8. λ 3639·71 (6R) $p_1-2s$.

This line has been found to possess two satellites and the following structure is obtained :—

−0·034 (3).
0·000 (10).
+0·027 (5).

The following lines are simple :—

9 ..... 3572·88 (5R).
10 ..... 2873·40 (4R) $p_2-3d_2$.

11. λ 2833·17 (6R) $p_0-2s$.

This line possesses two satellites, one of which is quite sharp while the other is very faint, and the position and the wave-length of this satellite is very difficult to measure. The following structure is obtained :—

−0·021 (4).
0·000 (10).
(?)

The following lines are again simple :—

12 ..... 2823·28 (4R).
13 ..... 2802·09 (5R) $p_2-3d_2$.
14 ..... 2697·72 (4RU).
15 ..... 2628·36 (2R) $p_2-3s$.

16. λ 2614·26 (3R).

This line has one satellite :—

−0·017 (5).
0·000 (10).

The following two more lines are found to be simple :—

17 ..... 2613·74 (3R).
18 ..... 2577·35 (4R).

*Term-Scheme of Lead.*

Very few lines of lead are found to possess complex structure. The classification of lines is that done by Thorsen [10] and later on confirmed by Gieseler and Grotrian[11]. It will be evident that the levels $p_0$, $p_1$, $p_2$, $P_2$, $3d_1$, $3d_2$, and $3s$ are all simple, while the only level which possesses a certain amount of structure is the level $2s$ which is common to the three lines 4058 ($p_2-2s$), 3640 ($p_1-2s$), and 2833 ($p_0-2s$).

The term-separations of the $2s$ level is given in the ollowing table :—

| λ in Å.Us. | ν in cm.$^{-1}$. | Δν in cm.$^{-1}$. |
|---|---|---|
| 4058·004 | 24635·746 | |
| | | ·184 |
| 7·990 | 35·930 | |
| | | ·249 |
| 7·929 | 36·179 | |
| 3639·737 | 27466·713 | |
| | | ·204 |
| 9·710 | 66·917 | |
| | | ·256 |
| 9·676 | 67·173 | |
| 2833·170 | 35285·796 | |
| | | ·262 |
| 3·149 | 86·058 | |

It will be seen that the $2s$ level is a triplet with term-separations of 0·194 cm.$^{-1}$ and 0·262 cm.$^{-1}$. It is here seen that the two separations are in the ratio 3 : 4, since

$$0{\cdot}194 : 3 = 0{\cdot}0647.$$
$$0{\cdot}262 : 4 = 0{\cdot}0655.$$

The line 2614·26, which possesses one satellite, has not been classified as yet.

*References.*

(1) Wali Mohammad & Mathur, Phil. Mag. iv. p. 112 (1927).
(2) Wali Mohammad & Mathur, *ibid.* v. p. 1112 (1928).
(3) Wali Mohammad & Sharma, *ibid.* x. p. 916 (1930).
(4) Wali Mohammad & Sharma, *ibid.* xii. p. 726 (1931).
(5) Gehrcke & von Baeyer, *Ann. d. Phys.* xx. p. 285 (1908).
(6) Janicki, *ibid.* xxix. p. 848 (1909).
(7) Lunelund, *ibid.* xxxiv. p. 526 (1911).
(8) Nutting, *Astrophys. Journ.* xxiii. p. 75 (1906).
(9) Wali Mohammad, *ibid.* xl. p. 196 (1914).
(10) Thorsen, *Naturwissensch.* xi. p. 78 (1923); xii. p. 705 (1924).
(11) Giesseler & Grotrian, *Zeit für Phys.* xxxiv. p. 374 (1925).

Department of Physics,
Lucknow University (India),
April 1931.

CVI. *Observations on the Paper by Messrs. Seth, Gulati, and Singh on the E.M.F. between Metals.* *By* Prof. P. E. Shaw, *M.A.*, *D.Sc.* *

In the issue of the 'Philosophical Magazine' for Aug. 1931 the above authors give results for the Volta contact force. They do not appear to have seen my results (Proc. Roy. Soc. A, cxxii. p. 42 (1929)), produced also by a dynamical method. I passed a stream of metal filings through a metal tube, and measured the resulting three voltages on (1) the tube, (2) the emerging filings, (3) the emerging air. The velocity was higher than that used in the above paper; and in accordance with Lafay's Law the values were high, as much as 1000 millivolts. I only used copper, zinc, iron, and brass amongst metals; but as far as I went the results, like those of Messrs. Seth and his colleagues, conform with the well-known Volta series.

In my results a notable effect was that when the metals were *alike* Zn/Zn, or Cu/Cu, or Brass/Brass, there was e.m.f. produced; in fact, the voltages were comparable with those for unlike metals. It would be interesting for Messrs. Seth and his colleagues to try *like* metals by their method, which seems to work with ease and reliability, and should be adaptable. As one who has spent much time in the last twenty years on this and kindred subjects, I should like to express the opinion that this large and fruitful field—contacts at solid surfaces—has been too long neglected, and

* Communicated by the Author.

will reward all the perseverance these investigators can summon.

As to theory, one must not press for a model before reliable data are to hand; but the suggestion by the authors that the surfaces are not in contact seems to involve something like a flight of electrons across the (air) space intervening between the two metal surfaces.

The reaction of the surfaces in contact varies according to the number (with range 0 to $10^{12}$ or so) of atoms in contact. It seems to me that light pressure, with relatively few atoms bearing, would so act as to account for the charges, resistances, and pressures observed in these experiments.

It should be possible by direct experiment to answer the important question, whether or not there is actual contact between the reacting surfaces. Especially easy this should prove as the surfaces are conducting.

CVII. *The Influence of Electrolytes on the Dielectric Constant of Water.*—Part I. (*Experimental Method*) *and* Part II. (*Uni-univalent Salts*). *By* R. T. Lattey *and* W. G. Davies *.

[Plate XXII.]

## Part I.

### *Introduction.*

MEASUREMENTS on the dielectric constants of electrolytic solutions are of interest in that they may be expected to supplement the knowledge we have acquired from the measurements of electrical conductivity.

While the electrical conductivities of solutions of salts have been measured in water and many other solvents by different observers with good agreement, the values which are available for the dielectric constants show little agreement. This is probably due to the many corrections which must be applied to obtain true values. Obviously, alternating currents must be used for any measurements of the dielectric constants of conducting solutions. We will here confine our attention to the solution of salts in water. Early investigators were under great disadvantage in that they were forced to work with damped oscillations, an added difficulty to the interpretation of results.

* Communicated by the Authors.

A summary of the position in 1926 is given by Blüh [3]. The first measurements appear to have been carried out in 1891. Rosa [28], measuring the force between two electrodes by means of the torsion balance, found that the force decreased on the addition of acid or copper sulphate to distilled water. Bouty [4] stated there was no change of dielectric constant on adding NaCl to water, while Cohn [8], who used a Lecher wire system excited by an Hertzian oscillator, found that the dielectric constant increased on the addition of NaCl. Later, experiments were carried out by Drude [12]. He showed, using his second method, that a 25 per cent. solution of NaCl had a dielectric constant of the same value as pure water. For $CuSO_4$ solution also he could detect no change. Smale [31], using an electrometer method, found that for KCl, HCl, and $CuSO_4$ solutions there was an increase of dielectric constant with increasing concentration. Nernst [24], using his bridge method, also found an increase for KCl solutions. Coolidge [37], using a modified arrangement of the Drude 2nd method, found no change for $CuSO_4$ solutions. Palmer [26] stated that a $CuSO_4$ solution of conductance 32·5 times that of water and a KCl solution of conductance 21 times had the same value of the dielectric constant as water. In all these cases damped oscillations were used, and the effect of the conductivity of the solutions on the measurements had never been properly realized.

The results have been criticized by Lattey [20] on these grounds. He used a "Current Tuning" resonance method and applied a correction for the conductance of the solutions. A correction was also applied for the inductance of the condenser leads. In each case it was found that the addition of a salt to water resulted in a decrease of the dielectric constant. The corrections to be applied are considerable and are difficult to evaluate to any great degree of accuracy. Sommer [32] [3], using the Nernst bridge method, also found a decrease for both NaCl and KCl solutions. Fürth [13] used the ellipsoid force method and found, on addition of NaCl, a decrease in dielectric constant which depended on the voltage applied. Carman and Schmidt [6], using an electrometer method, showed that there was a decrease in value at small concentrations, but that on further increase of concentration the dielectric constant increased to a value above that of water. The current passing through the solution was sufficient to raise its temperature a few degrees while observations were being taken, and since the frequency used was quite low it is probable that there were appreciable

polarization effects. Hellman and Zahn [15] stated that solutions of NaCl, HCl, LiCl, and $CuSO_4$ all lowered the dielectric constant of water, but in the case of $CuSO_4$ further increase in concentration resulted in an increase to a value above that of water. Their results could be obtained only for concentrations above 0·03 N. The extrapolation of their results to obtain an initial decrease does not seem entirely justifiable. Sack [29] used the bridge method at a frequency of $2 \times 10^6$ for a larger number of salts. He found in each case a decrease in dielectric constant which was proportional to the concentration and to the valencies of the ions present. If D represents the dielectric constant of pure water while $D_1$ is the dielectric constant of a solution of concentration $c$ mols per litre, then $D_1 = D(1-\gamma c)$. From theoretical considerations he concluded that the value of $\gamma$ for different salts should be given by $\gamma = 3{\cdot}3\Sigma\nu_i z_i^{3/2}$, where the salt consists of $\nu_1$, $\nu_2$, . . . $\nu_s$ ions of valencies $z_1$, $z_2$, . . . $z_s$. The factor 3·3 was chosen to fit the experimental values. The following values are given for different salts :—

| | KCl. | NaCl. | LiCl. | $BaCl_2$. | $MgSO_4$. | $CuSO_4$. | $La(NO_3)_3$. | $LaCl_3$. |
|---|---|---|---|---|---|---|---|---|
| (exp.)..... | 6·9 | 7·1 | 7·4 | 16·5 | 17·3 | 19·0 | 24·2 | 26·5 |
| ± ..... | 1·0 | 1·2 | 1·4 | 2·8 | 2·7 | 2·3 | 3·4 | 3·5 |
| (calc.) ... | 6·6 | 6·6 | 6·6 | 15·8 | 18·5 | 18·5 | 27·1 | 27·1 |

Corrections were made for conductivity but not for lead inductance. Skancke and Schreiner [30] also used a bridge method and showed the effect of various errors in the use of this method. They corrected for conductivity and lead inductance and found a decrease in the dielectric constant of water on addition of KCl, LiCl, $BaCl_2$, $MgSO_4$, and $K_4Fe(CN)_6$. The decrease was greater than that obtained by Sack. Pechold [27] used the Fürth ellipsoid method and found a decrease in dielectric constant followed by a rise, for solutions of KCl, LiCl, HCl, NaCl, and NaOH. Deubner [10] and Voigt [33] used the 1st and 2nd Drude methods respectively. While Voigt found a decrease in the dielectric constant for NaCl solutions, Deubner found no change up to 0·0032 N. For $CuSO_4$ he found a decrease proportional to the concentration. Walden and Werner [35], using the "Current Tuning" resonance method over a small concentration for a great number of salts, found in each case a lowering of dielectric constant proportional to the concentration. Their results have, however, been criticized by Hellmann and Zahn [16], Lattey [21], and Astin [2]. Bramley [5] found a decrease with increasing concentration

for NaCl solutions by means of an interferometer method. Carman and Smith [7], using an improved form of the Carman and Schmidt apparatus, found that for $CuSO_4$ solutions the dielectric constant always had a value greater than that of water, while for $BaCl_2$ and KCl it first increased and then decreased with increasing concentration. The results differ considerably from those obtained by the earlier method. Astin [2] used the "Voltage Tuning" resonance method and found values for KCl solutions, which he stated were dependent on the coupling with his oscillator. Subsequent work on his part has failed to confirm this. Astin made no correction for the capacity of the condenser plates with near objects such as the walls of the containing vessel. His earlier measurements were at a frequency where any inductance due to the condenser leads had a negligible effect, but he did not correct for the effect of the conductivity of his solutions on the apparent value of the lead inductance. In his later note he states that he is unable to find any change in the value of the dielectric constant on increasing the concentration of KCl solutions up to 0·01 N. It has been previously pointed out by us [23] that the correction for conductivity is almost independent of the frequency. Dielectric constant-concentration curves similar to those of Astin were obtained by us before the importance of this correction was realized. Drake, Pierce, and Dow [11] used a modification of the Drude 2nd method at wave-lengths of 4 to 25 metres, and could find no change in the value of the dielectric constant on increasing the concentration of KCl up to N/70. Haverstadt and Fricke [14] have used the bridge method and found a decrease in value for KCl solutions which was many times that obtained by Sack and by Skancke and Schreiner, who used the same method.

To illustrate the divergence which exists between the results of various observers all the results which are available for KCl solutions are plotted in Graph 1. It will be seen that there is little or no agreement and that it is desirable that some new method should be adopted in which the many corrections which have to be applied should be eliminated or otherwise accurately determined.

The dielectric constants of insulating dielectrics are probably best determined by bridge methods. When the dielectric is also a conductor serious difficulties are introduced. In these cases resonance methods which depend on the determination of a position of maximum current are much more satisfactory. The usual method is to adjust the circuit by means of a variable condenser until the current is

a maximum, and then to connect the unknown capacity in parallel with the variable and to adjust until resonance is again obtained. This method was used by Walden, Ulich, and Werner [34] and by Lattey [20] for electrolytic solutions. Considerable corrections have to be applied, and the method is not considered very satisfactory. The "Voltage Tuning"

Graph 1.

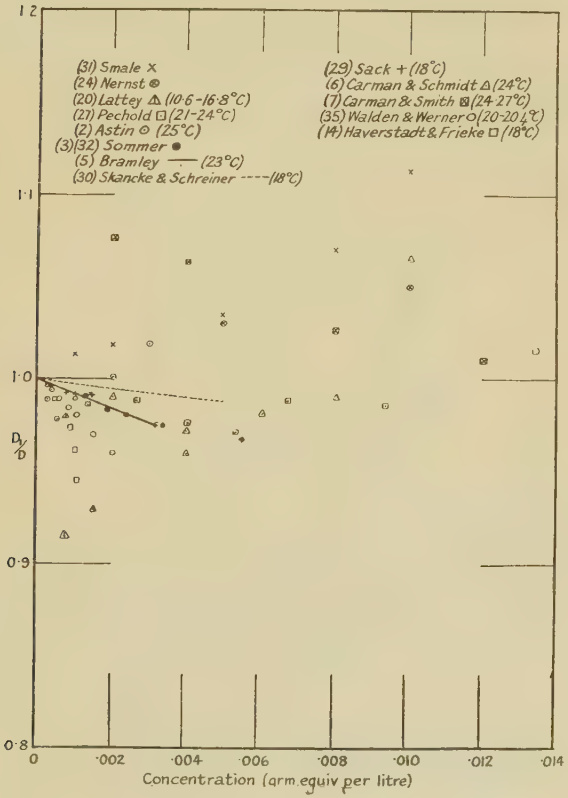


method which has been used by us can be adapted so that no correction must be made for the conductance, and it seems to be a considerable improvement on the older methods for this reason.

## *Theory.*

Consider the oscillating circuit which is represented in fig. 1. Suppose that this circuit is loosely coupled to an

oscillator which generates pure sine waves. We can assume that there is no reaction from the oscillating circuit on the generator. R represents the resistance of the coil L, X is a resistance in parallel with the condenser K, $i$ etc., represent the instantaneous currents in the various circuits, and $v$ represents the instantaneous voltage between the points A and B. We consider the effect of an impressed electromotive force $E_0 \sin pt$ on the circuit ; then

$$L\frac{di_1}{dt} + Ri_1 - E_0 \sin pt = \int \frac{i_2 . dt}{K} = -v \quad . \quad . \quad (1)$$

and

$$i_1 + i_2 = \frac{v}{X} . \quad . \quad . \quad . \quad . \quad . \quad . \quad (2)$$

Fig. 1.

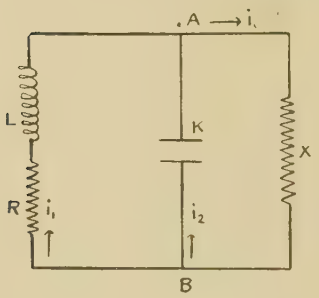


Combining these equations

$$\frac{d^2v}{dt^2} + \left(\frac{R}{L} + \frac{1}{XK}\right)\frac{dv}{dt} + \frac{1}{LK}\left(1 + \frac{R}{X}\right) = \frac{E_0}{LK} \sin pt ; \quad (3)$$

therefore $$v = A \sin (pt - \alpha),$$

where

$$A = \frac{E_0}{LK\sqrt{\left(\frac{R}{L} + \frac{1}{XK}\right)^2 p^2 + \left\{\frac{1}{LK}\left(1 + \frac{R}{X}\right) - p^2\right\}^2}} . \quad (4)$$

The value of $v$ is a maximum when A is a maximum, that is, when

$$K = \frac{L}{p^2L^2 + R^2} . \quad . \quad . \quad . \quad . \quad . \quad . \quad (5)$$

If the condenser is adjusted so that the voltage across AB is a maximum, then the value of K is independent of any resistance X which is in parallel with it.

A condenser containing a conducting solution is equivalent to the arrangement in fig. 1 of a condenser with a resistance in parallel. The capacity for which the voltage across the terminals of this conducting condenser is a maximum is independent of any leakage resistance.

This theory has been worked out by Jezewski [17], Kniekamp [18], who used it to determine the dielectric constants of sugar and urea in water, Lattey and Gatty [22], who measured the dielectric constants of a number of organic liquids and water, and Appleton and Childs [1], who made measurements on ionized air.

In this simple theory we have entirely neglected any effects which may be due to the inductance of the condenser leads. That these may attain considerable importance has

Fig. 2.

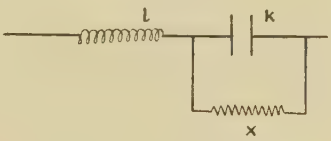


Fig. 3.

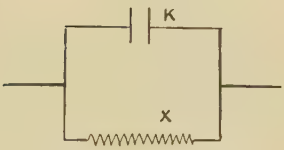


been pointed out by Watson [36] and by Lattey and Gatty [22]. The latter have shown that a condenser of capacity $k$ in parallel with a resistance $x$ and having leads of inductance $l$ (fig. 2) is equivalent to a condenser K in parallel with a resistance X (fig. 3), where

$$\mathrm{X} = x(1-p^2kl)^2 + \frac{p^2l^2}{x} \quad . \quad . \quad . \quad . \quad (6)$$

and

$$\mathrm{K} = \frac{kx^2(1-p^2kl)-l}{x^2(1-p^2kl)+p^2l^2} = \frac{k\left(1-\frac{l}{kx\mathrm{X}}\right)}{(1-p^2kl)} \; ; \quad . \quad . \quad (7)$$

$p$ is the periodicity of the oscillations. The corrections which have to be applied to the observations for the effect of lead inductance will be introduced with the aid of these equations.

The circuit, which is used experimentally, is represented diagrammatically in figs. 4 and 5. R represents the resistance of the coil L ; $k_1$ is a well insulated variable condenser with leads of inductance $l_1$ ; $k$ represents the condenser containing the conducting dielectric under test, its leakage resistance being $x$ and its leads having an inductance $l$. The maximum voltage across its terminals is measured by finding the maximum current in the thermo-

Fig. 4.

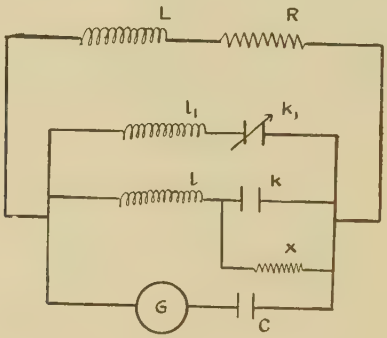


Fig. 5.

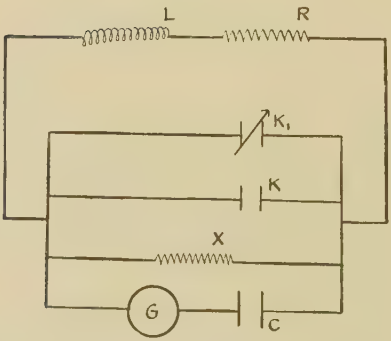


junction and the galvanometer G which is coupled through the condenser C. The circuit is equivalent to that represented in fig. 5, where $k_1$, $K_1$, and $l_1$ are connected by the equation

$$K_1 = \frac{k_1}{(1-p^2k_1l_1)} \quad . \quad . \quad . \quad . \quad . \quad . \quad (8)$$

(putting $x=\infty$ in equation (7)), while $k$, K, $l$, $x$, and X are connected by (7).

$k_1$ is first adjusted in the absence of $k$ so that the current through the galvanometer is a maximum. Suppose its value equals $k_0$. $k$ is then introduced and the variable condenser is readjusted until there is again resonance. Let the new value equal $(k_0-\Delta)$; then the capacity of the liquid condenser uncorrected for the inductance of its own leads is given by

$$K = \frac{k_0}{(1-p^2l_1k_0)} - \frac{k_0-\Delta}{(1-p^2l_1(k_0-\Delta))}$$

or

$$\frac{1}{K} = \frac{(1-p^2l_1k_0)^2}{\Delta} + p^2l_1(1-p^2l_1k_0). \quad . \quad . \quad . \quad (9)$$

The true capacity of the liquid condenser is obtained from K by equation (7). This equation involves $x$ and X, which must be expressed in terms of measurable quantities.

Lattey and Gatty [22] showed that if the value of the variable capacity equals $k_0$ when it has been adjusted for voltage resonance, and if the corresponding current through G is $I_0$, then, when $k_1$ is detuned an amount $(k_0\sim k_1)$ and the current through G is $I_1$,

$$\frac{k_0\sim k_1}{\sqrt{\frac{I_0^2}{I_1^2}-1}} = \frac{1}{p}\left(\frac{1}{X} + \frac{R}{(R^2+p^2L^2)} + \frac{p^2C^2G}{(1+p^2C^2G^2)}\right); \quad (10)$$

G represents the resistance of the galvanometer. The r.h.s. is dependent only on the circuit constants if $p$ is kept constant.

We may write

$$\frac{k_0\sim k_1}{\sqrt{\frac{I_0^2}{I_1^2}-1}} = \phi, \quad . \quad . \quad . \quad . \quad . \quad (11)$$

where $\phi$ is called the tuning factor; $k_0$, $I_0$, $k_1$, and $I_1$ are measurable quantities, so that the value of $\phi$ can be calculated.

When the condenser $k$ is absent X becomes infinite, and we may rewrite (10)

$$\phi = \left(\frac{R}{R^2+p^2L^2} + \frac{p^2C^2G}{1+p^2C^2G^2}\right)\frac{1}{p}. \quad . \quad . \quad (12)$$

If we denote the two values of $\phi$ by $\phi_1$ and $\phi_2$, then

$$\Delta\phi = \phi_2-\phi_1 = \frac{1}{pX}. \quad . \quad . \quad . \quad . \quad (13)$$

Using equations (6) and (13) we rewrite (7) in the form

$$\frac{1}{k} = \frac{1}{K} + p^2 l - \frac{p^2 l(\Delta\phi)^2}{K\{p^2 l(\Delta\phi)^2 + K(1+p^2 KL)\}}; \quad (14)$$

$p$, $l$, K, and $\Delta\phi$ may be found experimentally so that K can be calculated.

It will be noticed that the observed capacity K is not independent of the conductance of the solution as was concluded from the simple theory. The capacity $k$ thus calculated is a function not only of the dielectric constant of the liquid between its plates, but also of the capacity of the leads and a capacity relative to the surroundings. Lattey and Gatty [22] connect $k$ with the dielectric constant D by means of the equation

$$k = k_l + C_0 D + \frac{AD}{B+D};$$

$k_1$ representing the capacity of the leads, $C_0$ the capacity *in vacuo*, while A and B are constants. Since it is $\frac{1}{k}$ which is determined by equation (14), we find it more convenient to use the approximate form

$$\frac{1}{k} = a + \frac{b}{D} + \frac{c}{D^2}, \quad . \quad . \quad . \quad . \quad . \quad (15)$$

where $a$, $b$, and $c$ are constants. Their values must be determined by the use of liquids of known dielectric constants.

By the aid of equations (9), (14), and (15) it is possible to determine D for any liquid which is contained in the condenser $k$. The evaluation of the many constants involved will be discussed later.

### *The Oscillator.*

The oscillations were produced by the triode arrangement which is shown in fig. 6.

The valve used was a Mullard O 30 requiring a filament voltage of 5 volts. The plate was kept at a constant voltage of 520. $c$ was a variable condenser having a maximum capacity of about 0·5 m.m.f. A fine adjustment of the capacity could be made on a small condenser in parallel with $c$. The large fixed condenser K was put in parallel with the plate battery, so that slight capacity

changes in the battery would have little effect on the wave-length of the oscillations produced. The fixed coils M and N consisted of a few turns of 16-gauge enamelled copper wire on ebonite cylinders of about 12 cm. diameter. For the production of the shorter waves both coils were wound on the same cylinder, since stronger coupling was required between M and N. The coils were connected in the circuit by plugs so that they could be easily changed. Using various combinations of M and N and varying $c$, oscillations were produced of any required wave-length between 35 and 300 m. This arrangement was found to be unaffected by stray capacities, so that there was little variation of wave-length. The complete oscillator, exclusive of batteries, was mounted on a trolly running on rails of about 1·5 m. length (fig. 7, Pl. XXII.). By this means the oscillator could be

Fig. 6.

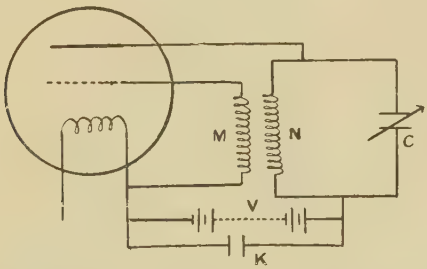


arranged easily at any distance from the receiving circuit. Its nearest distance of approach to the coil L of the receiving circuit was 35 cm.

*The Receiving Circuit.*

The circuit is shown diagrammatically in figs. 4 and 5, and the geometrical arrangement may be seen in fig. 7 (Pl. XXII.).

The inductance L was made of brass strip $0{\cdot}3 \times 0{\cdot}8$ cm. and constructed in the shape of a helix. Four helices, consisting of two or three turns and having diameters of from 12 to 22 cm., were used. They were attached by screws so that they could easily be changed. The variable condenser $k_1$ was of the rotating-vane type. It was enclosed completely in an earthed square brass box of side 11 cm. The scale was etched on the ebonite dial, which was covered with a brass disk so that only the scale was visible. The dial was fitted with an ebonite handle, 26 cm. long, so that the condenser could be be adjusted without any part of the

observer's body being brought near to it. The scale was read by a pointer marked on the brass box. The scale was divided into 180 units, each having a value of approximately 1/3 cm.

The fixed condenser C consisted in reality of a pair of condensers in series, each having the same capacity. Each condenser was shielded from the remainder of the circuit by an earthed brass sheet, and they were arranged so that they could be easily changed. Two pairs of condensers were used, one pair having capacities 0·5 m.m.f. each and the other 1·0 m.m.f. Various combinations of L and C were used so that measurements could be made at a variety of wave-lengths.

Fig. 8.

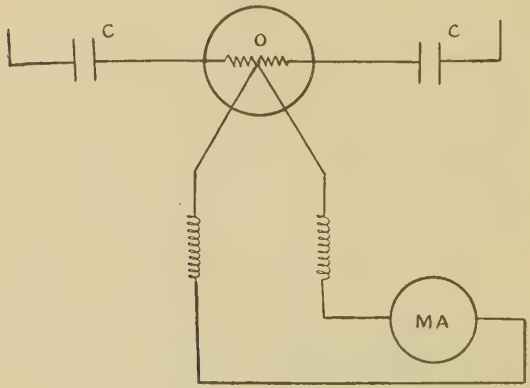


High frequency currents are best measured by their heating effects. Therefore the galvanometer G consisted of a Fleming vacuum electric couple connected through a choke to the recording milliammeter. The heating filament of the couple was connected between two fixed condensers, as shown in fig. 8. The choke prevented any leakage of high frequency current through the milliammeter, and the whole circuit was arranged symmetrically about the point O. The vacuum couple used had a heating resistance of 2·93 ohms (G) and a couple resistance of 5·26 ohms, while the milliammeter resistance was 10 ohms. All connexions in the high frequency part of the circuit were made of brass strip ensuring good contact, a point of great importance.

It is seen from equations (10) and (11) that the value of $\phi$ is increased on increasing the value of C and G. For the

accurate determination of $k_1$ it is essential that the tuning factor $\phi$ should be small. C and G cannot, however, be decreased indefinitely, since decreasing their value also decreases $I_0$. Many values of C and G were tried by us to determine their most suitable values under these two opposing conditions.

When X is small, as is the case for conducting solutions, $\phi = \frac{1}{pX}$ approximately. For a given solution X is fixed and $\phi$ can only be decreased by increasing $p$, the periodicity of the oscillations used.

The chief correction to be applied to the readings involves the inductance of the leads, and it is desirable that this correction should be as small as possible. The inductance of the leads, which are in the form of parallel wires, are given by

$$L = 4s\left[\log\left(\frac{d}{r}\right) - \frac{d}{s}\right], \quad . \quad . \quad . \quad . \quad (16)$$

where $s$ is the length of each wire, $r$ their radii, and $d$ the distance between them[25]. The inductance will depend chiefly on the length of lead $s$. The lengths of the leads $l$ and $l_1$ were reduced so as to be as small as possible, and the branch circuits containing $k$, $k_1$, and the galvanometer were consequently brought very close together. Considerable trouble was then encountered by capacity coupling between the circuits. If such capacity effects were assumed the results were such as would be expected from the mathematical theory. For example: various geometrical arrangements gave either two values of $l_1$ depending on the value of C, denoting a coupling between the galvanometer and the $l$ and $l_1$ circuits, or one value of $l_1$ whatever the value of C, but a value of $l$ which varied with $k$, denoting a coupling between the $l$ circuit and some other. After considerable experimental work the circuit was given its present geometrical arrangement, an arrangement which has been found to be free from all these coupling effects and which has proved very satisfactory.

Four condensers of different capacities were used for the electrolytes. Three had leads of about 10 cm. length (fig. 9), while the fourth had leads of about 2 cm. (fig. 10).

The electrodes E (fig. 9) were in the form of thin platinum disks 1 cm. in diameter. Their distances apart in the condensers A, B, and C were 0·2, 0·3, and 1·5 cm. respectively. Their platinum leads were fused into the glass-containing vessel and fixed into the thick copper leads T. These were

held rigidly by soldering to the screw S, held in position by the nuts N, and passed through the two rectangular covers F and G. The filling tube of the glass vessel also passed through F and G, and was gripped tightly by the lead ring R when the two plates were fastened together by means of the screw D. The copper wires fitted into brass slots so that they were always the same distance, 4·5 cm., apart. The condensers had capacities of about 100, 70, and 20 arbitrary units when filled with water. They were arranged in a thermostat so that they were immersed almost to the ebonite plates.

Fig. 9.

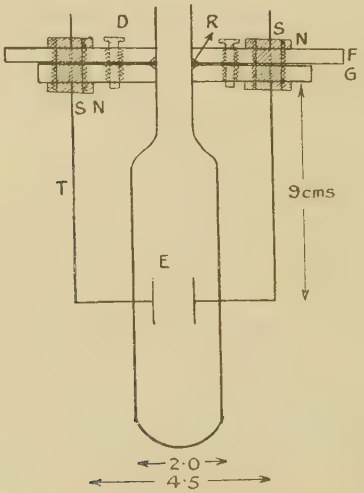


The thermostat consisted of a large copper vessel of diameter 24 cm. and depth 20 cm. supported by a wooden stand in an outer metal vessel, the space between them being filled with felt. The two vessels were in electrical contact and were earthed ; they were arranged concentrically and were mounted so that they could rotate about a common axis. The copper vessel was fitted with a wooden cover into which were cut three rectangular slots arranged symmetrically, and into these the ebonite plates (fig. 9) just fitted. The plates F were slightly bigger and supported the condensers on the cover. Each condenser had a fixed position in the bath, and by rotating the whole thermostat each condenser could be brought in turn into the circuit. The thermostat was filled with paraffin and was electrically

heated by passing a current through a coil of insulated wire wound non-inductively around a cylindrical frame, which was screwed on to the under side of the wooden cover. The frame consisted of eight metal rods insulated by means of glass tubing. The bath was stirred by paddles which were fitted on a vertical axis, on top of which a pulley was mounted. The pulley was rotated by an electric motor. The bath was kept at any desired temperature by a temperature control consisting of a coil of bimetallic strip which was arranged to cut off the heating current through a relay.

Fig. 10 *a*.

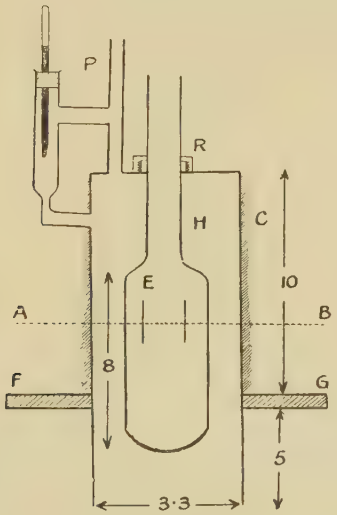


For electrolytic solutions the bath was controlled at two temperatures, $18 \pm 0{\cdot}2^{\circ}$ C. and $25 \pm 0{\cdot}2^{\circ}$ C. The paraffin in the bath was kept at the same height throughout, and the whole thermostat was shielded from the observer's body by means of an earthed metal sheet.

The fourth condenser used for the liquids had very short leads and is shown in figs. 10 *a* and 10 *b*.

The electrodes E were thin disks of platinum of 1 cm. diameter and fixed 1 cm. apart. The containing vessel was cylindrical ; it was fitted inside a copper cylinder C. The glass tube H was rigidly fixed by a rubber ring at R which gripped it tightly when the head was screwed up. The outer vessel had a side tube in which a thermometer was placed. The platinum leads of the electrodes came out

horizontally and passed into the rubber bung D, where they were fixed into thick copper leads. The bung was cut in half to do this, and after replacement was covered with wax to keep the leads in a fixed position. The connexions at R and D were both made air-tight. The lower end of C was arranged to dip into the paraffin of the thermostat, the remainder being supported by the ebonite ring FG, which rested on the wooden cover of the thermostat. By means of the tube P the paraffin was sucked up into C and the vessel containing the electrolyte was completely immersed. Radiation losses were diminished by surrounding the outside of C with asbestos. The capacity of this condenser was about 30 units when it contained water.

Fig. 10 *b*.

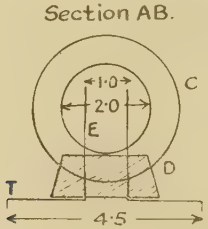


*Method of Measurement.*

(a) $p$.

The wave-length was determined by a wave-meter. $p = \frac{2\pi c}{\lambda}$, where $\lambda$ is the wave-length and $c$ = velocity.

Table I.

| λ. | L. | | C. |
|---|---|---|---|
| | No. of turns. | Diameter. | |
| metres. | | cm. | m.m.f. |
| 36 | 2 | 12 | 0·25 |
| 41·5 | 2 | 17 | 0·25 |
| 47 | 2 | 22 | 0·25 |
| 59 | 2 | 22 | 0·50 |
| 62 | 3 | 22 | 0·25 |
| 77·5 | 3 | 22 | 0·50 |

Measurements have been carried out on electrolytes at six wave-lengths. The particulars given in Table I. refer to the receiving circuit.

(b) $k_0$, $\Delta$, and $\Delta\phi$.

$k_0$, the capacity for resonance, was approximately determined by rotating the variable condenser until the reading of the ammeter was a maximum. The milliammeter was calibrated to read the square of the current directly. The distance between the oscillator and the receiving circuit was adjusted until the reading of the ammeter, $I_0^2$, corresponding to the resonance capacity $k_0$ was 100 units or some simple fraction of it. Various known values were given to the variable condenser and the corresponding readings of the ammeter noted.

Suppose we have two values of the variable condenser, $k_1$ and $k_1'$, one on each side of the resonance capacity $k_0$, the corresponding currents being $I_0$ and $I_0'$. Then

$$\frac{k_0 - k_1}{\sqrt{\frac{I_0^2}{I_1^2} - 1}} = \phi \quad . \quad . \quad . \quad . \quad . \quad (11)$$

and

$$\frac{k_1' - k_0}{\sqrt{\frac{I_0^2}{I_1'^2} - 1}} = \phi.$$

Eliminating $k_0$

$$\phi = \frac{k_1 - k_1'}{\sqrt{\frac{I_0^2}{I_1^2} - 1} + \sqrt{\frac{I_0^2}{I_1'^2} - 1}} \quad . \quad . \quad . \quad . \quad (17)$$

The value of $\phi$ can be calculated from (17), and by substitution of its value in (11) $k_0$ can be accurately determined.

The variable condenser had a capacity even when its pointer read zero. This capacity correction was found by varying the wave-length emitted by the oscillator so as to put the receiving circuit in resonance when the variable condenser $k_0$ had a fixed value near the lower end of its scale, and then to a wave-length for which $k_0$ had a fixed value near the upper end of its scale, and lastly when $k_0$ was disconnected. Since the square of the wave-length is proportional to the total capacity in the circuit for resonance in each of the three cases, this zero correction may be calculated. A series of observations gave it a mean value of 32 units.

The resonance value of $k_0$ is determined before and after the liquid condenser is introduced. The difference $k_0 - k_0' = \Delta$ and $\Delta\phi$ is given by the difference in value of the tuning factor in the two cases.

Table II. gives a series of observations taken on a potassium iodate solution at 18° in condenser D at a wavelength of 77 metres.

Experiments were carried out to find whether the value of the resonance capacity was dependent on the distance between the oscillator and the receiving circuit, as was found by Astin [2]. It was found that the value $k_0$ was independent of the distance between the circuits.

TABLE II.

D absent.

| $k_1$. | $I^2$. | $\left(\frac{I_0^2}{I^2}-1\right)^{\frac{1}{2}}$. | | $k_0$. |
|---|---|---|---|---|
| $150=k_0$ (approx.) | $100=I_0^2$ | | | |
| 130 | 69·4 | 0·664 | | 148·12 |
| 170 | 61·1 | 0·798 | | 148·20 |
| 160 | 84·1 | 0·435 | | 148·10 |
| 140 | 91·7 | 0·301 | | 148·24 |
| $\phi_1=27·38$ | | | Mean..... | 148·17 |

D present.

| $118=k_0'$ (approx.) | $100=I_0^2$ | | | |
|---|---|---|---|---|
| 50 | 77·9 | 0·533 | | 116·00 |
| 170 | 84·0 | 0·436 | | 115·98 |
| 160 | 88·9 | 0·3535 | | 116·25 |
| 60 | 83·0 | 0·453 | | 116·02 |
| $\phi_2=124·0$ | | | Mean..... | 116·06 |

$k_0=148·17+32·00=180·17.$

$\Delta=(148·17+32·00)-(116·06+32·00)=32·11.$

$\Delta\phi=124·0-27·38=96·6.$

By (13) $\Delta\phi=\frac{1}{pX}$, *i. e.* $\Delta\phi$ varies linearly with H the specific conductivity of the solution. The values of $\frac{\Delta\phi}{\lambda}$ have been plotted against $\kappa$ for solutions of KCl, NaCl, NaF, and $KIO_3$ at 18° in Graph 2. $\Delta\phi$ is expressed in our arbitrary units. The values of $\kappa$ are expressed in ohm$^{-1}$ cm.$^{-1}$, and are interpolated from Kohlrausch's figures [19]. The results given are those obtained for the smallest condenser where the range of concentration was greatest. They served as a useful check on the concentration of the solutions, which were made up by weight.

(c) $l$ and $l_1$.

If the condenser $k$ contains a perfect insulator and its leads are very short so that $\Delta\phi=0$ and $l=0$, then from (9) and (14)

$$\frac{1}{k}=\frac{(1-p^2l_1k_0)^2}{\Delta}+p^2l_1(1-p^2l_1k_0). \quad . \quad . \quad (18)$$

Graph 2.

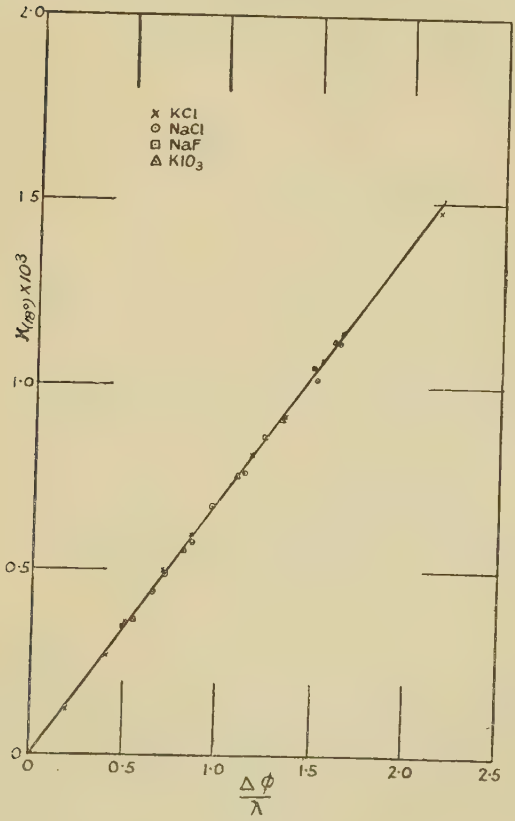


Suppose $k$ is given two values $k'$ and $k''$ and the corresponding settings of the variable condenser are $k_1'$ and $k_1''$, the setting being $k_0$ when $k$ is absent; then from (18)

$$\frac{1}{k'}-\frac{1}{k''}=\left(\frac{1}{\Delta_1}-\frac{1}{\Delta_2}\right)(1-p^2l_1k_0)^2, \quad . \quad . \quad (19)$$

where $\Delta_1 = k_0 - k_1'$ and $\Delta_2 = k_0 - k_1''$. If $p$ is varied $\left(\frac{\Delta_1\Delta_2}{\Delta_1 - \Delta_2}\right)^{\frac{1}{2}}$ should be a linear function of $p^2k_0$ from which $l_1$ may be determined.

All these conditions were satisfied by using two small mica condensers attached by leads of about 1 cm. length. All readings were carried out in a few hours, so that there was little possibility of variation in the capacity of the mica condensers. Unfortunately it was not found possible to determine $l_1$ with sufficient accuracy by this method and another was tried.

We may rewrite (18) in the form

$$\frac{\sqrt{\Delta}}{\left(1 + \frac{p^2 l_1 \Delta}{2(1 - p^2 l_1 k_0)}\right)} = \sqrt{k}(1 - p^2 l_1 k_0). \quad . \quad . \quad (20)$$

Giving an approximate value to $l_1$ in the expression $\frac{p^2 l_1}{2(1 - p^2 l_1 k_0)}$, plotting the left-hand side against $p^2k_0$, and extrapolating to $p^2k_0 = 0$ gives a value for $k$. $l_1$ is then given by the slope of the line.

The measurements previously taken with mica condensers were used to give an approximate value of $l_1$, for use in the expression $\frac{p^2 l_1 \Delta}{2(1 - p^2 l_1 k_0)}$.

If the liquid condenser having leads of inductance $l$ contained a perfect insulator, then from (14)

$$\frac{1}{k} = \frac{1}{\mathrm{K}} + p^2 l.$$

If the frequency is varied K is a linear function of $p^2$ and $l$ may be determined. The liquid condensers were filled with water or sugar solutions and the value of K was determined at various frequencies. Series of observations were taken at various temperatures. Although not perfect insulators, the values of $\Delta\phi$ for these liquids were very small and any effect of conductivity could be neglected. The values obtained for $l_1$ and $l$ by these methods were in good agreement with those calculated by the aid of equation (16).

We have pointed out[23] that the correction term due to the conductivity of the solution can attain considerable importance. It was thought desirable that this term should be eliminated, and it was for this reason that the condenser

with leads of negligible length was used. This condenser has been previously described (fig. 10). The value of $l$ was found experimentally to be negligible. The expression for the true capacity then reduces to

$$\frac{1}{k} = \frac{(1-p^2 l_1 k_0)^2}{\Delta} + p^2 l_1 (1-p^2 l_1 k_0).$$

Table III. gives the values which were obtained for the dielectric constants of KCl solutions at 18° C. in the four condensers used. The capacities of A, B, C, and D when containing water are 100, 70, 20, and 30 units respectively. D is the condenser with very short leads.

TABLE III.

| Concentration in gram equivalents per 1000 gm. of solution. | $\lambda$. | Condenser. A. | B. | C. | D. |
|---|---|---|---|---|---|
| 0·000,963 | 36 | 79·10 | 81·15 | 80·76 | |
| | 41·5 | 80·13 | 80·40 | 80·46 | |
| | 47 | 81·98 | 81·74 | ... | 81·71 |
| | 59 | 81·65 | 80·87 | ... | 81·24 |
| | 62 | 80·65 | 80·50 | | |
| | 77·5 | 81·42 | 80·57 | ... | 81·62 |
| | | | Mean..... | 81·09 | |
| 0·002,133 | 36 | ... | ... | 82·73 | 80·92 |
| | 41·5 | ... | ... | 81·77 | 83·04 |
| | 47 | 82·17 | 81·84 | 82·57 | 83·17 |
| | 59 | 83·09 | 81·94 | 83·29 | 82·37 |
| | 62 | 81·69 | 81·69 | 82·31 | 83·72 |
| | 77·5 | 81·29 | 81·00 | 83·33 | 81·62 |
| | | | Mean..... | 82·28 | |
| 0·002,830 | 36 | ... | ... | 82·22 | |
| | 41·5 | ... | ... | 83·13 | 82·85 |
| | 47 | 82·63 | 81·79 | 81·68 | 83·21 |
| | 59 | 82·58 | 82·46 | 82·82 | 83·48 |
| | 62 | 84·58 | 81·84 | 80·59 | 83·37 |
| | 77·5 | 82·63 | 80·80 | ... | 83·07 |
| | | | Mean..... | 82·54 | |
| 0·003,983 | 36 | | | | |
| | 41·5 | ... | ... | 84·82 | 83·04 |
| | 47 | ... | 83·58 | 84·50 | 83·41 |
| | 59 | 85·34 | 84·44 | 84·82 | 82·30 |
| | 62 | ... | ... | ... | 83·76 |
| | 77·5 | ... | 83·11 | 83·56 | 82·15 |
| | | | Mean..... | 83·76 | |

TABLE III. (*cont.*).

| Concentration in gram equivalents per 1000 gm. of solution. | λ. | Condenser A. | B. | C. | D. |
|---|---|---|---|---|---|
| 0·004,783 | 36 | ... | ... | 82·95 | |
| | 41·5 | ... | ... | 84·08 | 83·08 |
| | 47 | ... | 84·06 | 84·27 | 83·33 |
| | 59 | ... | 85·09 | 85·03 | 82·60 |
| | 62 | ... | ... | 82·56 | 82·87 |
| | 77·5 | ... | 85·29 | 83·06 | 83·65 |
| | | | Mean..... | 83·71 | |
| 0·006,658 | 36 | ... | ... | 86·83 | 83·98 |
| | 41·5 | ... | ... | 87·41 | 86·03 |
| | 47 | ... | ... | 85·95 | 83·52 |
| | 59 | ... | 86·93 | 87·92 | 85·30 |
| | 62 | ... | ... | 82·89 | 85·36 |
| | 77·5 | ... | ... | 83·91 | |
| | | | Mean..... | 85·50 | |
| 0·007,452 | 47 | ... | ... | 87·74 | 83·76 |
| | 59 | ... | ... | 86·40 | 86·89 |
| | 62 | ... | ... | 84·27 | 83·32 |
| | 77·5 | ... | ... | 86·67 | |
| | | | Mean..... | 85·58 | |
| 0·008,658 | 47 | ... | ... | 85·78 | 85·23 |
| | 59 | ... | ... | 85·79 | 87·25 |
| | 62 | ... | ... | 85·17 | 86·63 |
| | 77·5 | ... | ... | 85·55 | 88·00 |
| | | | Mean..... | 86·28 | |
| 0·009,303 | 47 | ... | ... | 85·51 | 86·31 |
| | 47 | ... | ... | 85·38 | |
| | 59 | ... | ... | 88·68 | 87·66 |
| | 59 | ... | ... | 89·54 | |
| | 62 | ... | ... | 84·66 | |
| | 77·5 | .. | ... | 86·76 | 88·40 |
| | | | Mean..... | 87·04 | |
| 0·010,225 | 47 | ... | ... | 88·80 | 85·63 |
| | 59 | ... | ... | 88·07 | 89·94 |
| | 77·5 | ... | ... | ... | 88·11 |
| | | | Mean..... | 88·00 | |

TABLE III. (*cont.*).

| Concentration in gram equivalents per 1000 gm. of solution. | λ. | Condenser. A. | B. | C. | D. |
|---|---|---|---|---|---|
| 0·012,092 | 47 | ... | ... | 87·69 | |
| | 47 | ... | ... | 91·38 | |
| | 47 | ... | ... | 90·90 | |
| | 59 | ... | ... | 95·65 | |
| | 59 | ... | ... | 91·92 | |
| | 59 | ... | ... | 92·21 | |
| | 77·5 | ... | ... | 95·42 | |
| | 77·5 | ... | ... | 86·59 | |
| | | | Mean..... | 90·22 | |

It will be seen that there is agreement between the results obtained by the use of the four condensers, and this conclusion has been confirmed by the results which have been obtained for other salts.

(d) *a*, *b*, and *c*.

These constants were evaluated by finding the capacities of the condensers when they contained four liquids of known dielectric constant. For this purpose we used

(1) Water at 18·7° C. . . . . D = 80·52
(2) Water at 29·2° C. . . . . D = 76·74
(3) 20 per cent. sugar solution at 14° C. . . D = 76·74
(20 gm. of sugar per 100 gm. of solution.)
(4) Water at 89·1° C. . . . . D = 58·33
(5) 20 per cent. sugar solution at 73·9° C. . . D = 58·33
(6) Nitrobenzene at 16° C. . . . . D = 36·165

The values for water and sugar solutions had been previously measured by us [9]. The value used for nitrobenzene is that determined by Lattey and Gatty [22].

## PART II.

### *Results.*

Measurements have been carried out on solutions of four uni-univalent salts at 18° and 25° C. The values obtained for the dielectric constant at various concentrations are given below, and they are plotted against the concentration in Graphs 3 and 4. The concentration is expressed in gram equivalents per 1000 gm. of solution. The second column

gives the number of independent values which have been obtained (see Table III.), and the third table gives the mean

Graph 3.

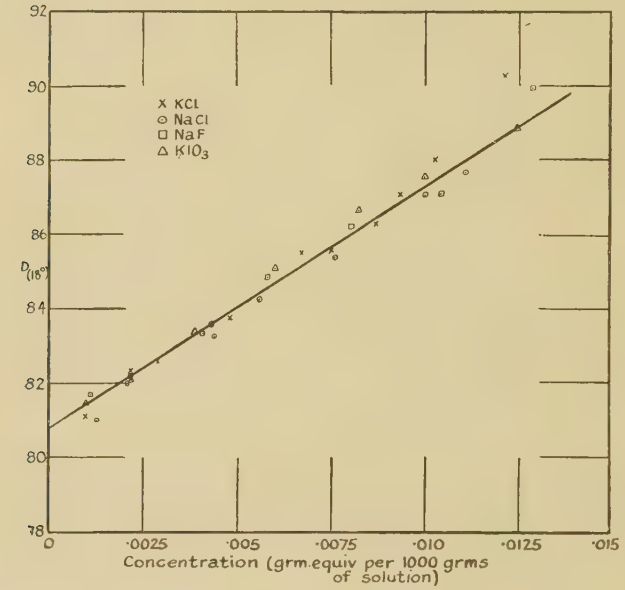


Graph 4.

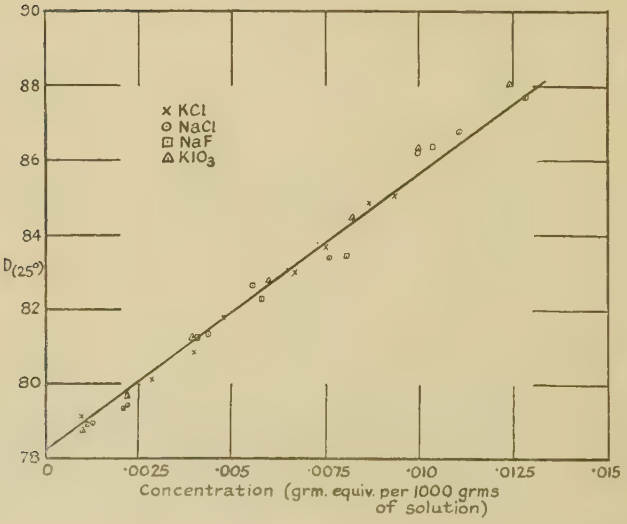

value. All the salts used were Kahlbaum preparations, and the solutions were made up from "conductivity water."

KCl solutions.

| Concentration. | 18°. | | 25°. | |
|---|---|---|---|---|
| | No. | D. | No. | D. |
| 0 | | 80·79 | | 78·24 |
| 0·000,963 | 20 | 81·09 | 22 | 79·11 |
| 0·002,133 | 20 | 82·28 | 19 | 79·79 |
| 0·002,830 | 18 | 82·54 | 18 | 80·10 |
| 0·003,983 | 13 | 83·76 | 15 | 80·82 |
| 0·004,783 | 14 | 83·71 | 14 | 81·76 |
| 0·006,658 | 12 | 85·50 | 8 | 82·98 |
| 0·007,452 | 7 | 85·58 | 7 | 83·64 |
| 0·008,658 | 8 | 86·28 | 6 | 84·83 |
| 0·009,303 | 9 | 87·04 | 6 | 85·03 |
| 0·010,225 | 5 | 88·00 | | |
| 0·012,092 | 5 | 90·22 | | |

NaCl solutions.

| | | | | |
|---|---|---|---|---|
| 0 | | 80·79 | | 78·24 |
| 0,001,205 | 12 | 80·97 | 12 | 78·93 |
| 0·002,124 | 14 | 82·18 | 12 | 79·42 |
| 0·004,225 | 5 | 83·54 | | |
| 0·004,340 | 10 | 83·21 | 15 | 81·35 |
| 0·005,561 | 9 | 84·22 | 7 | 82·62 |
| 0·007,550 | 9 | 85·39 | 9 | 83·38 |
| 0·009,965 | 8 | 87·06 | 23 | 86·20 |
| 0·011,013 | 4 | 87·66 | 2 | 86·79 |

NaF solutions.

| | | | | |
|---|---|---|---|---|
| 0 | | 80·79 | | 78·24 |
| 0·001,072 | 11 | 81·69 | 11 | 78·90 |
| 0·002,057 | 16 | 81·97 | 16 | 79·38 |
| 0·004,040 | 22 | 83·33 | 14 | 81·23 |
| 0·005,789 | 23 | 84·83 | 9 | 82·25 |
| 0·008,000 | 10 | 86·21 | 11 | 83·42 |
| 0·010,375 | 10 | 87·04 | 7 | 86·36 |
| 0·012,800 | 5 | 89·92 | 3 | 87·70 |

$KIO_3$ solutions.

| | | | | |
|---|---|---|---|---|
| 0 | | 80·79 | | 78·24 |
| 0·000,984 | 12 | 81·44 | 12 | 78·76 |
| 0·002,184 | 16 | 82·08 | 15 | 79·69 |
| 0·003,899 | 15 | 83·38 | 13 | 81·24 |
| 0·005,970 | 10 | 85·10 | 10 | 82·74 |
| 0·008,190 | 9 | 86·63 | 9 | 84·42 |
| 0·009,978 | 10 | 87·54 | 9 | 86·30 |
| 0·012,400 | 5 | 88·84 | 7 | 88·09 |

It is seen that the presence of a salt in water produces an increase in the dielectric constant. The increase is proportional to the concentration and is the same for each

uni-univalent salt within the limits of experimental error. The increase at 18° C. is equal to that at 25° for salts of the same concentration.

The method is now being used for measurements on solutions of salts of other types. We hope to publish shortly the results we have obtained.

We are indebted to Prof. J. S. Townsend for the facilities which have been offered us to complete this work in his laboratory.

*References.*

(1) Appleton and Childs, Phil. Mag. vii. p. 969 (1930).
(2) Astin, Phys. Rev. xxxiv. p. 300 (1929) ; and 25th April, 1930.
(3) Blüh, *Phys. Zeit.* xxvii. p. 226 (1926).
(4) Bouty, *C. R.* cxiv. p. 533 (1892).
(5) Bramley, Journal Franklin Institute, ccvi. (May 1928).
(6) Carman and Schmidt, Phys. Rev. xxx. p. 925 (1927).
(7) Carman and Smith, Phys. Rev. xxxiv. p. 1042 (1929).
(8) Cohn, *Wied. Ann.* xlv. p. 370 (1892).
(9) Davies, Thesis, Oxford, 1929.
(10) Deubner, *Ann. d. Phys.* lxxxiv. p. 429 (1927).
(11) Drake, Pierce, and Dow, Phys. Rev. xxxv. p. 613 (1930).
(12) Drude, *Wied. Ann.* lxi. p. 466 (1897).
(13) Fürth, *Phys. Zeit.* xxv. p. 676 (1924).
(14) Haverstadt and Fricke, *Zeit. anorg. Chem.* clxxxviii. p. 357 (1930).
(15) Hellman and Zahn, *Ann. d. Phys.* lxxxi. p. 711 (1926).
(16) Hellman and Zahn, *Zeits. phys. Chem.* cxxxii. p. 399 (1928).
(17) Jezewski, *Zeit. f. Phys.* xlviii. p. 123 (1928).
(18) Kniekamp, *Zeit. f. Phys.* li. p. 95 (1928).
(19) Landolt-Börnstein Tabellen, p. 1079.
(20) Lattey, Phil. Mag. xli. p. 829 (1921).
(21) Lattey, *Zeit. phys. Chem.* cxix. p. 104.
(22) Lattey and Gatty, Phil. Mag. p. 985 (1929).
(23) Lattey and Davies, Phil. Mag. xi. p. 997 (1931).
(24) Nernst, *Wied. Ann.* lx. p. 600 (1897).
(25) Nottage, 'Measurement of Inductance and Capacity.'
(26) Palmer, Phys. Rev. xiv. p. 38 (1902).
(27) Pechold, *Ann. d. Phys.* lxxxiii. p. 427 (1927).
(28) Rosa, Phil. Mag. (5) xxxi. p. 188 (1891).
(29) Sack, *Phys. Zeit.* xxviii. p. 199 (1927).
(30) Skancke and Schreiner, *Phys. Zeit.* xxviii. p. 597 (1927).
(31) Smale, *Wied. Ann.* lx. p. 625 (1897).
(32) Sommer, Thesis, Berlin, 1923.
(33) Voigt, *Zeit. f. Phys.* xliv. p. 70 (1927).
(34) Walden, Ulich, and Werner, *Zeit. phys. Chem.* cxv. p. 177 (1925).
(35) Walden and Werner, *Zeit. phys. Chem.* cxxix. p. 389 (1927).
(36) Watson, Proc. Roy. Soc. cxvii. p. 43 (1927).
(37) Coolidge, *Wied. Ann.* lxix. p. 125 (1899).

Electrical Laboratory,
Oxford.

# CVIII. *The Aluminium-Manganese System of Alloys.*

*By* A. J. Bradley, *Ph.D.*, *and* Phyllis Jones, *Ph.D.**

[Plates XXIII.–XXV.]

## Introduction.

THE Aluminium-Manganese System of Alloys is one which has not been dealt with very thoroughly in the past. This is partly because serious difficulties accompany the preparation and examination of these alloys. Pure manganese is very difficult to obtain, and the fact that it attacks everything siliceous in nature introduces a further difficulty, namely, the choice of a suitable crucible for the melting of the alloys. With open-air melting other troubles are introduced due to the ease with which manganese oxidises. It is not surprising, therefore, to find that the earlier work on the Aluminium-Manganese System was somewhat contradictory. Leon Guillet † carried out some extensive investigations on the aluminium-manganese series in 1902, but the usually accepted equilibrium diagram is that published by Hendricks ‡ in 1908. A great objection to the examination of the alloys of this system from the metallographic point of view is that, apart from those rich in aluminium, they do not lend themselves easily to microscopical analyses. Hendricks obtained his data from thermal observations alone, and his equilibrium diagram by taking cooling curves for each of a series of alloys. His results show the existence of a eutectic at the aluminium end of the diagram, also a miscibility gap in the liquid state, extending from 57 to 86 per cent. aluminium.

According to Hendricks there exist two compounds which are represented by the formulæ $Mn_3Al$ and $MnAl_3$.

W. Krings and W. Ostmann § have examined the ternary system MnCuAl, and confirm that the alloys of maximum magnetic properties exist along the line joining the $Cu_3Al$ and $Mn_3Al$ compounds. In their examination of the Al–Mn system, they found that the compound $Mn_3Al$ dissociated below 1040° C. They also found, contrary to Hendricks's results, that the compound $Al_3Mn$ did not exist, but that the characteristic needle structure found in the system was due to a compound $Al_4Mn$.

* Communicated by Prof. W. L. Bragg, M.A., F.R.S.

† *Compt. Rend.* cxxxiv. p. 236 (1902).

‡ *Z. anorg. Chem.* lix. p. 444 (1908).

§ *Z. anorg. Chem.*, p. 163 (1927).

The equilibrium relations in aluminium-manganese alloys of high purity have been investigated by E. J. Dix and W. D. Keith * with a view to examining the eutectic which occurs at the Al end of the diagram. These investigators followed the generally accepted view that the light grey constituent which formed a eutectic with Al was the compound $MnAl_3$. The solid solubility of Mn in Al was found by them to be very small.

The constitution of the Mn–Al alloys within the range of compositions 0–40 per cent. Mn has recently been studied thermally and microscopically by E. Rassow †, while the present research was in progress. The existence of a miscibility gap in the liquid state, as found by Hendricks was not confirmed. The constituent which exists in the Al rich alloys was found to be the compound $Al_7Mn$ and not $Al_3Mn$ as formerly supposed. According to these investigators the compound $Al_7Mn$ is formed at 870° C. by a peritectic reaction between the melt (containing 13 per cent. Mn) and a solid solution in the compound $Al_3Mn$ (40·4 per cent. Mn). The compound $Al_3Mn$ was found to melt at about 1000° C., whereas the compound $Al_7Mn$ was found to undergo a polymorphic transformation at a temperature of 670° C.

From the brief survey given above it is apparent that there is much uncertainty concerning the equilibrium diagram of the Al–Mn system. No two investigators have succeeded in obtaining results which are absolutely in agreement, and the most recent researches of Rassow, on the Al rich alloys of the Al–Mn system, are almost in entire disagreement with the earlier work of Hendricks.

In view of the lack of concordant results it was decided to re-examine the system. This is justified by the rapid development in recent years of the technique involved in the preparation and examination of alloys. In the present research the alloys were prepared under a low pressure of hydrogen and examined by an X-ray method. There was thus no contamination of material, and no appreciable furnace loss ; so that the final alloy was not far removed in composition from that which it was intended to be. Moreover, by the employment of induction heating, the alloy was thoroughly stirred up during preparation. In view of these several improvements a new investigation of this system seemed justified, in spite of the fact that only moderately pure Mn was available. The best of the samples available

* Trans. A.I.M.E. p. 315 (1927).

† Hauszeit, V. A. W. u. d. Erftwerk, A. G., Al. p. 187 (1927).

gave the following analyses: 0·71 per cent. Si, 0·36 per cent. Fe, 0·95 per cent. Al, and 0·04 per cent. C. Al–Mn alloys made up of this specimen will contain impurities ranging from a low value at the Al end to approximately 1 per cent. at the Mn end. The results of the present investigation should give a fair representation of the nature of the Al rich alloys. On the other hand, the most that can be claimed for the Mn rich alloys is that they will probably provide a rough indication of the nature of the changes at the Mn end of the diagram.

## Experimental.

The alloys were melted in a high-frequency coreless induction furnace made by Metropolitan-Vickers. The required quantities of Al and Mn were loosely packed into a fire-clay crucible lined with an alumina mixture. By this means the interaction between the fire-clay crucible and the Mn was eliminated. The Al, being lighter than Mn, was placed at the bottom of the crucible to facilitate the mixing of the two metals, and the resulting alloy was inverted in the crucible and remelted in order to ensure a perfectly homogeneous product. The alloys were kept in the molten state for as short a time as possible in order to reduce to a minimum any possibility of the distillation of Mn and to prevent the formation of blow-holes. The alloys thus prepared in the induction furnace, in an atmosphere of hydrogen, were found to be very satisfactory. On analysis the composition of the alloys was found to agree remarkably well with the quantities of metal weighed out originally.

## Heat-Treatment.

The alloys were annealed in the lump form at temperatures from 502–600° C. for some considerable time, and finally ground up to powder for the X-ray analysis. The powder was annealed *in vacuo* for 5 or 6 hours.

Rosenhain's method was used for quenching, water being admitted to the evacuated furnace at the required temperature. This was only satisfactory when the alloy was in powder form. An alloy quenched in the solid form only was found to give very ambiguous results when subjected to X-ray powder analysis. There was apparently a change of structure due to the cold working of the alloy in powdering; but after the second quench in powder form consistent results were obtained.

The powdered material was passed through a sieve of very small mesh, and the resulting fine-grained material was subjected to X-ray analysis. Iron radiation was employed from a Shearer Gas Tube, and powder photographs were taken in a Phragmèn* type of Precision Camera which operates over the range of glancing angles between $\theta = 45°$ and $\theta = 80°$. A series of these photographs is shown in Pl. XXIII.

Table I.

Heat-treatment of Alloys.

| Alloy. | Per cent. Mn. | Annealing temperatures. | | | |
|---|---|---|---|---|---|
| | | Lump form. | | Powder form. | |
| | | Time. | Temp. | Time. | Temp. |
| Al ..... | 0 | | | 2 hrs. | 550° C. |
| 2 ..... | 7 | 3 days. | 490° C. | $2\frac{1}{2}$ ,, | 530 ,, |
| 3 ..... | 19 | $4\frac{1}{2}$ ,, | 500 ,, | 6 ,, | 520 ,, |
| 4 ..... | 21 | 4 ,, | 600 ,, | $4\frac{1}{2}$ ,, | 570 ,, |
| 5 ..... | 21·9 | 4 ,, | 590 ,, | 5 ,, | 590 ,, |
| 6 ..... | 29·6 | 3 ,, | 560 ,, | $4\frac{1}{2}$ ,, | 570 ,, |
| 7 & 7 B ..... | 39 | 7 ,, | 565 ,, | 5 ,, | 550 ,, |
| 8 ..... | 44 | $4\frac{1}{2}$ ,, | 500 ,, | $4\frac{1}{2}$ ,, | 510 ,, |
| 9 ..... | 50·5 | 2 ,, | 585 ,, | 8 ,, | 550 ,, |
| 10 ..... | 59·2 | $2\frac{1}{2}$ ,, | 570 ,, | 5 ,, | 570 ,, |
| 11 ..... | 65·5 | 3 ,, | 600 ,, | 5 ,, | 570 ,, |
| 12 ..... ..... | 83·2 | 1 ,, | 550 ,, | 3 ,, | 550 ,, |
| 13 ..... | 98 | 3 ,, | 530 ,, | | 530 ,, |

Results of the X-Ray Analysis.

*Phases* 1 ($Al$), *and* 2 ($Al_7Mn$) *and their eutectic.*

The first photograph is that of pure Al. No filter is used in conjunction with the iron radiation which is employed, so that the $\beta$ lines appear on the film in addition to the $\alpha$ doublets. Since Al is known to be based on a simple face-centred cubic lattice, each of the lines is easily identified. The positions of the lines on the film were measured and the value of $\sin^2\theta$ obtained from the calibration curve of the camera. The value obtained from the above data for the lattice constant of Al was 4·040 Å., as compared with 4·042 Å. obtained by Westgren and Bradley.

* A. Westgren, Trans. Amer. Inst. Min. and Met. Eng., Feb. 1931. The camera was kindly supplied by Dr. G. Phragmèn.

Photograph 2 (Pl. XXIII.) is of an alloy containing about 7 per cent. Mn heat treated at a temperature of about 500° C.

Photograph 2 shows that with the addition of Mn, the pattern typical of the Al face-centred cubic lattice still persists, the lines remaining in exactly the same position on the film and the relative intensities remaining the same. The film was measured and the lattice constant of the face-centred cubic lattice was again found to be 4·040 Å., which value agrees with that obtained for Al. This shows that on adding Mn to Al the Mn atoms do not replace the Al atoms on the face-centred cubic lattice to any appreciable extent. The atomic volume of Mn is smaller than that of Al, and if Mn dissolved in Al the lattice constant would be diminished. Other faint lines appear on photograph 2 which signify the existence of another structure. This represents the appearance of a new phase with quite different properties from those of Al. Alloy No. 2 is a mixture of pure Al and the second phase.

Photographs 3 and 4 (Pl. XXIII.) represent alloys made up to correspond to compositions of 19 and 21 per cent. Mn respectively, and were annealed at temperatures of 520° and 570° respectively. It was not necessary to analyse alloys 2, 3, and 4 because they are in a two-phase region. All the other alloys in the series were, however, subjected to analyses.

With increasing Mn content the lines characteristic of the second lattice increase in intensity at the expense of the Al lattice. The positions of the lines on the film, however, remain unchanged. This clearly means that alloys 2, 3, and 4 are mixtures of Al and phase 2, the proportion of the latter phase increasing with increasing Mn content.

With still further increase of Mn content the Al lines disappear and photograph 5 corresponds almost entirely to the second phase. Alloy 5, which contains 21·9 per cent. Mn, is, therefore, very close to the constituent which has been represented by the new lattice in the previous photographs. Alloys 2, 3, and 4 are, therefore, mixtures of alloy 5 and Al.

It has already been pointed out that thermal and microscopical evidence indicate the existence of a eutectic in the Al rich alloys of the Al–Mn system.

From the point of view of X-rays a eutectic, or primary crystals in a eutectic, simply consists of a mixture of two different constituents. On the X-ray evidence it is impossible to distinguish between a eutectic and any other mixture of two different phases, since the essential characteristic of the

eutectic is that the two constituents have the same melting-point. This influences the mode of distribution of the constituents, and hence the microscopical structure, but not the atomic structure revealed by X-rays. The X-ray results, in showing alloys 2, 3, and 4 to be mixtures of alloys 1 and 5, do not prove this to be a eutectic range, but the results are such as could be explained by the existence of a eutectic, confirming the results of previous investigations.

E. H. Dix and W. D. Keith * have examined the Al end of the Al–Mn diagram with the idea of determining the composition of the eutectic. One of its constituents was found to be a solid solution of Mn in Al. According to these investigators Mn dissolved in Al to the extent of 0·65 per cent. at the eutectic temperature. This value dropped rapidly to less than 0·23 per cent. at 550° C. and then decreased to less than 0·14 per cent. at 220° C. The light grey constituent forming the eutectic with Al (or Al solid solution) was assumed to be the compound $Al_3Mn$, following the findings of all previous investigators. This constituent was referred to as $Al_3Mn$ throughout their communication.

According to the present investigation the first constituent of the eutectic was identified with Al from the agreement of their lattice constants. Such a small amount of Mn as was found by Dix and Keith to be dissolved in Al (viz. 0·21 per cent. at 550° C.) would, however, be imperceptible. It is possible, therefore, that the Al constituent of the eutectic contains in solid solution the very small amount of Mn determined by Dix and Keith.

The other constituent of the eutectic cannot possibly be the compound $Al_3Mn$ of composition 40 per cent. Mn, 60 per cent. Al. An alloy of this composition has been examined, and its pattern is entirely different from that of the second constituent of the eutectic. (Compare photographs 5 and 7 (Pl. XXIII.).) The present work proves the constituent to have a composition 21·9 per cent. Mn. Alloy 5, which represents this composition, has a matt bright fracture which shows a fibrous effect.

In Table I. a list of the heat-treatments of the alloys is given corresponding to the photographs taken, from which it may be seen that the temperatures of the heat-treatments of these alloys varied between 500° and 600° C. In this connexion it should be remarked that however slowly the alloys (1 to 5) were cooled from these temperatures, they always gave the same photographic results. Photographs 1 to 5 (Pl. XXIII.) can, therefore, in all probability be taken

* Trans. Amer. Journ. of Mining & Met. Engineers, p. 315 (1927).

as representing the stable state of equilibrium of these alloys from room temperature up to 500–600° C.

On pursuing the study of the system still further, photograph 6 (Pl. XXIII.) of an alloy containing 29·6 per cent. Mn annealed at 570° C. shows the existence of phase 2, together with some extra lines. It is interesting to note that the lines characteristic of phase 2 occupy the same position on the film for this alloy as for the other alloys in which the phase has appeared. This is shown in Table II., where the observed values of $\sin^2\theta$ for phase 2 are tabulated for alloys 2, 4, and 6. Many more lines were measured for alloy 4, where phase 2 is very prominent, but for the purpose of comparison the only ones tabulated are those which correspond

TABLE II.

Values of $\sin^2\theta$ for phase 2.

| 7 per cent. Mn. | | 21 per cent. Mn. | | 29·6 per cent. Mn. | |
|---|---|---|---|---|---|
| Int. | $\sin^2\theta$. | Int. | $\sin^2\theta$. | Int. | $\sin^2\theta$. |
| vw | ·541 | vs | ·541 | w | ·541 |
| vw | ·548 | vs | ·548 | w | ·549 |
| vw | ·595 | s | ·595 | s | ·595 |
| vvw | ·604 | m | ·603 | w | ·603 |
| vw | ·614 | s | ·613 | s | ·613 |
| abs. | — | s | ·625 | w | ·624 |
| vw | ·751 | s | ·751 | w | ·752 |
| vw | ·754 | s | ·755 | w | ·754 |
| vw | ·811 | s | ·811 | w | ·811 |
| vvw | ·813 | m | ·814 | vw | ·813 |

to the lines which could be measured for the alloys on the other side.

The agreement between the values for $\sin^2\theta$ for phase 2, whether found associated with phase 1, as in alloys 2 and 4, or with phase 3, as in alloy 6, proves that phase 2 is unique in having a characteristic structure which dissolves neither of the constituents on either side, and so has an extremely narrow range of composition. Phase 2 may, therefore, be regarded as an intermetallic compound, the composition of which must be very close to that of alloy 5. Alloy 5, containing 21 per cent. Mn, is approximately represented by a chemical formula $Al_7Mn$. The light grey constituent of the eutectic is, therefore, identified with the compound $Al_7Mn$ and is definitely not the compound $Al_3Mn$.

While this work was near completion the results of a thermal and microscopical study of the Al rich alloys of the Al–Mn system were published by Rassow *. It is interesting to note that Rassow finds that the grey constituent of the eutectic is not the compound $Al_3Mn$. Instead he establishes it as the compound $Al_7Mn$, in agreement with the results of the present investigation.

### *Phase* 3.—$Al_3Mn$.

The next alloy in this series was made up to correspond to the formula $Al_3Mn$. This alloy, like the others, was prepared under an atmosphere of hydrogen in an induction furnace. In the interior of the resulting product was a cavity in which were revealed some very beautiful needle-shaped crystals embedded in a light grey constituent. The cavity was formed, presumably, by the expulsion of dissolved gases, and the nature of the temperature change was apparently of such a kind as to produce very favourable conditions for the free development of crystals from the saturated melt.

A preliminary attempt was made to obtain a rotation photograph of one of these crystals. For this purpose the crystal was set with its long natural axis vertical and was bathed in a beam of iron radiation, the crystal being rotated throughout the exposure. The length of the axis parallel to which the crystal was rotated was then determined from a measurement of the distance between the layer lines on the rotation photograph.

From a rough measurement of the photograph obtained, the value of "$c$," the spacing of the axis of rotation was calculated to be 12·3 Å.

Further investigations by J. D. Bernal have shown that the crystal is pseudo-tetragonal and probably extremely complicated.

In order to see how this alloy fitted in with the rest of the system it was necessary to take a powder photograph as for the other alloys. Unfortunately it requires a fair amount of material for a precision photograph, and as the crystals needed analysing, the supply of single crystals was limited. There was, however, an abundant supply of the grey material in which the needle-shaped crystals were embedded. If it could be proved that the grey material was similar in structure to the single crystals, the former consisting of an

* *Loc. cit.*

aggregate of small crystals of the same structure as the latter, then the problem of obtaining sufficient material would be solved. It was possible to test this point by means of a circular camera which, fortunately, needs very little powder. For this purpose some of the single crystals were crushed into a powder, and without re-annealing a photograph was taken in the circular camera. Iron radiation was used as before. The result obtained is represented in photograph 7 *a* (Pl. XXIV.). The grey material associated with the crystals was annealed for a week at 550° C. and a photograph of the annealed powder was taken in the circular camera. The pattern obtained is shown in photograph 7 *b* (Pl. XXIV.) The two photographs 7 *a* and 7 *b* are extremely similar but not identical. This may be due to the fact that the single crystals were not annealed after being powdered. The slight differences in the photographs may, therefore, arise solely from the fact that the structure corresponding to alloy 7 is easily subject to distortion.

A precision photograph of the grey material is shown in photograph 7 (Pl. XXIII.). An outstanding feature of this photograph is the diffusenesses of the lines. On comparison with the previous photograph it is apparent that this pattern indicates the presence of an entirely new phase which occurs alone in alloy 7, and as a mixture with phase 2 in alloy 6. Reference to the complete powder photograph in Pl. XXIV. confirms this. This will be referred to as phase 3. The structure of phase 3 is apparently capable of some modification. This is borne out by the difference between the two Debye photographs.

Alloy 7 was found to contain 39 per cent. Mn. This composition corresponds approximately to the formula $Al_3Mn$, so that the characteristic needle-shaped crystals found in the Al–Mn alloys are in all probability represented by this formula.

Hendricks * found a compound $Al_3Mn$ in the Al–Mn system, but W. Krings and W. Ostmann failed to find such a compound. They attributed the characteristic needle-shaped crystals to a compound $Al_4Mn$. A compound having the formula $Al_4Mn$ would correspond to a composition of 30 per cent. Mn. The alloy containing 29·6 per cent. Mn is, however, shown from photograph 6 to be in a two-phase region (see Pls. XXIII. & XXIV.). There is no indication, therefore, of the existence of a compound $Al_4Mn$. The results of the present research agree with Hendricks in

* *Loc cit.*

attributing the needle-shaped crystals to an alloy whose composition may be represented by a formula $Al_3Mn$.

*Phase* 4.

At a composition of 50·5 per cent. Mn another new structure occurs, and as photograph 9 shows, phase 3 has now completely disappeared. The phase corresponding to this structure will be referred to as phase 4. Alloy 10, with a composition of 59·2 per cent. Mn, again shows the same characteristic lines as alloy 9, the pattern being displaced to the right on the film. Phase 4, therefore, exists over a range of compositions. The alloys in this range have a very bright fracture, are silvery in appearance, and are characterized by the ease with which they tarnish. Photographs 9 and 10 (Pl. XXIII.) correspond to annealing temperatures of about 570° C. and are the same whether the alloys are cooled quickly or slowly to room temperature. There is, therefore, apparently no phase change in this temperature range. When quenched from a temperature of 860° C. the alloys again give precisely the same photographs. Phase 4 is, therefore, the stable form up to a temperature of at least 860° C. The structure of this phase is again very complicated, as shown by the powder photographs. It is clear from the displacement of the lines on the film and the range over which the phase exists that the atoms are able to displace each other to a large extent on the space lattice underlying the structure. From this it may be deduced that phase 4 is a solid solution. A complete powder photograph of this alloy is shown in Pl. XXIV. (9).

Alloy 8, containing 44 per cent. Mn, gives a very diffuse precision photograph which it is difficult to interpret. It seems possible, however, to identify some of the lines on the precision photograph with the pattern characteristic of phase 4 (photograph 9, Pl. XXIII.). The lines in 8 are very slightly displaced compared with those in photograph 9 (Pl. XXIII.), showing that phase 4 contains more Al in alloy 8 than in alloy 9.

Other lines on photograph 8 appear to belong to phase 3, thus indicating alloy 8 to be a mixture of two phases, and this is fully borne out by the complete powder photograph (see Pl. XXIV. (8)).

Photograph 11 (Pl. XXIII.) is of the annealed alloy 11 containing 34·4 per cent. Al, and represents a mixture of two patterns. Lines characteristic of phase 4 are easily identified in this photograph and are found to be still further displaced

to the right relative to the same set of lines appearing in previous photographs. This means that the lattice corresponding to the previous alloy (alloy 10) now holds more Mn in solution. Alloy 10, therefore, falls well within the range of homogeneity of phase 4. The boundary occurs at a composition corresponding to the lattice constant of the phase found as a mixture in alloy 11.

Alloy 11 was also quenched from a temperature of 900° C. and gave photograph 11 Q (Pl. XXV.). This shows that phase 4 is still stable at a temperature of 900° C. The lines are, however, displaced to the left relative to those found for the alloy at a temperature of 570° C. This means that the lattice characteristic of this phase is not able to hold as much Mn in solid solution at the high temperature as at the low. In other words, the line marking the Mn end of the phase 4 boundary on the equilibrium diagram is not vertical but is inclined to the Al end at high temperatures.

### *βMn—dissolving Al.*

The photographs of the next two alloys in the series, alloys 12 and 13, represent another structure which is like βMn. The lines in both photographs are displaced with respect to those in pure Mn. These alloys, therefore, must be solid solutions of Al in the β lattice of Mn. Their lattice constants differ from each other and from that of pure βMn, due to the replacement of some of the Mn atoms in the parent lattice by the slightly bigger Al atoms. The increase in the size of the lattice with increasing Al content is made apparent in the photographs by the displacement of the lines to the left. The measurements for alloy 13 are given in Table III., from which the side of the unit cell was found to be 6·31 Å., as compared with 6·29 Å. obtained by Westgren and Phragmèn for pure βMn. A similar set of measurements was obtained for alloy 12, from which a value of 6·37 Å was obtained for the lattice constant.

Returning to photograph 11 (Pl. XXIII.) the extra lines found in addition to those characteristic of phase 4 are easily identified with those of the β structure. Alloy 11 is, therefore, a mixture of phase 4 and the β phase. In alloy 11 the displacement of the β lines is carried to its limit, the corresponding lattice constant being determined as 6·41 Å. From this data, used in conjunction with Végard's law, it was possible to determine approximately the composition corresponding to the end of the β range. According to Végard's law, which was assumed to be true for the small

range of the $\beta$ alloys, the side of the unit cell is linearly proportional to the composition of the alloy. Having determined the lattice constants for alloys 12 and 13, the composition corresponding to the extreme lattice constant of 6·41 Å. was found, by extrapolation from Végard's law, to be approximately 25 per cent. Al. This composition should correspond to the boundary of the $\beta$ phase.

TABLE III.

Measurements for Alloy 13 ($\beta$ phase).

| $\Sigma h^2$. | Int. | Obs. $\sin^2\theta$. | $\sin^2\theta/\Sigma h^2$. $a_1$. | $a_2$. |
|---|---|---|---|---|
| 25..... | vw | ·5870 | ·02348 | |
| | vvw | ·5900 | | ·02360 |
| 26..... | vs | ·6100 | ·02346 | |
| | m | ·6130 | | ·02358 |
| 27..... | m | ·6340 | ·02348 | |
| | m | ·6360 | | ·02356 |
| 29..... | vs | ·6790 | ·02341 | |
| | m | ·6825 | | ·02354 |
| 30..... | m | ·7020 | ·02340 | |
| | m | ·7050 | | ·02350 |
| 34..... | m | ·7960 | ·02341 | |
| | m | ·7985 | | ·02349 |
| 35..... | s | ·8200 | ·02343 | |
| | m | ·8235 | | ·02353 |
| 36..... | s | ·8445 | ·02346 | |
| | m | ·8480 | | ·02355 |
| 37..... | m | ·8670 | ·02343 | |
| | m | ·8700 | | ·02351 |
| 38..... | m | ·8910 | ·02345 | |
| | w | ·8940 | | ·02353 |
| 40..... | vw | ·9390 | ·02347 | |
| | vvw | ·9420 | | ·02355 |
| 41..... | s | ·9620 | ·02346 | |
| | ms | ·9650 | | ·02354 |
| | Mean ..... | | $\sin^2\theta/\Sigma h^2$=·02344 | ·02354 |
| | | | $\sqrt{\sin^2\theta/\Sigma h^2}$=·1532 | ·1534 |
| | $\alpha_1$=1·9323 | | | |
| Fe | | | $a$=6·310 | 6·311 |
| | $\alpha_2$=1·9365 | | | |
| | | $a$=6·31 Å | | |

Photographs 11, 12, and 13 (Pl. XXIII.) correspond to a heat-treatment of the alloys at a temperature of about 570° C. However slowly the alloys were cooled from these temperatures they always gave the same photographs. On annealing the alloys at a lower temperature, 360° C. or thereabouts, for a fortnight they still gave the same results. Photographs 11, 12, and 13 can therefore be taken as represent

the stable state of the alloys at room temperature. Alloy 12, which is typical of the range over which the $\beta$ phase exists at room temperature, is silvery in appearance, and has a bright, hard, irregular surface of fracture.

For pure Mn the $\beta$ structure is a high temperature modification only existing above the transformation temperature of 742° C. Below this temperature $\alpha$Mn is the stable form *. The presence of Al in these alloys has lowered the $\alpha\beta$ transformation point, so that the $\beta$ modification is stable at room temperature.

Pure $\beta$Mn is only stable up to a temperature of 1191° C., above that temperature $\gamma$Mn is the stable form. Quenching experiments were performed in order to ascertain whether this temperature was lowered by the presence of large amounts of Al. Photograph 11 Q (Pl. XXV.) of the alloy, quenched from 1000° C., shows that the $\beta$ phase has now completely disappeared, and that in addition to phase 4, which was present in the annealed alloy, there is another new structure. This phase has not been investigated in detail. Alloy 12, quenched from 900° C., shows no trace of this phase and has only the pure $\beta$Mn structure.

The Mn used was not pure enough to give any reliable data regarding the confines of the $\beta$ phase in the Mn rich area, but the results indicate that there is probably quite a wide area where the $\alpha$ and $\beta$ phases co-exist

Photographs 14 (*a*), (*b*), and (*c*) in Pl. XXV. represent a sample of Mn which has been quenched from various temperatures. Sample 14 is of the same order of purity as alloy 13 and gives the following analyses :—0·71 per cent. Si, 0·36 per cent. Fe, 0·95 per cent. Al, and 0·04 per cent. C. The Al content is just a trifle less than that of specimen 13, which may account for the photograph being somewhat different.

Photograph 15 (Pl. XXV.) contains only the lines of a pure $\alpha$Mn structure. The specimen which photograph 14 (*a*) represents was annealed at a temperature of 550° C. and quenched. The same pattern was also obtained when the specimen was annealed at a much lower temperatnre and cooled very slowly. Specimen 14, therefore, consists of a mixture of the $\alpha$ and $\beta$ phases in equilibrium up to a temperature of 550° C. When quenched from 700° C. the $\alpha$ phase disappears completely and the $\beta$ phase only remains, as shown in photograph 14 (*c*) (Pl. XXV.). At 660° C., represented in photograph 14 (*b*) (Pl. XXV.), the specimen

Dr. Marie Gayler, Journ. Iron & Steel Inst. p. 1 (1927), Personn and Öhman, 'Nature' (Aug. 31, 1929).

consists of a mixture of the $\alpha$ and $\beta$ phases, the quantity of $\alpha$ phase being extremely small. On further examining photographs 14 (*a*), (*b*), and (*c*), the $\beta$ lines are observed to be displaced very slightly to the right with increase of temperature. This means that at the high temperature the $\beta$ lattice contains more Mn in solution than at the lower temperature. This suggests a slope of the boundary line towards the Mn end of the diagram at higher temperatures. This is what would be expected to happen from a knowledge of the transformation points for pure Mn. The inference from these photographic results is best shown diagrammatically as in fig. 1.

Fig. 1.

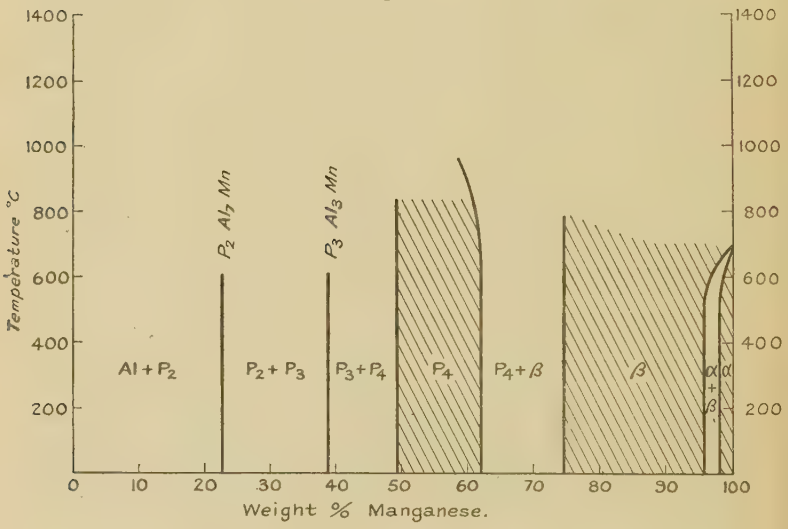


Aluminium—Manganese.

## *$Mn_3Al$.*

It has already been pointed out that previous investigators have found the existence of a compound $Mn_3Al$ in the Al–Mn system of alloys. This is the compound so often quoted in connexion with the Heusler alloys. Alloy 12 in the present series of alloys is not far removed from the composition corresponding to the formula $Mn_3Al$, but this alloy at room temperature falls within a solid solution range based on the $\beta$ structure. A compound $Mn_3Al$ cannot, therefore, possibly exist at room temperature. Moreover, alloy 12, quenched from 900° C., still exhibits the $\beta$ structure, thus showing that

the compound MnAl, if it exists at all, is not stable below a temperature of 1000° C.

W. Krings and W. Ostmann maintain that the compound $Mn_3Al$ dissociates below 1049° C. Whether the compound $Mn_3Al$ exists above a temperature of 1049° C. has not been tested in the present investigation.

## Summary.

An attempt has been made to obtain a general survey of the Al–Mn system of alloys with the aid of the X-ray powder method of investigation.

The impurity of the alloys is small at the Al end but increases up to about 1 per cent. at the Mn end. The results for the Al rich alloys should, therefore, be reliable enough, but the Mn rich alloys can only serve as an indication of the nature of the changes.

1. X-ray investigations show the existence of seven different phases which are summarized in the form of a preliminary equilibrium diagram shown in fig. 1.

2. In this diagram $P_2$ is an intermetallic compound $Al_7Mn$. It exists in equilibrium with Al on the one hand, and with $P_3$ on the other, up to a temperature of at least 600° C.

3. $P_3$ in all probability is represented by the formula $Al_3Mn$. The phase occurs in the form of needle-shaped crystals which are pseudotetragonal.

4. The compound $Al_4Mn$ does not exist at a temperature of 570° C.

5. Phase 4 is a solid solution existing over a range represented roughly in the diagram, extending beyond 50 per cent. Mn on the one hand and beyond 59 per cent. on the other. Phase 4 is stable up to a temperature of at least 860° C. on the Al rich side and up to 1000° C. on the Mn side. The boundary at the Mn end of the range is curved towards the Al end at a temperature of 1000° C. as deduced from the displacement of the lattice pattern.

6. A phase based on the $\beta$ form of Mn exists over a wide range of compositions.

7. The compound $Mn_3Al$ does not occur up to a temperature of 1000° C.

8. The addition of Al to Mn lowers the $\alpha\beta$ transformation point to such an extent that the $\beta$ modification becomes stable at room temperature.

9. A two-phase range of the $\alpha$ and $\beta$ phases is indicated at room temperature for a low Al content. The lines in this

part of the diagram are merely tentative, the compositions corresponding to the boundary lines being somewhat arbitrary.

The authors wish to thank Professor W. L. Bragg, F.R.S., for his kind interest in the work, which was carried out in the Physical Laboratories of the University of Manchester. Mr. Cuthbertson has kindly analysed the alloys. One of us (P. H. J.) is indebted to the University of Wales for a Fellowship, and one (A. J. B.) to Mr. A. P. M. Fleming, C.B.E., Director of Research, Messrs. Metropolitan-Vickers, for enabling the work to proceed.

Manchester University,
Sept. 20, 1931.

---

CIX. *Note on Heat-flow through a Granulated Material.* *By* J. H. Awbery, *B.A., B.Sc., F.Inst.P., Physics Department, National Physical Laboratory, Teddington, Middlesex* *.

IN this note the granulated material contemplated consists of an aggregate of exactly similar particles, packed in such a manner that every one bears the same relation to its neighbours as any other. Thus they might be equal spheres, ellipsoids, tetrahedra, or more irregular figures, provided only that they all occupy similar positions in the material.

It follows that if the aggregated material is placed between two parallel plates—a hot plate and a cold plate—we shall be able to distinguish layers of the material running parallel to the surfaces of the plates. Since the geometrical composition of all the layers is identical and the same heat-flow takes place across each, the temperature difference across a layer is independent of the position of the layer.

Consider now any single body from the aggregate, and for simplicity assume that it only touches two neighbours, one in the next upper and one in the next lower layer. The contact may be of finite area, if it is proportional to the size of the body.

* Communicated by Dr. G. W. C. Kaye, O.B.E.

Let $h$ be the heat-flow through this body, $\theta$ the temperature difference between the two points of contact, and $a$ a typical linear dimension which determines its size. Then, if we take a series of such single bodies, all geometrically similar, and having the points of contact at corresponding positions, we may apply the principle of similitude.

The heat-flow per second ($h$) has dimensions $ML^2T^{-3}$ in mass, length, and time, and depends only on $\theta$, $a$, and $k$. These have dimensions $\theta$, L, and $MLT^{-3}\theta^{-1}$ respectively. Thus $h/\theta ak$ is dimensionless, and must be equal to a constant $\lambda$. In other words,

$$h=\lambda\theta ak. \quad . \quad . \quad . \quad . \quad . \quad . \quad . \quad (1)$$

This equation is interesting in itself. It is evident from first principles that the heat-flow is proportional to the temperature difference and to the conductivity, but it is not so obvious that for a fixed temperature difference the flow is proportional to the size. It implies, for example, that if a number of spheres of different sizes but of the same material were studied, keeping opposite ends of a diameter at temperatures of 0° C. and 100° C., then the heat-flow would be greater for the larger spheres; the explanation is evidently that the greater mean area of the large sphere more than compensates for the increased distance apart of the "electrodes" with its reduction of the temperature gradient. The rationale of the process is clearly seen if we take the case of a slab, where the area increases as the square of the linear dimensions, whilst the temperature gradient only falls off as the first power. Thus the heat-flow increases (as in the general equation (1)), proportionately to the linear dimensions.

When the body considered touches more than one neighbour in the contiguous layers we associate the points of contact in pairs; the heat-flow due to each pair is, by the above argument, proportional to $ak$, and thus the total flux is also proportional to $ak$. We are now in a position to study the conduction through the granulated material. Considering a block of area S and thickness $b$, filled with the material, let a temperature difference $\theta_1$ be applied. If there are $m$ layers the temperature difference across each is $\theta_1/m$, and (from equation (1))

the heat conducted per second through a layer is $\lambda \cdot \frac{\theta_1}{m} akp$, where $p$ is the number of bodies in a layer.

Thus the heat conducted per second per unit area is $\lambda\theta_1 akp/m\mathrm{S}$, and the effective thermal conductivity $k_1$ is this quantity divided by the whole temperature gradient $\theta_1/b$, *i. e.*,

$$k_1 \text{ is } \lambda abkp/m\mathrm{S}.$$

Now magnify the linear dimensions of the whole system $n$-fold, but retain $\theta_1$ as the temperature difference across the faces. We now have a block of area $n^2\mathrm{S}$ and thickness $nb$, containing $m$ layers, with $p$ bodies in each layer. The heat conducted per second across a layer is $\lambda \cdot \frac{\theta_1}{m} \cdot na \cdot kp$, and the heat conducted per second per unit area is $\lambda\theta_1 akp/mn\mathrm{S}$, giving an effective thermal conductivity $k_1 = \lambda pabk/m\mathrm{S}$. This is the same conductivity as before. Thus we reach the conclusion that the effective thermal conductivity through a medium of the type mentioned in the opening paragraph is independent of the size of the individual particles.

So far we have considered the medium to be entirely composed of the bodies under consideration, the intervening spaces playing no part in the conduction. But it is clear that in many cases (*e. g.*, if spheres are packed in open or "cubical" piling) the conditions imposed on the first set of bodies will at the same time cause the spaces between them to assume geometrical forms such that any space is related to its neighbouring spaces in exactly the same way as any other. Thus the spaces might be filled with a conducting medium, the original bodies being insulators, and the same theorem would apply. The conduction through this second medium would be independent of the size of the bodies forming the first medium, and hence, proceeding one step further and allowing both materials to conduct, the conduction through a mixture of materials would be independent of the size of the particles of either component. This conclusion, however, is much less generally true than the first conclusion, where only one medium is effective; it would break down, for example, if there is appreciable heat interchange between the bodies of the two media.

An interesting example of the general result may be found in a calculation by C. H. Lees (Phil. Mag. lix. p. 221, 1900). He investigated in detail the flow of heat across a material made in chess-board fashion, so that the black and white squares have different conductivities, and the heat flows in the plane of the board. His result for the effective conductivity is independent of the actual size of the squares. As another example, it is obvious that with this "chessboard" medium the heat-flow per unit area perpendicular to the board would be independent of the actual size of the squares.

---

CX. *An Investigation into some of the Properties of Porous Building Materials.*—Part I. *The Absolute Porosity and Saturation Coefficient. By* E. Madgwick, *M.C., M.Sc., Ph.D., Professor of Physics, Raffles College, Singapore*.*

*Introduction.*

THE present investigation, although it has a close application to various practical building problems and may also be of service in expressing the qualities of porous bodies generally, was undertaken primarily to elucidate certain properties of building stone which are believed to be of importance from the weathering standpoint.

The weathering problem briefly is to predict in terms of its chemical and physical properties, the ability of a stone to resist prolonged exposure to atmospheric conditions, to determine how its powers of endurance may be enhanced, and to devise the means of preserving ancient buildings and monuments which are in process of decay. Because of the wide variation both in the constitution and structure of different stones and also of the conditions under which they may be exposed, the problem is one of unusual complexity, and in spite of the notable advances which have been made by such experimenters as Hirschwald [1], Kreüger [2], Laurie [3], and Russell [4], the subject must be regarded as yet in its preliminary stages. It is generally conceded, however, that of the multiplicity of possible contributory causes of stone decay some of the most potent are those which depend for their action upon the presence of absorbed water.

When water freezes within the pores of a stone considerable stresses may be set up in consequence of the volumetric

* Communicated by Sir F. E. Smith, K.B.E., Sec.R.S.

expansion which it undergoes. But when the water is absorbed under natural conditions not all the pore spaces are occupied, and it may be that the unfilled spaces are able, by virtue of their size and distribution, to accommodate the increased volume without stress. The extent to which such unfilled spaces exist in a stone is denoted by a saturation coefficient. This has been defined rather differently by different experimenters. Hirschwald, for example, regards it as the ratio of the quantity of water absorbed by a specimen under conditions which he describes as "slow immersion"—(the specimen is placed in a trough into which water is passed at such a rate as to cover it after four hours; it is then allowed to stand until it attains a constant weight)—to that which is absorbed *in vacuo* followed by a pressure of 120 atmospheres; Kreüger as the ratio of the volume of water absorbed per cubic centimetre during a four days immersion to the porosity (or pore space per cubic centimetre) as determined by measuring the true specific gravity of the material after powdering, and the apparent specific gravity of the material in bulk. Various freezing tests have been devised which, although differing in details, are similar in principle. Rectangular blocks are wetted and subjected to a number of cycles of freezing and thawing from all sides; they are then examined for loss of weight and strength. Hirschwald has found that practically all stones may be broken by freezing after saturation at high pressures, and that when the saturation takes place at normal pressures disintegration is generally the more likely to take place the higher the saturation coefficient. Kreüger has concluded that materials with a saturation coefficient greater than 0·85 are destroyed by freezing, while those with a saturation coefficient less than 0·8 are generally able to withstand the action of frost. The results of such tests, however, are relative only, since in practice freezing proceeds from one face of the material. Even so, it is agreed that the saturation coefficient of a stone is not an absolute criterion of its frost resisting qualities, and that the nature of the pore spaces exerts a considerable influence. A detailed study of the pore spaces within a stone at any stage of its decay has been rendered possible by the work of Russell, who has developed a technique for impregnating the stone with a synthetic resin in the liquid form, converting it there to the solid form, and cutting thin sections which can be subjected to microscopic examination.

Various chemical actions take place due to the presence in the atmosphere of such impurities as carbon dioxide and

sulphur compounds, which enter the stone in solution in absorbed water. Rain water exercises a solvent action on limestones, and attacks the calcareous binding material of sandstones. Laurie has adduced considerable evidence in support of the view that a serious factor in chemical weathering is the recrystallization within the stone of such salts as calcium sulphate, a circumstance conducive to flaking. His conclusions have been borne out by the work of Russell. Lucas [5] has shown that disintegration may result from the recrystallization at or near the surface of the stone of salts which are carried into the stone by ground water.

Stresses may be set up due to thermal or moisture expansion. The latter is likely to be the more serious, since whereas high temperature gradients are uncommon, the transition between complete saturation and almost complete dryness often occurs across a very short distance.

An examination of the water absorbing qualities of stone is therefore essential to a study of the general problem. A great deal of experimental work has already been carried out by Hirschwald, Kreüger, Laurie, Douty and Beeby [6], Kersler [7], and Wig and Bates [8], who have determined, by weighing, the amounts of water absorbed by rectangular specimens of various sizes under such diverse conditions as slow immersion, quick immersion, immersion under reduced pressure, immersion under high pressure, sprinkling, and immersion in boiling water.

The first efforts at stone preservation were directed to the obvious course of sealing up the surface pores and so preventing the absorption of water. This method is now widely discredited, on what appears to the writer to be inadequate evidence. Long range and large scale tests have been carried out with coatings of various kinds and many failures have been encountered ; but these tests have not been backed by the preliminary work necessary to demonstrate whether the stone has in fact been adequately rendered waterproof.

The present work is concerned with an examination of the principal properties of such porous bodies as stone, and the reduction of the experimental determination of the attendant constants to a simple form suitable for routine testing. It will be described in the order in which these tests are carried out.

*The absolute porosity and saturation coefficient.*

When one face of a slab of porous material is maintained in contact with water, the water penetrates with a uniformity depending on the homogeneity of the material, which to a

certain depth is "saturated." The conditions are then at once well defined and representative of the extreme practical case. The amount of water absorbed by each cubic centimetre of material saturated in this way will be termed the absorption porosity, or simply the *porosity*; the total pore space per cubic centimetre of material the *absolute porosity*;

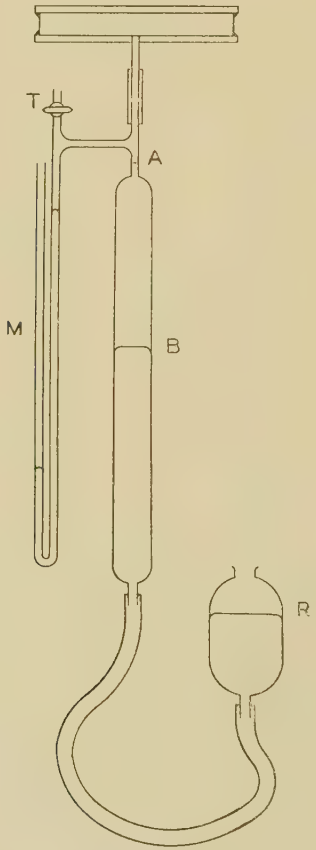


and the ratio of the absorption porosity to the absolute porosity the *saturation coefficient*. The amount of water which is absorbed by the specimen is measured in the course of the absorption experiments to be described later. The total pore volume is estimated by determining the volume of air which is withdrawn from the specimen in consequence of a measured reduction in pressure.

The specimen consists of a slab of the material, generally cylindrical in form, and from one-half to two inches in thickness. After having been thoroughly dried out it is clamped between two brass caps, each of which is fitted with a rubber disk to take up any slight irregularities of the surface, and the sides are rendered air-tight with a thin coating of Faraday wax. A central hole passes through one cap and rubber disk, so that air can be withdrawn from the specimen by reducing the pressure. The general arrangement is shown in the figure. M is a capillary manometer, and AB a vertical glass tube which is carefully calibrated from the mark A. In carrying out an experiment the tap T is opened and the level of the reservoir R is adjusted until the mercury in the tube AB is at A. The tap T is then closed and R is lowered until the mercury in AB falls to a suitable level B. This is read on a scale and the volume $v$ between A and B is determined from the calibration curve. The manometric height $h$ is also noted. The noted pore volume of the specimen is then

$$V=\left(\frac{H}{h}-1\right)\left(v-\frac{\alpha h}{2}\right)-v_0, \quad . \quad . \quad . \quad . \quad (1)$$

where H = barometic height in cm. of mercury,

$v_0$ = volume of air in manometer and connexions,

$\alpha$ = area of cross-section of manometer tube.

It is advisable to make $\alpha$ and $v_0$ small. In the present apparatus they have the values 0·06 sq. cm. and 4·0 c.c. respectively. A number of readings corresponding to different pressures are taken in the same way.

The results of a typical experiment are set out below :

Specimen ..... Whitbed.
Volume of specimen ... 533 c.c.
Barometric height ..... 74·90 cm.

| $v$ c.c. | $h$ cm. | V c.c. |
|---|---|---|
| 61·9 | 24·2 | 124·2 |
| 57·0 | 22·8 | 124·7 |
| 40·3 | 17·7 | 124·6 |
| 31·0 | 14·3 | 125·4 |
| 28·9 | 13·6 | 124·0 |
| 13·3 | 6·9 | 124·0 |
| 5·5 | 3·0 | 125·7 |
| | Mean ..... | 124·7 |

Absolute porosity ..... 124·7/533 = ·234

From the water absorption test on the same specimen the total amount absorbed was found to be 86·5 c.c. Hence

Porosity ..... 86·5/533 = ·162

and Saturation coefficient.. ·162/·234 = ·694

It is to be noted that the determination of the saturation coefficient does not involve the measurement of the volume of the specimen. For the purpose of calculating the porosities in these experiments this has been obtained by direct measurement of the mean thickness with a screw gauge and the mean diameter with a travelling microscope. It can be determined alternatively by the displacement of mercury.

Other results are as follows :—

| Material. | Porosity. | Absolute porosity. | Saturation coefficient. |
|---|---|---|---|
| Box Ground ..... | ·174 | ·255 | ·682 |
| Bath ..... | ·262 | ·314 | ·835 |
| Monks Park ..... | ·219 | ·307 | ·713 |

*References.*

(1) *Handbuch der bautechnischen Gesteinsprüfung*, Berlin, 1912.
(2) Trans. Acad. Eng. Sci. No. 24, 1923, Stockholm.
(3) Journ. Soc. Chem. Ind. Feb. 27th, 1925.
(4) Report of the Stone Preservation Committee. H.M. Stationery Office, 1927.
(5) "Disintegration and Preservation of Building Stones in Egypt." Ministry of Finance, Egypt Survey Dept. 1915.
(6) Proc. Amer. Soc. Testing Materials (1912).
(7) Tech. Paper of the Bureau of Standards, No. 133 (1919).
(8) Tech. Paper of the Bureau of Standards, No. 3 (1912).

## CXI. *Some Properties of Porous Building Materials.*—Part II. *The Flow of Air through Porous Bodies.* By E. Madgwick, *M.C., M.Sc., Ph.D.**

*Introduction.*

It has been pointed out that certain impurities which are carried in solution by rain water may act chemically on some constituents of stone after absorption, and that the

* Communicated by Sir F. E. Smith, K.B.E., Sec.R.S.

soluble products of the chemical changes may be dissolved by the water and deposited at or near the surface when evaporation takes place. The gaseous impurities of the atmosphere may also enter the pores of stone under the action of wind pressure, and the principal object of the present section is to obtain data which will lead to an estimation of the magnitude of this effect. The results are also of use in deciding to what extent air may flow through the porous walls of a building—a matter of interest in connexion with heating and ventilating.

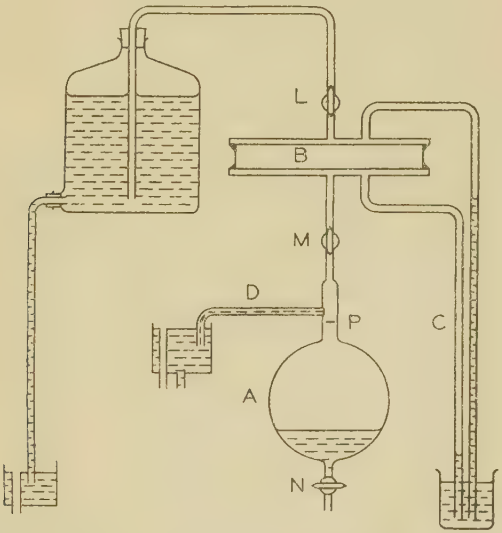


The pressure P, due to a wind of velocity V, has been expressed by the empirical formula $P = kV^2$, where $k$ is constant. The value of $k$ when V is expressed in miles per hour, and P in pounds per square foot is given by Stanton [1] as 0·0032. A hundred miles an hour gale thus gives rise to a pressure equal to that exerted by about 6 ins. or 15 cm. of water, and this may be taken as the upper limit of the pressures with which we are concerned.

*Experimental Method.*—The specimen which has been used in the absolute porosity test is transferred to a fresh pair of holders, which are the same as are employed for the water absorption test to be described later. In the figure it is shown in position at B. The pressure on the upper side is reduced

by means of an aspirator, and air enters the specimen from the bulb A. The side tube D has a flexible connexion and dips into a constant level reservoir from which water flows into A as the air is withdrawn. The pressures at the faces of the specimen are measured with the manometer C.

In carrying out an experiment the tube D is raised and the taps L, M, and N are opened. When the manometer readings are steady, N is closed and D is lowered into the reservoir. The time is then measured for the bulb to be filled up to the mark P, the volume up to this mark being known. To prevent water reaching the specimen the taps L and M are closed, or the tube D is raised, at the conclusion of each test. A set of four bulbs ranging in volume from 100 c.c. to 1 litre is used. By adjusting the pressure across the specimen and selecting the most suitable bulb a test is arranged to be of a few minutes duration.

*The Law of Flow.*—Consider a slab of material of thickness $l$, on one side of which the gas is maintained at a pressure $p_1$, on the other at a pressure $p_2$, $p_1$ being greater than $p_2$. Then there will be a steady flow through the material from the side of higher to that of lower pressure. At a depth $x$ let the pressure be $p$ and the volume of gas flowing per second across each square centimetre at right angles to the direction of flow be $q$. Then we have the condition that $pq$ is constant and equal to $p_1q_1$, where $q_1$ is the volume entering each square centimetre of the material per second. Thus $q=\frac{p_1q_1}{p}$. Suppose the resistance to flow to be proportional to the average velocity, which is proportional to $q$. (The assumption is here implied that the distances across the pores are not small compared with the mean free path of the gas molecules, *i. e.*, that streaming does not occur and that the resistance to flow is independent of the pressure. The distances in question are in fact of the same order as the mean free path, but so far as the experiments have shown, no correction on that account appears to be necessary.) Then, considering unit area of an element of the material of thickness $dx$, we may write for the resistance $k\,q\,dx$, or $k\frac{p_1q_1}{p}dx$, where $k$ is constant. Also the force across this element $\mathrm{B}\,dp$, where $dp$ is the pressure difference between the faces, and B is the absolute porosity. Hence for steady flow

$$k\frac{p_1q_1}{p}dx=\mathrm{B}\,dp,$$

and integrating over the thickness of the material we obtain

$$q_1 = \frac{B}{k} \cdot \frac{p_1^2 - p_2^2}{2lp_1}$$

$$= P \cdot \frac{p_1^2 - p_2^2}{2lp_1}, \quad \ldots \ldots \quad (2)$$

writing $\frac{B}{k} = P$: or, if $Q_1$ is the volume entering an area A per second,

$$Q_1 = A \cdot P \cdot \frac{p_1^2 - p_2^2}{2lp_1}. \quad \ldots \ldots \quad (3)$$

When $p_1 - p_2$ is small compared with $p_1$ and $p_2$, equation (3) simplifies to

$$Q_1 = A \cdot P \cdot \frac{p_1 - p_2}{l}. \quad \ldots \ldots \quad (4)$$

P is the *permeability* to the gas, and may be defined as the rate of flow through each square centimetre of material of one centimetre thickness under the action of unit pressure difference, provided the unit of pressure is small compared with the actual pressure. By analogy with the corresponding case of the steady flow of heat or electricity it may be termed the conductivity, and $\frac{1}{P} = \sigma$ the *resistivity*. Equations (3) and (4) may thus be written

$$Q_1 = A \cdot \frac{p_1^2 - p_2^2}{2\sigma lp} \quad \ldots \ldots \quad (5)$$

and

$$Q_1 = A \cdot \frac{p_1 - p_2}{\sigma l} \quad \ldots \ldots \quad (6)$$

respectively.

The approximation involved in equation (6) is valid when $\frac{p_1 - p_2}{2p_1}$ is small compared with unity. In considering wind pressure we have seen that the maximum value of $p_1 - p_2$ is 15 cm. of water; also, $p_1$ is of the same order as the atmospheric pressure, or rather more than 1000 cm. of water. In this case, therefore, equation (6) is sufficiently accurate. In the experiments values of $p_1 - p_2$ up to 200 cm. of water are employed and $\sigma$ is calculated from equation (5), which has been shown to hold within the limits of experimental error. The following are the results of a typical experiment to test equation (5), which may be written:

$$\sigma = \frac{At}{lV}(p_1 - p_2)\left(1 - \frac{p_1 - p_2}{2p_1}\right),$$

where V is the volume of the bulb and $t$ the time in seconds for it to be filled. The readings are divided into groups, each group containing between ten and fifteen readings corresponding to values of $p_1-p_2$ which are nearly the same. Each figure represents the average for the group, and in addition the extreme values of $\sigma$ are given. In the third column are shown the values of the factor which differentiates the exact from the simplified equation.

TABLE I.

Specimen ..... Whitbed.

V=587 c.c., $l$=2·54 cm., A=139 sq. cm.

| $p_1-p_2$. | | $1-\frac{p_1-p_2}{2p_1}$. | $t$ secs. | $\sigma$ C.G.S. units $\times 10^6$ (extreme values and averages). |
|---|---|---|---|---|
| Dynes cm.$^2\times 10^3$. | cm. of water. | | | |
| 141·5 | 144·2 | 0·925 | 92·5 | $\left\{\begin{matrix}1·112\\1·138\end{matrix}\right\}$ 1·125 |
| 99·8 | 101·8 | 0·950 | 127·0 | $\left\{\begin{matrix}1·112\\1·137\end{matrix}\right\}$ 1·123 |
| 66·2 | 67·5 | 0·967 | 189·6 | $\left\{\begin{matrix}1·116\\1·140\end{matrix}\right\}$ 1·132 |
| 41·6 | 42·4 | 0·979 | 296·7 | $\left\{\begin{matrix}1·118\\1·139\end{matrix}\right\}$ 1·129 |
| 5·37 | 5·48 | 0·997 | 2255 | $\left\{\begin{matrix}1·110\\1·143\end{matrix}\right\}$ 1·129 |
| | | | | Mean..... 1·128 |

Table II. gives some values of the resistivity and permeability which have been determined in this way for a number of materials. Each material shows considerable variations, and the figures represent the average of a number of tests on different specimens.

*The Flow through Compound Bodies.*—The flow through slabs consisting of uniform layers of different materials will now be considered. Let

$l_1, l_2 \ldots\ldots l_n$ be the thicknesses of the layers.

$\sigma_1, \sigma_2 \ldots\ldots \sigma_n$ their resistivities.

$p_1, p_2 \ldots\ldots p_{n+1}$ the pressures at the successive faces.

$q_1, q_2 \ldots\ldots q_{n+1}$ the values of $q$ at these faces.

Then from equation (5)

$$q_1=\frac{p_1^2-p_2^2}{2p_1\sigma_1 l_1}, \qquad q_2=\frac{p_2^2-p_3^2}{2p_2\sigma_2 l_2}, \text{ etc.,}$$

and hence, remembering that

$$p_1q_1=p_2q_2=\ldots\ldots=p_{n+1}q_{n+1},$$
$$p_1^2-p_2^2=2p_1q_1\sigma_1 l_1,$$
$$p_2^2-p_3^2=2p_2q_2\sigma_2 l_2=2p_1q_1\sigma_2 l_2,$$
$$\ldots\ldots\ldots\ldots\ldots$$
$$p_n^2-p_{n+1}^2=2p_nq_n\sigma_n l_n=2p_1q_1\sigma_n l_n.$$

TABLE II.

| | | *Resistivity* C.G.S. units $\times 10^6$. | *Permeability* C.G.S. units $\times 10^{-6}$. |
|---|---|---|---|
| Limestones. | Portland Basebed | 7·76 | 0·129 |
| | Portland Roach | 2·90 | 0·345 |
| | Anston | 0·28 | 3·57 |
| | Ham Hill | 2·80 | 0·357 |
| | Bathstone | 13·3 | 0·075 |
| Sandstone .. | Darley Dale | 2·26 | 0·442 |
| | Longridge | 10·5 | 0·095 |
| Bricks | Fletton | 0·019 | 52·6 |
| | Wire Cut | 0·65 | 1·54 |
| | Sand faced | 0·61 | 16·4 |
| | Sand and lime | 0·023 | 43·5 |
| Plasters | Gypsum plaster | 4·51 | 0·222 |
| | Gypsum and sand | 1·23 | 0·813 |
| | Gypsum and pit sand | 0·78 | 1·28 |
| | Lime putty and pit | 2·79 | 0·358 |
| | Sand and 10 % plaster | | |

Adding

$$p_1^2-p_{n+1}^2=2p_1q_1(\sigma_1 l_1+\sigma_2 l_2+\ldots+\sigma_n l_n),$$

whence

$$q_1=\frac{p_1^2-p_{n+1}^2}{3p_1\Sigma\sigma l},$$

or

$$Q_1=A\cdot\frac{p_1^2-p_{n+1}^2}{2p_1\Sigma\sigma l}. \qquad \ldots\ldots\ldots \quad (7)$$

For small values of $p_1-p_{n+1}$ this equation simplifies, in the same way as equation (4), to

$$Q_1=A\frac{p_1-p_{n+1}}{\Sigma\sigma l}. \qquad \ldots\ldots\ldots \quad (8)$$

Equation (7) has been verified by finding the resistance $\frac{\sigma l}{A}$ separately for a number of specimens by means of equation (5), and of $\frac{\Sigma\sigma l}{A}$ for pairs of the specimens connected in series. The total resistance as calculated in this way was found to agree excellently with the sum of the resistances which were determined separately. This will be seen from the following results :—

TABLE III.

| Specimen. | Resistance $\frac{\sigma l}{A}$. C.G.S. units $\times 10^5$. | |
|---|---|---|
| 1″ Bathstone (B) | 2·53 | |
| 1″ Portland Roach (PR 1) | 0·475 | |
| 3″ Portland Roach (PR 2) | 1·27 | |
| Specimens in Series. | Total resistance $\frac{\Sigma\sigma l}{A}$. C.G.S. units $\times 10^5$. | |
| | Calculated. | Measured. |
| B+PR 2 | 3·80 | 3·76 |
| PR 1+PR 2 | 1·745 | 1·735 |
| B+PR 1 | 3·00 | 3·02 |

*The Resistance of a Thin Coating.*—Protective coatings such as paints and distempers often offer a very considerable resistance to the passage of gases. This resistance is measured as follows :—A plain specimen of, *e. g.*, plaster is tested in the usual way. Then by equation (5) its resistance per unit area is

$$\sigma l = \frac{A(p_1^2 - p_2^2)}{2Q_1 p_1}.$$

The coating is then applied and the test is repeated under a pressure difference $p_3 - p_4$, say. Then if $l_1$ is the thickness

of the coating and $\sigma_1$ its resistivity, its resistance per square centimetre is $\sigma_1 l_1$. By equation (7)

$$Q_2 = \frac{A(p_3^2 - p_4^2)}{2p_3(\sigma l + \sigma_1 l_1)},$$

whence

$$\sigma_1 l_1 = \frac{A(p_3^2 - p_4^2)}{2p_3 Q_2} - \sigma l. \quad . \quad . \quad . \quad . \quad (9)$$

The following values of $\sigma_1 l_1$ have been obtained for specimens of the coatings mentioned. In each case they were applied to gypsum plaster.

TABLE IV.

| Coating. | $\sigma_1 l_1$. C.G.S. units $\times 10^6$. |
|---|---|
| Priming coat | 33·5 |
| Priming coat and undercoat | 73·0 |
| Priming coat, undercoat, and paint | impermeable. |
| Priming coat, undercoat, and enamel | impermeable. |
| Size and distemper | 21·5 |
| Size and paper | 35·5 |
| Size, paper, and distemper | 48·0 |

*The Flow of Air through Walls.*—The rate of flow of air under the action of wind pressure can be calculated from equation (8). Consider, for example, a 9-inch brick wall with 1 inch of plaster sized, papered, and distempered. Then we have for the resistance $\sigma l$ of 1 square centimetre :

of the brick (taking $\sigma = 0{\cdot}2 \times 10^6$), $4{\cdot}6 \times 10^6$ C.G.S. units :
of the plaster (taking $\sigma = 4 \times 10^6$), $10{\cdot}2$ „ „
and of the size, paper, and distemper, $48{\cdot}0 \times 10^6$ „
a total of $62{\cdot}8 \times 10^6$ C.G.S. units.

Adopting the maximum permissible value of $15 \times 980$ dynes per square centimetre for $p_1 - p_{n+1}$, the rate of flow is found to be 0·0084 cubic metre per square metre per hour. Considering only the resistance of the brick, the rate is 0·115 cubic metre per square metre per hour. These are small when compared with the other factors which influence air interchanges.

*Application to the weathering problem.*—The amounts of gaseons impurities which are driven into the wall of a buiiding under the action of wind pressure may be computed on the above considerations from a knowledge of the structure of the wall together with certain meteorological data. As an illustration we shall consider at what rate sulphur dioxide will enter a stone wall 30 cm. thick, due to a wind of velocity 100 miles per hour, incident normally. The amount of sulphur dioxide present in the atmosphere varies from time to time and from place to place, but Hacknel's[(2)] value of 0·00112 per cent. by volume may be taken as representative. Using the values $\sigma = 10^6$ for Whitbed and $\sigma = 13 \times 10^6$ for Bath stone, it is found with the aid of equation (6) that under these conditions the rate at which sulphur dioxide enters each sq. cm. of the wall is

for Whitbed $4{\cdot}7 \times 10^{-4}$ c.c. per day,

and for Bath $0{\cdot}3 \times 10^{-4}$ c.c. per day.

The Advisory Committee on Atmospheric Pollution have obtained data regarding the amount of sulphuric acid present in rain water. This corresponds to an amount of sulphuric acid of the order of 0·03 gram per litre, or about 0·01 c.c. per c.c. of water. Thus in this particular case more sulphuric acid enters the stone in the course of the absorption of an amount of rain water equal to 1 c.c. per sq. cm. of surface than is carried into it by a 100 miles an hour gale lasting 20 days in the case of Whitbed and 300 days in the case of Bath stone.

*References.*

(1) Proc. Inst. C. E. clxxi.
(2) *Zeits. F. anorg. Chem.* xxxv. p. 618 (1922).

CXII. *The Colour of the Light from High-Frequency Discharges in Helium.* *By* J. S. Townsend, *M.A., Wykeham Professor of Physics, Oxford, and* S. P. McCallum, *M A., University Demonstrator and Fellow of New College, Oxford* *.

1. In the course of various investigations of the electrical properties of helium we have had occasion to examine the radiation from high-frequency discharges in wide tubes containing gases at various pressures. Large variations

* Communicated by the Authors.

were observed in the colour of the discharges in helium, depending on the pressure of the gas, the difference of potential between the electrodes, the shape and size of the electrodes, and the distance between the electrodes.

Some changes of colour are due to bands which appear in the spectrum of the discharge in addition to the line spectrum of helium (ordinary helium lines). In the parts of the tube where the bands may be seen with a small direct-vision spectroscope the discharge has a purple colour which is easily distinguished from the colour due to the ordinary helium lines. The principal bands were in the positions determined by Curtis *.

Other changes of colour are obtained when there are no bands in the spectrum of the gas due to changes in the relative intensities of the lines. These changes are similar to those which have been observed in direct-current discharges or in the discharges obtained with induction coils. The principal change due to this cause is the change from the yellow or pink colour (generally obtained in the uniform glow when the electrodes are far apart) to a bright green colour. The bright green discharge may be obtained throughout the space between the electrodes when the pressure is low. Also at some pressures glows of different colours may be obtained in the same discharge, the glow being of a uniform yellow or pink colour in the space where the electric force is small, and bright green in the spaces near the electrodes where the force is high.

2. The conditions under which the purple glow is obtained with bright bands in the spectrum, and the colour-changes due to intensities in the ordinary spectral lines, may be explained by describing the effects observed in three quartz tubes, 4 cm. in diameter and 30 cm. long, containing helium at the pressures ·62, 3, and 12·5 mm. The band spectrum is obtained at the two higher pressures, and is very bright when the high-frequency potential is applied by narrow electrodes close to the tube.

In the experiments described in the following sections, 3, 4, 5, and 6, a few turns of insulated wire wound round the tube were used as external electrodes, and the wave-length of the oscillations was 140 metres.

3. The purple glow becomes very bright and widely distributed in the discharges through helium at 3 mm. pressure as the potential difference between the electrodes is increased. The distribution and the colour of the glows

* W. E. Curtis, Proc. Roy. Soc. lxxxix. p. 146 (1913).

in the tube with the gas at 3 mm. pressure and with electrodes 6 cm. apart are shown by figs. 1–3. The distribution changes with the potential between the loops of wires $W_1$ and $W_2$, which were used as external electrodes. When the potential is small there is a faint uniform yellow glow, as shown by the shading of the tube in fig. 1. The minimum potential required to maintain the discharge was 77 volts *.

Fig. 1.

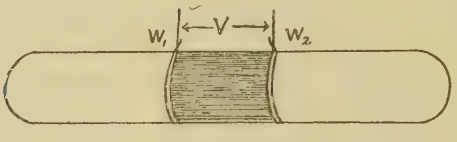


Helium 3 mm. pressure.
Electrodes 6 cm. apart.
Potential V=77 to 260.

Tho yellow glow increases in intensity without any marked change in the distribution of the light as the potential is increased from 77 to 260 volts. At this point the yellow glow becomes separated by two dark spaces from the glows near the electrodes.

The distribution of the light with potentials from 300 to 600 volts is shown in fig. 2. The glows in the spaces near the electrodes (shaded in the figure with vertical lines) are purple in colour and bands are seen in the spectrum of the

Fig. 2.

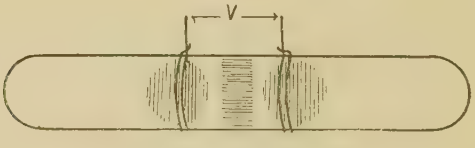


Helium 3 mm. pressure.
Electrodes 6 cm. apart.
Potential V=300 to 600.

light; the glow midway between the electrodes (shaded with horizontal lines) is yellow, and there are no bands in the spectrum. The glows are separated by two dark spaces, the yellow glow being about 2 cm. wide when the potential is 600 volts.

* The values of the potentials which are given are the root mean square values.

The space filled with the yellow glow diminishes and the spaces filled with the purple glow increase as the potential is increased.

The yellow glow disappears when the potential is increased to 770 volts, and at this point there are two purple glows in the tube, with a dark space about 2 cm. wide between them. The distribution of the light obtained with potentials from 770 to 1100 is shown in fig. 3. The purple glows near the electrodes are very bright and the bands in the spectrum are nearly as bright as the lines. At the higher potentials faint yellow glows showing no trace of bands appear at the ends of the tube remote from the electrodes.

4. Similar changes are observed with the same tube (containing helium at 3 mm. pressure) when the distance between the electrodes is increased. There is an increase in the space filled with the yellow glow corresponding to the increase in the distance between the electrodes. With the

Fig. 3.

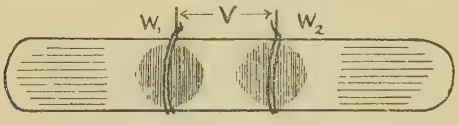


Helium 3 mm. pressure.
Electrodes 6 cm. apart.
Potential V=770 to 1100.

distance of 9 cm. the minimum potential required to maintain a faint uniform (yellow) glow was 105 volts ; the intensity of the glow increases with the potential between the electrodes, and with 300 volts the yellow glow is separated by two dark spaces from the glows near the electrodes, which are purple. With larger potentials the yellow glow contracts and purple glows extend over wide spaces near the electrodes. With a potential of 900 volts the yellow glow midway between the electrodes is about 3 cm. wide, and it is separated by two dark spaces about 1·5 cm. wide from the two purple glows.

5. When the distance between the electrodes is reduced there is a corresponding reduction in the space filled with the yellow glow. With the tube containing helium at 3 mm. pressure the minimum potential required to maintain a discharge was 60 volts, with the electrodes 2·5 cm. apart. The glow is yellow, and it increases in intensity as the potential is increased from 60 to 190 volts.

The space filled by the yellow glow diminishes and becomes separated by two dark spaces from the glows near the electrodes when the potential is increased above 190 volts. The yellow glow disappears when the potential is raised to 440 volts, and at this point there are two purple glows near the electrodes with a dark space between them. With further increases in the potentials the width of the dark space diminishes. When the potential is increased to 700 volts the dark space disappears and the purple glow extends throughout the whole space between the electrodes and projects beyond the electrodes towards the ends of the tube. With potentials from 700 to 1100 volts the glow is very bright, and the band spectrum is seen in all parts of the discharge.

In the experiments with the tube containing helium at 3 mm. pressure the yellow glows were uniform, and no striations were observed at the higher potentials.

6. With the tube containing helium at 12·5 mm. pressure a yellow glow is obtained in the space between the electrodes, which is uniform with small potentials but becomes striated as the potential is increased. There are also glows of different colour near the electrodes, but the yellow glow extends over a larger space and the glows near the electrodes over narrower spaces than the corresponding glows in the gas at lower pressures.

With loops of wire wound round the tube as electrodes the minimum potential required to maintain the discharge in the tube with helium at 12·5 mm. pressure was 208 volts when the electrodes were 6 cm. apart. With a potential of 250 volts there are four yellow striations in 5 cm. of the tube between the electrodes. The space filled with the yellow striations and the number of striations diminishes as the potential is increased. Thus with a potential of 350 volts there are three striations in the length of 4·2 cm., and with 1000 volts there are two striations in the length of 3 cm.

The length of the striated column and the number of striations increases with the distance between the electrodes. With the electrodes 9 cm. apart the minimum potential required to maintain a discharge is 264 volts, and the glow becomes striated with the potential of 290 volts. With the potential of 310 volts there are six striations in the length 7·5 cm.; with 400 volts there are five striations in the length 7 cm.; and with 1000 volts there are four striations in the length 6 cm.

The colour (yellow) and the relative intensities in the

lines of the spectrum of the striated column do not change with the distance between the electrodes or with the potential. It is possible to observe bands in the spectrum of the striated column, but they are very faint compared with the ordinary helium lines, and the effect of the bands on the colour of the discharge is not noticeable.

The intensity of the bands increases with the pressure, and at about 20 mm. pressure a continuous spectrum is obtained which makes it difficult to observe traces of impurities by a spectroscope. Experiments were therefore made with a large tube containing parallel plate electrodes, and the method described in a previous paper * was used to test the gas by measuring the sparking potential. It was thus found that at the higher pressures where several bands and continuous spectrum were obtained in a striated discharge at high pressures, there were no impurities in the gas.

Fig. 4.

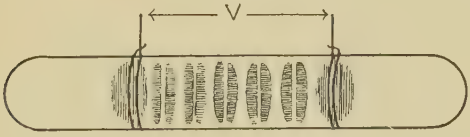


Helium 12·5 mm. pressure.
Electrodes 9 cm. apart.
Distance between striations 1·5 cm.
Potential V=400

7. The appearance of the striated column obtained in the tube containing helium at 12·5 mm. pressure with the electrodes $W_1$ and $W_2$ 9 cm. apart is shown in fig. 4. The yellow colour is represented by the shading. The distance between the centres of the striations was 1·5 cm. Each striation consists of two bright yellow disks separated by a narrow dark space.

The form of the yellow column depends on the pressure of the gas, the shape of the electrodes, the current, and the wave-length of the oscillations.

With electrodes in the shape of sleeves there were traces of striations in the yellow column when the wave-length was 140 metres and the currents large, but the column became uniform when the current or the wave-length was reduced.

* Phil. Mag. vi. p. 857 (Nov. 1928).

With the same tube (containing helium at 12·5 mm. pressure) and electrodes in the form of sleeves 6 cm. apart the yellow column, obtained with potentials from 180 to 270 volts was uniform when the wave-length of the oscillations was 100 metres. With the electrodes at the same distance apart the yellow column was uniform with potentials from 176 to 220 volts when the wave-length was 140 metres, but the column became striated (3 striations) when the potential was increased to 260 volts.

8. With the gas at 12·5 mm. pressure the glows near the electrodes are in rings, with a dark space in the centre about 2·5 to 3 cm. in diameter. With large currents the glow near the inner dark space is purple and the bands in the spectrum appear to be nearly as intense as the lines. The most intense bands are obtained with the electrodes $W_1$ and $W_2$ about 2·5 cm. apart. With this pressure the purple glow is very intense, but it is confined to a much smaller space than in the tube where the pressure is 3 mm.

9. When the pressure is reduced below a certain value the band spectrum tends to disappear.

With the tube containing helium at ·62 mm. pressure the purple glow was not obtained and there were no bands in the spectrum of the gas. The uniform glow in the middle of the tube is pink rather than yellow, and the glows near the electrodes are bright green, due to an increase in the intensity of the prominent green line in the spectrum.

When the electrodes are 6 cm. apart the minimum potential required to maintain a current is 75 volts. With small potentials the distribution of the light is uniform, as shown in fig. 1, but as the potential increases the pink glow diminishes and the green glows near the electrodes increase.

With a potential of 750 volts between the electrodes the distribution of the light is similar to that shown in fig. 2. At this point the pink glow in the centre of the tube is about 2·5 cm. wide and the green glow extends about 1·5 cm. on each side of the electrodes. A sudden change in the distribution occurs when the potential is increased to 850 volts. The pink glow disappears and the green glows extend about 2·5 cm. each side of the electrodes. Similar changes take place with any distance between the electrodes. When the distance is increased or diminished there is a corresponding change in the length of the pink column. With this tube ($p = ·62$) the minimum potential required to maintain a discharge was 65 volts when the electrodes were 2·5 cm. apart and 84 volts when the electrodes were 6 cm. apart.

The increase in the intensity of the green line is due to

the increase in the energy of agitation of the electrons. This may be deduced from Hanle's * experiments or from the experiments on the changes in the intensities of the lines in discharge tubes due to changes of pressure †.

Experiments were also made with direct-current discharges maintained by a battery of small accumulators in a tube 3 cm. in diameter. The band spectrum in the positive column was not sufficiently intense to affect the colour of the discharge, but in part of the negative glow, near the end of the positive column, the colour was purple, and bright bands were observed in the spectrum of that part of the discharge.

---

## CXIII. *The Theory of the Electrification of Aerosols.* *By* H. S. Patterson ‡.

WHEN an aerosol is dispersed in a closed chamber, the electrical character of the system formed depends chiefly upon the method used for its dispersal. Violent chemical reactions, arc discharges, etc. give rise to highly charged systems containing a large fraction of electrified particles which persists almost unchanged for a period of an hour or two, though the number of particles may have diminished to a comparatively small percentage of those originally present. Materials volatilized from a boat at relatively a low temperature on the other hand form systems which may be initially practically uncharged or only contain quite a small fraction of charged particles. With lapse of time, however, this fraction increases, and after a few hours the system may contain nearly as great a percentage of charged particles as an aerosol produced by the arc discharge.

Experimental results illustrating both types of system have already been described (Patterson, Whytlaw-Gray, and Cawood, Proc. Roy. Soc. A, cxxiv. p. 526 (1929)), but no quantitative explanation was advanced of the constancy or variation with time of the fraction of particles charged. In this communication the conditions likely to determine the electrical behaviour of aerosols are considered, and it will be seen that it is possible to deduce equations giving

* W. Hanle, *Zeit. f. Phys.* lvi. p. 94 (1929).
† J. S. Townsend and F. Ll. Jones, Phil. Mag. xii. (Oct. 1931).
‡ Communicated by the Author.

numerical results in satisfactory agreement with the experimental data.

If an aerosol is uncharged initially it can only become electrified by catching ions from the air. The increase in the number of electrified particles will depend therefore on the rate of production of ions. In the earlier stages these electrified particles will tend consequently to carry unit charges, since a large fraction of the particles will be uncharged, and so the greater number of ions will be caught by neutral particles. It is obvious, however, that later on, when the fraction of electrified particles has increased, multiple charges might be acquired in this way. If now we consider the effect of coagulation on such a charged aerosol, we see that though the actual number of electrified particles cannot be increased the fraction present may be altered considerably. Charges will only be neutralized by the collision of particles carrying equal charges of opposite sign, and in the initial stages such collisions will be rare compared with those occurring in the system as a whole. Coagulation will, therefore, at first tend to increase the fraction of particles charged, though at a later stage it might have the reverse effect. It appears therefore that in such a system both the number and fraction of particles charged should increase rapidly at first, but with lapse of time this rate of increase should gradually diminish.

With a highly charged aerosol, such as the smoke produced by burning magnesium ribbon, the conditions are entirely different. The particles are mostly electrified and many carry multiple charges. Under ordinary conditions therefore the electrification is little affected by the catching of ions. Coagulation, on the other hand, produces practically the same rate of decrease of charged particles as of the total particles. In this case the range of charge carried by the particles is long, so that the chance of equally and oppositely electrified particles meeting is small, and accordingly few neutral complexes will be formed.

The two systems just described are those most frequently met with and are extreme types. As yet no complete mathematical theory which will include both types and also the intermediate conditions has been devised. We will therefore consider each of these systems separately.

### (a) *Slightly Charged Aerosols.*

Suppose we consider an aerosol containing at any time $n$ particles per c.c., of which $n_e$ per c.c. are charged. We

will assume that each electrified particle carries a unit charge and that equal numbers of each sign are present. The rate of decrease of the total number with increase of time is $Kn^2$, where K is the coagulation constant for the smoke (Patterson, Whytlaw-Gray, and Cawood, Proc. Roy. Soc. A, cxxiv. p. 502 (1929)). The rate of decrease of charged particles with time is, on the other hand, $1{\cdot}5\,Kn_e^2$, since if two particles of the same sign coagulate there is a decrease of one in the number of charged particles, whilst if two of opposite sign coagulate there is a decrease of two. On the average then there is a decrease of 1·5, as compared with a decrease of 1 for the system as a whole. Suppose now that A is the rate of production of ions in the air per c.c. in which the aerosol is dispersed: all these ions will be caught by the particles of the aerosol, since the latter are very large and numerous compared with the ions (Patterson, Whytlaw-Gray, and Cawood, *loc. cit.* p. 516). The number caught by the neutral particles will clearly be $A\,\frac{n-n_e}{n}$, and this gives the rate of increase of charged particles, whilst the number caught by the electrified particles will be $A\,\frac{n_e}{n}$. Of these latter collisions one half will cause a neutralization of the electrified particles, so that the rate of decrease of electrified particles thus brought about will be $A\,\frac{n_e}{2n}$. We have therefore for the increase of electrified particles with time the equation

$$\frac{dn_e}{dt} = -1{\cdot}5\,Kn_e^2 + A\frac{n-n_e}{n} - A\frac{n_e}{2n}. \quad . \quad . \quad (1)$$

If we transform into particulate volumes instead of numbers, *i.e.*, we put $n=\frac{1}{\sigma}$ and $n_e=\frac{1}{\sigma_e}$, we obtain

$$\frac{d\sigma_e}{dt} = 1{\cdot}5\,K - A(\sigma_e - 1{\cdot}5\sigma)\sigma_e. \quad . \quad . \quad . \quad . \quad (2)$$

For the decrease of the particles as a whole we have

$$-\frac{dn}{dt} = Kn^2$$

or

$$\frac{d\sigma}{dt} = K. \quad . \quad . \quad . \quad . \quad . \quad . \quad . \quad . \quad . \quad . \quad (3)$$

Eliminating time between equations (2) and (3) we have

$$\frac{d\sigma_e}{d\sigma} = 1{\cdot}5 - \frac{A}{K}(\sigma_e - 1{\cdot}5\sigma)\sigma_e.$$

By substituting a new variable for $(\sigma_e - 1{\cdot}5\sigma)^{-1}$ we can transform this equation to a linear equation of the first order. On integration and simplification we obtain

$$\sigma_e = 1{\cdot}5\sigma + \left[\frac{e^{b^2(\sigma^2-\sigma_0^2)}}{\sigma_{e_0} - 1{\cdot}5\sigma_0} - \frac{b^2}{0{\cdot}75}\right.$$
$$\left. e^{b^2\sigma^2}\left(\int_0^{\sigma} e^{-b^2\sigma^2}d\sigma - \int_0^{\sigma_0} e^{-b^2\sigma^2}d\sigma\right)\right]^{-1}, \quad . \quad (4)$$

where $b^2 = \frac{1{\cdot}5\ A}{2\ K}$.

We may find the variation of $\sigma_e$ with time instead of with $\sigma$ by substituting $\sigma = \sigma_0 + Kt$, obtained by the integration of equation (3).

It must be borne in mind that equation (4) only holds good accurately so long as the number of particles carrying multiple charges is small compared with those carrying unit charges. In practice, however, the calculated figures agree quite well with those obtained experimentally when the aerosol contains up to 40 per cent. or 50 per cent. of charged particles.

We will now compare the results given by equation (4) with the experimental data for ammonium chloride (Patterson, Whytlaw-Gray, and Cawood, *loc. cit.* p. 526). As typical experiments we will take the 15 mg. smoke (*a*) and the 60 mg. smoke (*b*).

For the 15 mg. smoke the experimental value for the coagulation constant was $K = 3{\cdot}5 \cdot 10^{-8}$ cm.$^3$/min., and for the initial particulate volume $\sigma_0 = 1{\cdot}1 \cdot 10^{-6}$ cm.$^3$. A is taken to be $3{\cdot}5 \cdot 10^3$ per min., and the initial number of charged particles $n_{e_0}$ to be $2{\cdot}10^4$. In Table I. are given he smoothed experimental values for the fraction and number of the particles charged at various times, and the theoretical values calculated from the above data by means of equation (4).

For the 60 mg. smoke the experimental value of the coagulation constant was $K = 3{\cdot}1 \cdot 10^{-8}$ cm.$^3$/mim., whilst the initial number of particles was $\sigma_0 = 0{\cdot}5 \cdot 10^{-6}$ cm.$^3$. A in this case is taken to be $4{\cdot}5 \cdot 10^3$ per min. and the initial number of charged particles to be $5 \cdot 10^4$. The comparison of the experimental and theoretical data is given in Table II.

It will be seen that in both cases the agreement between theory and experiment is very satisfactory for 70 or 80

TABLE I.

Ammonium chloride, 15 mg. per cubic meter.

| Time from start, min. | Experimental. | | Calculated. | |
|---|---|---|---|---|
| | Fraction of particles charged. | Number per c.c. charged $\times 10^{-6}$. | Fraction of particles charged. | Number per c.c. charged $\times 10^{-6}$. |
| 0 | (0·02) | (0·02) | 0·02 | 0·02 |
| 10 | 0·08 | 0·06 | 0·08 | 0·06 |
| 20 | 0·15 | 0·08 | 0·14 | 0·08 |
| 30 | 0·22 | 0·10 | 0·20 | 0·10 |
| 40 | 0·28 | 0·11 | 0·29 | 0·12 |
| 50 | 0·35 | 0·12 | 0·36 | 0·13 |
| 60 | 0·41 | 0·13 | 0·42 | 0·13 |
| 70 | 0·47 | 0·13 | 0·47 | 0·14 |
| 80 | 0·52 | 0·13 | 0·52 | 0·13 |
| 90 | 0·57 | 0·13 | 0·55 | 0·13 |
| 100 | 0·62 | 0·13 | 0·58 | 0·13 |

TABLE II.

Ammonium chloride, 60 mg. per cubic meter.

| Time from start, min. | Experimental. | | Calculated. | |
|---|---|---|---|---|
| | Fraction of particles charged. | Number per c.c. charged $\times 10^{-6}$. | Fraction of particles charged. | Number per c.c. charged $\times 10^{-6}$. |
| 0 | (0·03) | (0·05) | 0·03 | 0·05 |
| 10 | 0·08 | 0·10 | 0·07 | 0·09 |
| 20 | 0·14 | 0·13 | 0·13 | 0·12 |
| 30 | 0·20 | 0·14 | 0·22 | 0·15 |
| 40 | 0·27 | 0·16 | 0·28 | 0·16 |
| 50 | 0·34 | 0·17 | 0·35 | 0·17 |
| 60 | 0·41 | 0·18 | 0·40 | 0·18 |
| 70 | 0·47 | 0·18 | 0·47 | 0·18 |
| 80 | 0·53 | 0·18 | 0·51 | 0·18 |
| 90 | 0·58 | 0·18 | 0·55 | 0·17 |
| 100 | 0·62 | 0·18 | 0·58 | 0·17 |

minutes. In the later stages, however, when multiply charged particles are present, the theory does not give accurate results, but, as would be anticipated, predicts too

small a number of charged particles. It appears to be necessary to assume that some charged particles are present initially. These are presumably due to thermionic emission from the heater during volatilization. It will be noticed that the value assumed for A is large, the rate of production of ions being of the order of 70 per second. At the time that the measurements were made a small quantity of free radioactive material was present in the laboratory, and measurements subsequently showed that, depending on conditions, the rate of production of ions might attain to 100 per second or more. The figure previously quoted (Patterson, Whytlaw-Gray, and Cawood, *loc. cit.* p. 532) was obtained in absence of the radioactive source. It will be seen that rather different values of A have been assumed in the two experiments, as this gave somewhat

Table III.

Stearic acid, 15 mg. per cubic meter.

| Time from start, min. | Fraction of particles charged. | Number per c.c. charged $\times 10^{-6}$. |
|---|---|---|
| $10\frac{1}{2}$ | 0·07 | 0·16 |
| 23 | 0·18 | 0·22 |
| $31\frac{1}{2}$ | 0·24 | 0·22 |
| $41\frac{1}{2}$ | 0·29 | 0·21 |
| $52\frac{1}{2}$ | 0·32 | 0·19 |
| $64\frac{1}{2}$ | 0·43 | 0·21 |

better agreement. If, however, an average value had been taken for the two cases, the agreement would still have been satisfactory.

A number of experiments have also been made on the electrification of blown smokes of stearic acid. The method used for their production has been described previously (Patterson, Whytlaw-Gray, and Cawood, *loc. cit.* p. 502). The results for a typical experiment are given in Table III.

The charged particles in this case consisted of approximately equal numbers of positives and negatives, though there was some slight tendency for the positives to be in excess. It will be seen that this aerosol is charged in quite a different way from those of ammonium chloride. Within the limits of error the number of charged particles appears to be practically constant throughout at about $2 \cdot 10^5$ per c.c. The low number at time $10\frac{1}{2}$ is not typical, and is probably due to experimental error, which is large in the early stages. It is obvious that the system contained initially a large

number of electrified particles. These were probably due to thermionic emission from the heater, which was at a considerably higher temperature than that used for the ammonium chloride aerosols.

We will now use equation (4) to calculate the fraction and number of charged particles present at various times for this smoke. The experimental value for the coagulation constant is $K = 8{\cdot}03 \cdot 10^{-8}$ cm.$^3$ per min. whilst the initial particulate volume is $0{\cdot}1 \cdot 10^{-6}$ cm$^3$. We will assume that $A = 2{\cdot}10^3$ per minute and that the initial number of charged particles $n_{e_0} = 2{\cdot}10^5$. The smoothed experimental data for the fraction and number of charged particles are given in Table IV. in comparison with the calculated figures.

TABLE IV.

Stearic acid, 15 mg. per cubic meter.

| Time from start, min. | Experimental. | | Calculated. | |
|---|---|---|---|---|
| | Fraction of particles charged. | Number per c.c. charged $\times 10^{-6}$. | Fraction of particles charged. | Number per c.c. charged $\times 10^{-6}$. |
| 0 | 0·02 | 0·20 | 0·02 | 0·20 |
| 10 | 0·08 | 0·20 | 0·08 | 0·20 |
| 20 | 0·15 | 0·20 | 0·15 | 0·20 |
| 30 | 0·21 | 0·20 | 0·21 | 0·20 |
| 40 | 0·27 | 0·20 | 0·26 | 0·19 |
| 50 | 0·33 | 0·20 | 0·31 | 0·19 |
| 60 | 0·39 | 0·20 | 0·35 | 0·18 |
| 70 | 0·46 | 0·20 | 0·40 | 0·17 |

As will be seen in this case also the agreement between theory and experiment is satisfactory, though, as before, the theory does not give accurate results in the later stages. There was no free radioactive material in the laboratory when the measurements were made, and the value of A was that determined in another chamber under similar conditions. The somewhat high rate of production of ions (30 per second) is almost certainly to be attributed to residual radioactive effects.

### (b) *Highly Charged Aerosols.*

With highly charged aerosols the range of charge carried by the particles is large. The chance of collision between two particles carrying equal and opposite charges is

consequently small, and so coagulation will give rise to few neutral particles. In this case therefore the rate of diminution of charged particles, $-\frac{dn_e}{dt}$, will tend towards the value $Kn_e^2$ instead of $1{\cdot}5\ Kn_e^2$ as for slightly charged aerosols. The few neutral particles formed will on the average rapidly become electrified again by collision with charged particles. It is obvious, however, that there must always be a proportion of neutral particles present and that this proportion will diminish the greater the range of charge carried by the particles.

An approximate solution of this case may be obtained in the following way. Since we may neglect the effect of the catching of ions in the electrification of the aerosol, equation (2) becomes to a first approximation

$$\frac{d\sigma_e}{dt}=K.$$

Eliminating time with equation (3), as before, we have

$$\frac{d\sigma_e}{d\sigma}=1,$$

or integrating,

$$\sigma_e=\sigma+C,$$

where C is a constant. This gives the approximate relationship between $\sigma$ and $\sigma_e$ for a highly charged aerosol.

The fraction of particles charged at any time is

$$\frac{\sigma}{\sigma_e}=1-\frac{C}{\sigma_e}.$$

For a highly charged aerosol $\sigma$ and $\sigma_e$ are nearly equal, and consequently C is small. Hence for variations of $\sigma$ and $\sigma_e$ which are not great the ratio $\frac{\sigma}{\sigma_e}$ is approximately constant.

The aerosol produced by burning magnesium ribbon is an example of this type of system, and the results previously given (Patterson, Whytlaw-Gray, and Cawood, *loc. cit.* p. 530) show that the percentage of charged particles remains constant within the limit of error of the experiments.

I wish to thank Mr. W. Cawood for his assistance with the experiment quoted on the electrification of stearic acid.

Chemistry Department,
The University, Leeds.
25th April, 1931.

CXIV. *The Elastic Ring. A Comparison of Strains Determined Experimentally with the Strains calculated from the Elastic Ring Theory.* *By* C. E. Larard, *M.Inst.C.E.* *

IN the 'Philosophical Magazine' for July last the author gave a mathematical investigation for the elastic ring and obtained expressions for the radial strains for a circular ring of uniform section when acted upon by any number, N, of equal and equiangular radial forces. He has since made an experimental investigation for a particular case to test the theoretical results, choosing for the purpose a ring loaded by two increasing compressive forces acting radially inwards at the extremities of a diameter. With increasing step-by-step loads, Q (fig. 1), the decrements in the vertical

Fig. 1.

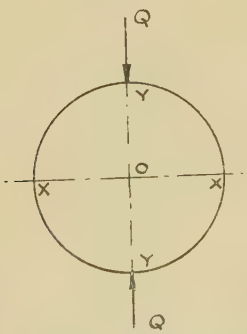


diameter YY and the increments in the horizontal diameter XX were measured. The results are given in columns Nos. 2 and 4 of the Table on p. 1188.

Experiments on such a ring, where $N=2$, furnish a very severe investigation, for an extreme case, of the validity of the theoretical results.

Consider first the case represented in fig. 2. The equations given † for the alteration in the lengths of the radii OY and OX for N equal forces P, and N equal forces Q are simplified by writing $N=2$, $\alpha=\frac{\pi}{2}$ and $P=0$. Remem-

* Communicated by the Author.

† Phil. Mag. xii. July 1931, Tables I. and II., p. 142.

bering also that the diametral strains for YY and XX are in each case twice the corresponding radial strains we obtain

$$\left.\begin{array}{l}\text{Decrement in vertical diameter YY}\end{array}\right\} = \frac{QR^3}{EI}\left(\frac{\pi}{4}-\frac{2}{\pi}\right)+\frac{\pi QR}{4EA}+\frac{C\pi RQ}{4GA}. \quad (1)$$

$$\left.\begin{array}{l}\text{Increment in horizontal diameter XX}\end{array}\right\} = \frac{QR^3}{EI}\left(\frac{2}{\pi}-\frac{1}{2}\right)-\frac{QR}{2EA}+\frac{CRP}{2GA}. \quad (2)$$

*Manufacture of the Ring.*—The ring was first machined to the near size out of suitable mild steel plate, and test specimens were also taken from the plate for the determination of Young's Modulus of elasticity. The ring and specimens were then annealed at a suitable temperature and allowed to cool slowly, after which they were machined and ground to the required dimensions.

Fig. 2.

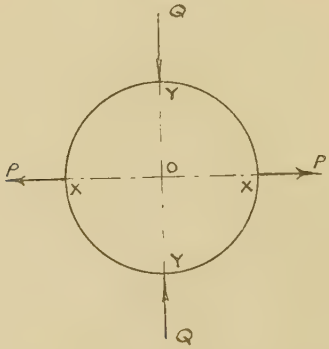


The finished dimensions of the circular ring, which was of rectangular section, were :—

Mean diameter, 9·9855 in. ; Mean radius, R=4″·99275.
Width, 0″·5015. Radial thickness, 0″·5005.

*Moduli of Elasticity.*—For the determination of Young's modulus of elasticity the Cambridge extensometer was used after calibration with the Johannson standard gauges, giving $E=29{\cdot}5772\times10^6$ (lb. inch units) and the transverse modulus G was taken equal to $\frac{2}{5}$E.

*Apparatus for applying the Load.*—Fig. 3 indicates the type of apparatus adopted by the author for loading the ring.

Increasing loads, Q, were applied to the vertical rods AA supported from the ends of a channel section beam BB, thus loading a plunger C capable of moving easily through

the central boss of a guide bracket D, the pressure being transmitted to the test-ring E. The ring was supported by a pressure foot F, carried by a second bracket G. Both brackets (or bridge pieces) D and G were bored near the ends, and were mounted on two vertical parallel cylindrical rods HH, fixed to the base K,—the lower bracket being supported by a vertical strut L.

For step-by-step increases in the load Q the vertical and horizontal strains on the diameters YY and XX were mea-

Fig. 3.

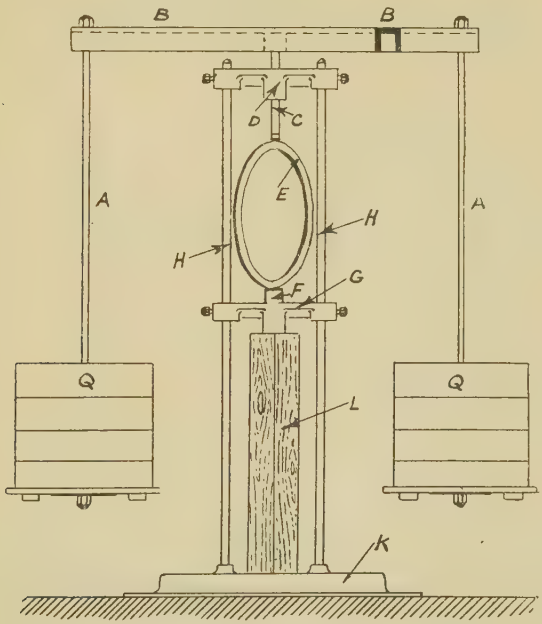


sured by a micrometer. Preliminary compression tests were made on the ring across three diameters at 60° to ascertain if the elastic properties were the same for all directions, and the results for the compressions per unit load were substantially the same for all diameters.

*Micrometer Instrument for Strain Measurement.*—For the accurate determination of small strains the author found it necessary to design and use the special instrument represented in fig. 4.

An enlarged B and S micrometer drum and sleeve MN are mounted in a frame F, the drum M being fixed to the frame. The screw of the micrometer is carried by the sleeve N and

has 50 threads per inch length. On the drum M is a scale giving tenths and fiftieths of an inch. The end of the sleeve N is bevelled and divided circumferentially into 20 equal divisions and numbered 0 to 20, thus indicating axial movements of the screw and gauge point G in thousandths of an inch. The interval between each pair of numbered divisions is divided into ten equal parts so that an angular movement of the sleeve through any one of these divisions represents an axial movement of the screw and gauge point G through the one ten-thousandth of an inch. The other end of the frame F carries a cylindrical rod H. The end K forms the other gauge point of the micrometer.

Fig. 4.

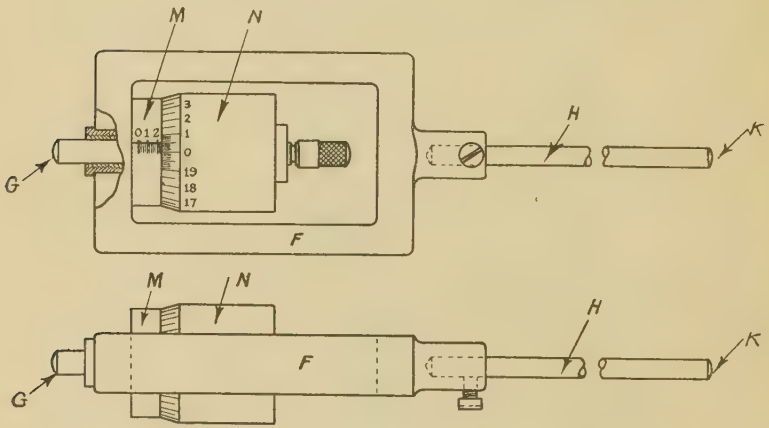


*Method of Experimenting.*—The loading of the ring by compressive forces at the extremities of a vertical diameter was effected by step-by-step increases of 40 lb. weights, and the micrometer was used to determine for each load first the vertical internal diameter of the ring YY, and second the internal horizontal diameter. The decrements for the vertical diameters and the increments for the horizontal diameters for the different loads are given in columns 2 and 4 of the table. The micrometer was handled by heat insulating material, and all measurements were made at temperature 17°·2 to 17°·7 C., the same temperature at which the tests were made for determining Young's modulus of elasticity for the test specimens.

*Comparison of Experimental with Mathematical Results.*—The vertical and horizontal strains given by equations (1) and (2) respectively are evaluated by substituting the following numerical values :—

$$R=4{\cdot}99275 \quad C=\tfrac{6}{5} \quad A=\cdot5015\times\cdot5005,$$
$$E=29{\cdot}5772\times10^{6} \quad G=\tfrac{2}{5}E,$$
$$I=\tfrac{1}{12}\times\cdot5015\times(\cdot5005)^{3}.$$

Equation (1) then becomes

$$\left.\begin{array}{l}\text{Vertical strain on}\\ \text{YY}\end{array}\right\} =(10^{-5}\times11{\cdot}948+10^{-7}\times5{\cdot}282 +10^{-7}\times15{\cdot}846)Q. \quad (3)$$
$$=10^{-5}\times12{\cdot}15928\,Q\ (\text{inch}).$$
$$\doteqdot10^{-5}\times12{\cdot}16\,Q\ (\text{inch}). \quad . \quad . \quad . \quad . \quad (4)$$

Equation (2) becomes

$$\left.\begin{array}{l}\text{Horizontal strain}\\ \text{on } XX\end{array}\right\} =10^{-5}10{\cdot}9725-10^{-7}\times3{\cdot}36262 +10^{-7}\times10{\cdot}0878)\,Q. \quad (5)$$
$$=10^{-5}\times11{\cdot}03975\,Q\ (\text{inch})$$
$$\doteqdot10^{-5}\times11{\cdot}04\,Q\ (\text{inch}). \quad . \quad . \quad . \quad . \quad (6)$$

The first, second, and third terms in equations (3) and (5) represent respectively the strains due to bending, hoop-stress, and shear. It will be noticed that the last two terms in each case are very small compared with the first due to bending.

The calculated values of the strains for the different loads from (4) and (6) above are given in columns (3) and (5) of the table. A comparison of these values with the experimental results in columns (2) and (4) shows remarkably close agreement. It has already been stated that the test is a severe one for a particular case. The substantial agreement between theory and experiment must therefore be regarded as satisfactory.

For the ring tested the ratio of the mean radius of the ring to the radial thickness is as 10 : 1.

Dr. A. J. S. Pippard gives experimental results for the deformation on the vertical diameter for a ring of $2\frac{1}{2}''$ mean radius and $\frac{1}{2}''\times\frac{1}{2}''$ section with a ratio of 5 : 1, and compares the vertical strains determined experimentally with the calculated strains *. The agreement between experiment and theory in this case is also shown to be very close indeed.

In giving a mathematical investigation for the elastic ring the author stated † that it is assumed that the radial thickness is small compared with the radius of the ring. The experimental results given in this paper and the ones given by Dr. Pippard show that theory and experiment agree in cases where the thickness is not small compared with the radius.

* 'Strain Energy Methods of Calculation,' p. 114 (Longmans).

† Phil. Mag. xii. p. 130, July 1931.

Experimental and Calculated Values of the two Principal Diametral Strains.

| 1. | 2. | 3. | 4. | 5. |
|---|---|---|---|---|
| | Decrease in Vertical Diameter. | | Increase in Horizontal Diameter. | |
| Force, pounds weight. | Determined experimentally (inch). | Calculated from equation (4) (inch). | Determined experimentally (inch). | Calculated from equation (6) (inch). |
| 0 | 0 | 0 | 0 | 0 |
| 40 | 0·0042 | 0·0048 | 0·0042 | 0·0044 |
| 80 | ·0095 | ·0097 | ·0089 | ·0088 |
| 120 | ·0142 | ·0146 | ·0129 | ·0132 |
| 160 | ·0193 | ·0195 | ·0178 | ·0177 |
| 200 | ·0240 | ·0243 | ·0217 | ·0221 |
| 240 | ·0287 | ·0292 | ·0263 | ·0265 |
| 280 | ·0338 | ·0340 | ·0310 | ·0309 |
| 320 | ·0386 | ·0389 | ·0351 | ·0353 |
| 360 | ·0438 | ·0438 | ·0394 | ·0397 |
| 400 | ·0482 | ·0486 | ·0436 | ·0442 |
| 440 | ·0527 | ·0535 | ·0480 | ·0486 |
| 480 | ·0582 | ·0583 | ·0525 | ·0530 |
| 520 | ·0629 | ·0632 | ·0574 | ·0574 |
| 560 | ·0679 | ·0681 | ·0618 | ·0618 |
| 600 | ·0729 | ·0730 | ·0662 | ·0662 |
| 640 | ·0780 | ·0778 | ·0707 | ·0706 |
| 680† | ·0829 | ·0827 | ·0747 | ·0751 |
| 720‡ | ·0896 | ·0876 | ·0794 | ·0795 |
| 760 | ·0980 | — | ·0855 | ·0839 |
| 800 | ·110 | — | ·095 | — |
| 840 | ·143 | — | ·115 | — |
| 880 | ·165 | — | ·172 | — |
| 960 | ·35 | — | ·25 | — |
| 1000 | ·5 | — | ·5 | — |
| 0 | ·42 | — | ·35 | — |

† Approximate limit of proportionality on vertical diameter.
‡ Approxmate limit of proportionality on horizontal diameter.

## CXV. *Vibrations of Revolving Shafts.*

*To the Editors of the Philosophical Magazine.*

GENTLEMEN,—

IN Dr. R. C. J. Howland's paper on "Vibrations of Revolving Shafts" in your August Supplementary Number the statement is made (p. 299) :—

"Assumption (3) has two important consequences. In the first place it is easily seen to lead to equations which are the same relative to axes rotating with the shaft as they would be with respect to fixed axes, except that a field of centrifugal force must be introduced. It also leads to the result that the motions in any two mutually perpendicular planes through the axis and revolving with it are sensibly independent."

These assertions may be seen to be inaccurate, as follows :— If $Oy$, $Oz$ are axes rotating with uniform angular velocity $\omega$ about a fixed axis $Ox$, the accelerations of a particle in motion in the $y-z$ plane are

$$\text{in direction } Oy, \text{ acceleration} = \ddot{y} - 2\omega\dot{z} - \omega^2 y,$$

$$\text{in direction } Oz, \text{ acceleration} = \ddot{z} + 2\omega\dot{y} - \omega^2 z.$$

In his analysis Dr. Howland has ignored the terms $-2\omega\dot{z}$, $+2\omega\dot{y}$; in consequence, his equation of motion (1) is incomplete, and the results which follow are inapplicable except to the special case of a revolving bar which is flexible in one transverse plane and is rigid in the perpendicular transverse plane. The same limitation applies to Dr. Howland's previous paper, "The Vibrations of Rods and Shafts with Tension or End-Thrust," Phil. Mag. i. p. 674 (1926), so far as it concerns rotating shafts.

I am,

Yours faithfully,

Metropolitan-Vickers Elect. Co., Ltd.
Trafford Park, Manchester.
August 20, 1931.

D. M. SMITH.

*To the Editors of the Philosophical Magazine.*

GENTLEMEN,—

I have to express my thanks to Mr. Smith for pointing out a misstatement in my paper, but I cannot agree with the conclusions that he draws. What I should have said was "the equations relative to fixed axes are the same when the shaft is rotating as when it is at rest, except that a field of centrifugal force must be introduced." I think it will be found that my equations interpreted as relative to fixed axes

are correct, and that, apart from a few slight verbal changes, no other alteration in the paper is needed.

Mr. Smith's reference to my previous paper does not appear to me relevant. In that paper rotating axes were not referred to. Nor is there, I think, any reason why in either paper the shaft should be supposed flexible in one plane only.

I am, Gentlemen,
Yours faithfully,
R. C. J. Howland,
Professor of Mathematics.

University College, Southampton.
October 30, 1931.

---

## CXVI. *Oberbeck's Vortices.*

*To the Editors of the Philosophical Magazine.*

Gentlemen,—

In the May number of your Magazine appears a paper "On Oberbeck's Vortices" by Dr. Banerji and Mr. Barave. We feel that section 7 of this paper cannot pass without comment.

The forces due to rotation set down in equation (5) are evidently considered by the authors to be external forces. Actually such inertia forces are completely covered by the terms :

$$\frac{Du}{Dt} = \frac{\partial u}{\partial t} + u\frac{\partial u}{\partial x} + v\frac{\partial u}{\partial y} \quad \text{and} \quad \frac{Dv}{Dt} = \text{etc.}$$

In equation (4) X and Y in their usual meaning (see Lamb's 'Hydrodynamics,' Ch. I. para. 6) denote forces acting quite independently of the fluid motion. Equation (6) is quite wrong. If viscous resistance were proportional to the velocity in the manner of equation (6), then a free stream of fluid moving with uniform velocity would experience frictional resistance. The correct form of the hydrodynamical equations with friction may be found in any text-book on hydrodynamics.

Equation (10) is an entirely arbitrary assumption, which will certainly not be fulfilled for a fluid with friction.

Equation (11) is remarkable for the sweeping nature of the assumptions made without any examination of the consequences. Consider the direction of resultant motion at any point, which will be at an inclination $\theta$ to the $x$-axis given by

$$\tan\theta = \frac{v}{u} = \frac{V}{U};$$

U and V are independent of $t$, so that the direction of flow at a given point cannot change with time if equation (11) is correct. The authors' own photographs show this to be wrong.

Another sweeping assumption is now made, namely, that $\lambda$ is uniform throughout the fluid. This is supposed to apply to the case of Oberbeck's vortices without any examination being made to see whether this possibly could be so. In solving equation (15) very special solutions are chosen without showing why these are preferred to more general ones. Why the arbitrary constant is omitted in equation (16) is not clear, and a comparison of equation (16) with equation (23) is interesting.

The fact that an equation like (21) was obtained should have shown the authors that something was seriously amiss with their work, as it is known that a stream function and a velocity potential exist only for the irrotational motion of a frictionless fluid. Also, from the elementary theory of complex functions it is known that the $\phi$ and $\psi$ lines of equation (21) intersect at right angles provided the $x$ and $y$ lines do so. Consequently the angle $\epsilon$ of equation (24) is $\frac{\pi}{2}$, and we then get from (28) that $r$ is a constant and that no spirals are formed.

Sufficient has been said to show that "the theory" given is in error, and that any observed agreement between results deduced from it and the experiments must be ascribed to coincidence. It is significant that no numerical agreement has been claimed, but only qualitative agreement.

D. E. Rutherford
(The University, St. Andrews),
John Caldwell
(The Royal Technical College,
Glasgow).

October 31, 1931.

---

## CXVII. *The Significance of the Compton Effect in Absolute Gamma-Ray Absorption Measurements.*

*To the Editors of the Philosophical Magazine.*

Gentlemen,—

In my recent paper, under the above title *, I regret that no mention was made by me of the work done in 1909 † and 1910 ‡ by F. and W. M. Soddy and Russell.

* Phil. Mag., November 1931.
† Phil. Mag., October 1909.
‡ Phil. Mag., May 1910.

They concluded that the gamma rays of radium are absorbed exponentially even in considerable thicknesses of lead, provided precautions are used to avoid the influence of a peculiar secondary radiation, apparently generated by lead. With the experimental precautions they outlined, these authors steered clear of disturbing phenomena such as the Compton Effect before this effect was discoved.

I am, Gentlemen,
Yours faithfully,
L. H. CLARK.

Barnato Joel Laboratories,
The Middlesex Hospital, W. 1.
20th November, 1931.

## CXVIII. *Notices respecting New Books.*

*Strahlenoptik.* By Dr. M. HERZBERGER. [Pp. xiv+196, 70 figures.] (Julius Springer, Berlin, 1931. R.M. 18, bound R.M. 19.40.)

DR. HERZBERGER has rendered a distinct service to students of optics in compiling this book. In recent years our knowledge of optical imagery has been greatly extended, the main contributions appearing in several scientific journals—German, Swedish, and English. As almost every writer has used a distinct notation, the task of making oneself familiar with even a portion of this work is a formidable one, but it has been greatly reduced by the collection into this volume, and the presentation in a single notation, of a number of the more fundamental results reached by these workers. The treatment of the subject is systematic, and the mathematical discussion is clear and sound. The whole structure has been built on the law of the stationary path. A large part of the book deals with the elements of imagery. Both symmetrical and unsymmetrical imageries are discussed, the media for the most part being supposed to be homogeneous and isotropic. Considerable space is very properly given to the exact laws of imagery known to us. The discussion of the third-order aberrations of a rotationally symmetrical instrument contains a good deal of matter not to be found in the older German treatises. The following chapter is concerned with schemes for the production of the most satisfactory images on the assumption that aberrations are not entirely removable. As the title of the book indicates, only the geometrical point of view is considered, and, in the absence of the wave-length as a factor in these problems, the propositions relate to the shapes, sizes, and positions of caustic surfaces. The book concludes with a chapter of historical remarks. Adequate indexes and a bibliography are included.

The work is unquestionably of great value to teachers, students, and workers in optics. It will serve admirably as an introduction to the most recent work in the subject.

[*The Editors do not hold themselves responsible for the views expressed by their correspondents.*]

# INDEX TO VOL. XII.

ADAMS (L. H.) on the critical temperature of magnetization for iron and other materials, 361.
Adsorption at the surface of a solution, 907.
Aerosols, theory of the electrification of, 1175.
Aluminium crystals, on the electrical conductivity of, 112.
Aluminium-manganese system of alloys, 1137.
Analogy between the electromagnetic field and a fluid containing a large number of vortex filaments, 1057.
Anderson (Dr. W.), note on the paper of D. S. Kothari on the limiting density of matter, 832.
Arkell (Dr. W. J.) and Douglas (Dr. J. A.) on the stratigraphical distribution of the cornbrash, 736.
Armature reaction in salient-point alternators, 690.
Ataka (H.) on a relation between continued fractions and hyperbolic functions, 551.
Atomic scattering factors, on some numerical calculations of, 81.
Awbery (J. H.), note on heat-flow through a granulated material, 1152.
Ballistic and perfect balances in bridges treated by the operational calculus, 265.
Barnett (Prof. S. J.) on a new electron-inertia effect and the determination of $m/e$ for the free electrons in copper, 349.
Bending of a thin circular plate, 185.
$\beta$-transformation, 439.
Bircumshaw (Dr. L. L.) on the surface-tension of liquid metals, 596.
Bode's law in relation to satellite systems, 67.
—— ——, observations on V. V. Narliker's paper, 602.
Boiling-point rules, on a general theory of, 685.
Bond (Dr. W. N.) on the electronic charge, 632.
Books, new :—D. Humphrey's Intermediate Mechanics: Statics and mechanics, 198; Alex. Findlay's Practical Physical Chemistry, 198; T. A. Ramos's Leçons sur le Calcul Vectoriel, 404; A. W. Porter's Thermodynamics, 405; F. S. C. Northrop's Science and First Principles, 405; H. C. Ives's Natural Trigonometric Functions, 604; T. Hodgson's Applied Mathematics for Engineers, 604; S. R. Williams's Magnetic Phenomena, 605; F. Wolfers's Deux Heures de Physique.—II. Structure de l'électricité, 605; Max Planck's The Universe in the Light of Modern Physics, 606; F. Wolfers's Les Ultra Sons et la Biologie, 606; P. A. M. Dirac's The Principles of Quantum Mechanics, 729; S. Timoshenko's The Strength of Materials, 730; R. O. Griffith and A. McKeown's Photo-processes in Gaseous and Liquid Systems, 731; G. P. Thomson's The Wave Mechanics of Free Electrons, 732; W. Heisenberg's The Physical Principles of the Quantum Theory, 732; F. E. Hoare's Thermodynamics, 733; H. A. Lorentz's Lectures on Theoretical Physics, 734; Bulletin of the National Research Council, the Age of the Earth, 734; Dr. Herzberger's Strahlenoptik, 1192.

Boswell (Prof. P. G. H.) on an ordovician grit from Anglesey, 406.
Boundary-layer equations, solutions of, 866.
Bowen (E. G.) on an X-ray investigation of the tin-antimony alloys, 441.
Bradley (Dr. A. J.) comparison of the crystal structures of $Cu_3Zn_8$ and $Cu_3Cd_8$, 143.
—— and Jones (Dr. Phyllis) on the aluminium-manganese system of alloys, 1137.
Bradley (R. S.) on the reaction rate in the system solid-solid-gas, 290.
Brindley (G. W.), some numerical calculations of atomic scattering factors, 81; correction, 729; on the turbulent and stream-line damping of a pendulum in viscous media, 522.
—— and Lavery (Dr. H.) on the refractivities and optical dispersions of methane and of its substituted chlorine derivatives, 945.
Burton (A. C.), McLennan (Prof. J. C.), Pitt (A.), and Wilhelm (J. O.) on the resistance of lead to high-frequency currents at superconducting temperatures, 707.
Caldwell (J.) and Rutherford (D. E.) on Oberbeck's vortices, 1190.
Campbell (Dr. N. R.) on the photoelectric emission of thin films, 173.
Carpenter (L. G.) on the thermal expansion and atomic heat of solid mercury, 511.
Cathode rays, the diffraction of, by thin films, 641.
Chromium, electroplated coatings, X-ray examination of, 853.
Clark (Dr. L. H.) on the significance of the Compton effect in absolute gamma-ray absorption measurements, 913, 1191.
Colwell (R. C.) on the vibrations of membranes and plates, 320.
Comparison of the crystal structures of $Cu_3Zn_8$ and $Cu_3Cd_8$, 143.
Compressibilities of the permanent gases, 41.
Compton effect in absolute gamma-ray absorption measurements, on the significance of the, 913, 1191.
Conduction of heat, on some problems in, 233, 1015.
Conductivity of gases in uniform electric fields, 384.
Conjugation, three different effects of, 768.
Continued fractions and hyperbolic functions, a relation between, 551.
Cook (W. R.) on the calculation of the mobility of mono-molecular ions, 554; on curve-fitting by means of least squares, 1025.
Coupled duplet and octet, 764.
Critical temperature of magnetization, the influence of hydrostatic pressure on, 361.
Crystal structure of copper-zinc and copper-cadmium alloys, 143.
Currie (Dr. B. W.) on electro-endosmosis in closed cylindrical tubes of large diameter, 429.
Curve-fitting by means of least squares, 1025.
Cylinder, heat loss from, embedded in insulating wall, 329.
Cylinders oscillating in a stream of water, 490.
Damping of a pendulum by viscous media, 396.
——, turbulent and stream-line, of a pendulum in viscous media, 522.
David (Prof. W. T.), Davies (W.), and Jordan (J.) on flame temperatures, 1043.
Davies (W.), David (Prof. W. T.), and Jordan (J.) on flame temperatures, 1043.
Davies (W. G.) and Lattey (R. T.) on the influence of electrolytes on the dielectric constant of water, 1111.
——, Lattey (R. T.), and Gatty (O.) on the temperature coefficient of the dielectric constant of water, 1019.
Determination of $m/e$ for the free electron in copper, 349.
Diaphragms, conical, used in acoustic apparatus for the reproduction of speech and music, 771.
Dielectric constant of water, the temperature coefficient of 1019; influence of electrolytes on, 1111.
Dielectrics, theory of, 197.
Diffraction of cathode rays by thin films, 641.

Donaldson (R. H.) and Gill (E. W. B.) on the sparking potential of air for high-frequency discharges, 719.
Doublets, steady motion of two, 993.
Douglas (Dr. J. A.) and Arkell (Dr W. J.) on the stratigraphical distribution of the cornbrash, 736.
Dufton (Dr. A. F.), observations on V. V. Narliker's paper on the significance of Bode's law, 602.
Elastic ring acted upon by equal radial forces, 129.
Electrical conductivity of single aluminium crystals, 112.
Electro-endosmosis in closed cylindrical tubes of a large diameter, 429.
Electromagnetic field and a fluid containing a large number of vortex filaments, on the analogy between, 1057
Electromotive force between two metals in relative motion, 409, 1110.
Electronic charge, 632.
Electron-inertia effect and the determination of $m/e$ for the free electrons in copper, 349.
Elliptic cylinder function, on an integral involving, 280.
—— hole, stresses due to small, on neutral axis of deep beam, 312.
Emeléus (Dr. K. J.) on the origin of the light from the negative glow, 73.
Energy of excitation by electron impact in helium, a precise experimental determination of, 962.
Equilibrium between radiation and matter and degeneracy, 657.
Falkner (V. M.) and Skan (Miss S. W.) on the solutions of the boundary-layer equations, 865.
Farquharson (Dr J.) on the magnetism of binary mixtures, 283.
Farr (C. C.) on the magnetic field of a circular cylindrical coil, 603.
Ferromagnetic ferric oxide, the structure of, 1089.
Films, on the photoelectric emission of thin, 173.
Fitch (A. A.) on the geology of the country between Ivybridge and Buckfastleigh, Devon, 407.
Flame temperatures, 1043.
Fraser (Dr. M.) on the electrical conductivity of single aluminium crystals, 112.
Frictional electric charges upon the surfaces of single metal crystals, 535.
Ganguli (A.) on the velocity of unimolecular reaction, 583.
Gardiner (C. I.) on the Loch Doon "granite" area, Galloway, 199.
Gatty (O.), Lattey (R. T.), and Davies (W. G.) on the temperature coefficient of the dielectric constant of water, 1019.
Ghosh (M.) on the theory of impacts of elastic hammer on a damped pianoforte string, 676.
Gill (E. W. B.) on electrical oscillations of very short wave-length, 843.
—— and Donaldson (R. H.) on the sparking potential of air for high-frequency discharges, 719.
Gravitational theories, classical and modern, 959.
Green (Dr. G.) on some problems in the conduction of heat, 233.
Green (Dr. J. J.) on the viscous layer associated with a circular cylinder, 1.
Green (J. W.) on the critical temperature of magnetization for iron and other materials, 361.
Greenly (Dr. E.) on an ordovician grit from Anglesey, 406.
Gregory (C. H.) on the comparison of the crystal structure of $Cu_3Zn_8$ and $Cu_3Cd_8$, 143.
Gulati (B.), Seth (Prof. J. B.), and Singh (S.) on an electromotive force between two metals in relative motion, 409.
Guében (Dr. G.), theory of dielectrics, 197.
Hamada (H.) on the molecular spectra of mercury, zinc, cadmium, magnesium, and thallium, 50.
Hartley (G. S.) on the theory of the velocity of diffusion of strong electrolytes in dilute solution, 473.
Hassé (Prof. H. R.) on the calculation of the mobility of monomolecular ions, 554.
Heat-flow through a granulated material, 1152.

Heat-loss from cylinder embedded in an insulating wall, 329.
Heaviside layer in Bengal, estimation of the height of, 897.
Helium, colour of the light from high-frequency discharges in, 1168.
——, energy of excitation by electron impact in, precise experimental determination of, 962.
——, excitation of the visible spectrum of, 815.
Higab (Dr. M. A.) on the steady motion of two doublets, 993.
Hill (A. G.) on the torsional oscillations of iron wire, 566.
Hoare (F. E.) on the damping of a pendulum by viscous media, 396.
Holtedahl (Prof. O.), some general structural features of the arctic and adjacent regions, 735.
Houstoun (Dr. R. A.), notes on Weber's law and the yellow spot effect, 538.
Howland (Dr. R. C. J.) on the vibrations of revolving shafts, 297, 1189.
Huxley (Dr. L. G. H.) on striated discharges, 380.
Hyperbolic functions and continued fractions, a relation between, 551.
Impacts of elastic hammer on a damped pianoforte string, 676.
Index operators, 201.
Ingram (W. H.) on armature reaction in salient-point armatures, 690.
Integral involving the elliptic cylinder function, 280.
International radium standard committee, report on the radioactive constants, 609.
Intrinsic magnetization, the temperature variation of, and associated properties of ferromagnetics, 737.
Ionium, the period of, 939.
Ionization in gas-filled photoelectric cells, 224.
James (R. W.) on some numerical calculations of atomic scattering factors, 81; correction, 729.
Jones (Prof. E. T.) on the diffraction of cathode rays by thin films, 641.
Jones (F. L.) on the conductivity of gases in uniform electric fields, 384.
—— and Townsend (Prof. J. S.) on the excitation of the visible spectrum of helium, 815.
Jones (H.), note on the physical significance of second order terms in the perturbation theory, 1063.
Jones (Dr. Phyllis) and Bradley (Dr. A. J.) on the aluminium-manganese system of alloys, 1137.
Jones (W. M.) on an X-ray investigation of the tin-antimony alloys, 441.
Jordan (J.), David (Prof. W. T.), and Davies (W.) on flame temperatures, 1043.
Kalman (Prof. E.) on two-dimensional linear elastic states, 572.
Kar (Dr. K. C.) on the theory of impacts of elastic hammer on a damped pianoforte string, 676.
Knowler (A. E.) on a balance method of measuring sound transmission, 1039.
Kothari (D. S.), note on the equilibrium between radiation and matter and degeneracy, 657; note on the white dwarfs and the electrostatic correction, 665.
Kuno (Prof. J.) on the law of photo-elastic extinction, 503.
Larard (C. E.) on the elastic ring acted upon by equal radial forces, 129; on the elastic ring, comparison of strains determined experimentally and calculated from theory, 1183.
Larmor (Sir J.), note on the significance of Bode's law in relation to satellite systems, 67.
Lattey (R. T.) and Davies (W. G.) on the influence of electrolytes on the dielectric constant of water, 1111.
——, Gatty (O.), and Davies (W. G.) on the temperature coefficient of the dielectric constant of water, 1019.
Lavery (Dr. H.) and Brindley (G. W.) on the refractivities and optical dispersions of methane and of its substituted chlorine derivatives, 945.
Lely (Dr. U. Ph.) on a simple experiment for investigating and demonstrating the Peltier-effect, 488.

Lemin (C. E.) on the motion of a sphere through a viscous liquid, 589.
Limiting density of matter, note on, 832.
Loewenthal (M.) on tears of strong wine, 462.
McCallum (Dr. S. P.) on the conductivity of gases in uniform electric fields, 384.
—— and Townsend (Prof. J. S.) on the colour of the light from high-frequency discharges in helium, 1168.
McLachlan (Dr. N. W.) and Sowter (G. A. V.) on the behaviour of conical diaphragms used in acoustic apparatus, 771.
McLennan (Prof. J. C.), Smith (C. E.), and Wilhelm (J. O.) on the effect of low temperatures on the ultra-violet transmission band of silver, 833.
——, Burton (A. C.), Pitt (A.), and Wilhelm (J. O.) on the resistance of lead to high-frequency currents at superconducting temperatures, 707.
Madgwick (Prof. E.) on an investigation into some of the properties of porous building materials, 1155, 1160.
Magnetic alloys and their properties, 255.
—— field of a circular cylindrical coil, 603.
Magnetism of binary mixtures, aqueous solutions of acids, 283.
Mahajan (Prof. L. D.) on the surface-tension of different solutions of Boys' soap solution, 954.
Mainstone (P. A.) on the frictional electric charges upon the surfaces of single metal crystals, 535.
Marcus (A.), note on classical and modern gravitational theories, 959.
Matley (Dr. C. A.) on the geology of the country around Mynydd Rhiw and Sarn, 405.
Mercury, thermal expansion and atomic heat of solid, 511.
Methane and its substituted chlorine derivations, on the refractivities and optical dispersions of, 945.
Mobility of monomolecular ions, 554.
Mohammad (Prof. W.) and Sharma (P. N.) on the fine structure of the spectrum lines of the zinc arc and the energy levels of zinc, 726; hyperfine structure of spectrum line of lead arc in the visible and ultra-violet regions, 1106.
Molecular spectra of mercury, zinc, cadmium, magnesium, and thallium, 50.
Narliker (V. V.) on the significance of Bode's law in relation to satellite systems, 67.
Negative glow, the origin of the light from the, 73.
Oakley (F. H.) on the thermal expansion and atomic heat of solid mercury, 511.
Oberbeck's vortices, on, 1190.
Operational calculus, method applied to the ballistic and perfect balances in bridges, 265.
Oscillations, electrical, of very short wave-length, 843.
Oxide cathodes, thermionic emission and electrical conductivity of, 1073.
Parkinson (M. M. L.) on the geological work of the Cambridge expedition to East Greenland in 1929, 607.
Patterson (H. S.) on the theory of the electrification of aerosols, 1175.
Peltier-effect, a simple experiment for investigating and demonstrating, 488.
Perturbation theory, note on the physical significance of second order terms in, 1063.
Photo-elastic extinction, the law of, 503.
Photoelectric cells, experiments on time-lag in gas-filled, 162, 230.
—— ——, on ionization in gas-filled, 224; inert gases in cæsium on silver, 224.
—— emission of thin films, 173.
Pitt (A.), McLennan (Prof. J. C.), Burton (A. C.), and Wilhelm (J. O.) on the resistance of lead to high-frequency currents at superconducting temperatures, 707.
Plate, bending of a thin circular, 185.
Porous building materials, investigation of some of the properties of 1155, 1160.

Potter (Dr. H. H.) on some magnetic alloys and their properties, 255.
Preston (G. D.) on an X-ray investigation of some copper-aluminium alloys, 980.
Radiation resistance in open wire radio transmission lines, distribution of, 392.
Radioactive constants—report of the international radium standard committee, 609.
Rakshit (H.) on an estimation of the height of the Heaviside layer in Bengal, 897.
Raman effect in some acid derivatives and esters, 823.
Reaction rate in the system solid-solid-gas, 290.
Refractivities and optical dispersions of methane and of its substituted chlorine derivatives, 945.
Reimann (Dr. A. L.) and Treloar (L. R. G.) on the thermionic emission and electrical conductivity of oxide cathodes, 1073.
Resistance of lead to high-frequency currents at superconducting temperatures, 707.
——, high, measurement by the bridge method, 840.
Revolving shafts, the vibrations of, 297, 1189.
Reynolds (Prof. S. H.) on the Loch Doon "Granite" area, Galloway, 199.
Richter (A. F.) on the coupled duplet and octet, 764; on three different effects of conjugation, 768.
Roberts (Dr. J. E.) and Whiddington (Prof. R.) on a precise exponential determination of energy of excitation by electron impact in helium, 962.
Rutherford (D. E.) and Caldwell (J.) on Oberbeck's vortices, 1190.
Satellite systems, the significance of Bode's law in rélation to, 67.
Schofield (F. H.) on the heat loss from a cylinder embedded in an insulating wall, 329.
Sen (B.) on the stresses due to a small elliptic hole on the neutral axis of a deep beam, 312.
—— on β-transformation, 439.
Seth (Prof. J. B.), Gulati (B.), and Singh (S.) on an electromotive force between two metals in relative motion, 409.
Sharma (P. N.) and Mohammad (Prof. W.) on the fine structure of the spectrum lines of the zinc arc and the energy levels of zinc, 726; hyperfine structure of spectrum lines of lead arc in the visible and ultra-violet regions, 1106.
Shaw (Prof. P. E.) on the electromotive force between metals, 1110.
Silver, ultra-violet transmission band of, effect of low temperatures on, 833.
Singh (S.), Seth (Prof. J. B.), and Gulati (B.) on an electromotive force between two metals in relative motion, 409.
Single metal crystals, frictional electric charges upon the surfaces of, 535.
Skan (Miss S. W.) and Falkner (V. M.) on the solutions of the boundary-layer equations, 865.
Sloane (R. H.) on the origin of the light from the negative glow, 73.
Smith (C. E.), McLennan (Prof. J. C.) and Wilhelm (J. O.) on the effect of low temperatures on the ultra-violet transmission band of silver, 833.
Smith (D. M.) on the vibrations of revolving shafts, 1189.
Smith (W. C.) on the xenoliths of igneous origin in the Trégastel granite, 199.
Soddy (Prof. F.) on the relation between uranium and radium, 939.
Sound transmission, a balance method of measuring, 1039.
Sowter (G. A. V.) and McLachlan (Dr. N. W.) on the behaviour of conical diaphragms used in acoustic apparatus, 771.
Sparking potential of air for high-frequency discharges, 719.
Spectrum lines of lead arc, hyperfine structure of, in the visible and ultra-violet regions, 1106.
—— —— of the zinc arc in vacuum, fine structure of, 726.
Sphere, motion of, through a viscous liquid, 589.

Starr (A. T.) on the ballistic and perfect balances in bridges treated by the operational calculus, 265.
Stoner (Dr. E. C.) on the temperature variation of intrinsic magnetization and associated properties of ferromagnetics, 737.
Stresses due to a small elliptic hole on neutral axis of a deep beam, 312.
Striated discharges, 380.
Strong electrolytes, on the velocity of diffusion, in dilute solution, 473.
Sumpner (Dr. W. E.) on index operators, 201.
Surface-tension of different dilutions of Boys' soap solution, 954.
Surface-tension of liquid metals—Part iv. surface-tension of mercury, 596.
Tears of strong wine, 462.
Tedham (W. F.) on ionization in gas-filled photoelectric cells, 224.
Teegan (J. A. C.) on the measurement of high resistance by the bridge method, 840.
Temperature variation of intrinsic magnetization and associated properties of ferromagnetics, 737.
Thatte (Prof. V. N.) on the Raman effect in some acid derivatives and esters, 823.
Thermal expansion and atomic heat of solid mercury, 511.
Thermionic emission and electrical conductivity of oxide cathodes, 1073.
Thewlis (J.) on the structure of ferromagnetic ferric oxide, 1089.
Thom (Dr. A.) on experiments on cylinders oscillating in a stream of water, 490.
Thomas (Dr. H. H.) on the xenoliths of igneous origin in the Trégastel granite, 199.
Thomson (Sir J. J.) on the analogy between the electromagnetic field and a fluid containing a large number of vortex filaments, 1057.
Time-lag in gas-filled photoelectric cells, experiments on, 162, 230.
Tin-antimony alloys, X-ray investigation of, 441.
Torsional oscillations of iron wire, 566.
Townsend (Prof. J. S.) and Jones (F. L.) on the excitation of the visible spectrum of helium, 815.
—— and McCallum (S. P.) on the colour of the light from high-frequency discharges in helium, 1168.
Treloar (L. R. G.) and Reimann (Dr. A. L.) on the thermionic emission and electrical conductivity of oxide cathodes, 1073.
Two-dimensional linear elastic states, 572.
Ultra-violet transmission band of silver, the effect of low temperatures on, 833.
Uranium and radium, relation between, 939.
Varma (R. S.) on an integral involving the elliptic cylinder function, 280.
Velocity of diffusion of strong electrolytes in dilute solution, 473.
—— of unimolecular reaction, 583.
Vibrations of membranes and plates, 320.
—— of revolving shafts, 297, 1189.
Vincent (J. J.) on the bending of a thin circular plate, 185.
Viscous layer associated with a circular cylinder, 1.
Walmsley (T.) on the distribution of radiation resistance in open wire radio transmission lines, 392.
Weber's law and the yellow spot effect, 538.
Wheatcroft (Prof. E. L. E.) on experiments on time-lag in gas-filled photoelectric cells, 162.
Wheeler (Dr. T. S.) on the general theory of boiling-point rules, 685.
Whiddington (Prof. R.) and Roberts (Dr. J. E.) on a precise experimental determination of energy of excitation by electron impact in helium, 962.
White dwarfs and the electrostatic correction, 665.
Whittard (Dr. W. F.) on the geological work of the Cambridge expedition to East Greenland in 1929, 607.
Wild (W.) on the compressibilities of the permanent gases, 41.

Wilhelm (J. O.), McLennan (Prof. J. C.), Burton (A. C.), and Pitt (A.) on the resistance of lead to high-frequency currents at superconducting temperatures, 707.
——, McLennan (Prof. J. C.), and Smith (C. E.) on the effect of low temperatures on the ultra-violet transmission band of silver, 833.
Wiseman (J. D. H.), a contribution to the petrology of the metamorphic rocks of East Greenland, 607.
Wood (W. A.) on the X-ray examination of electroplated chromium coatings, 853.
Wright (C. E.), note on a problem in the conduction of heat, 1015.
Wynne-Jones (W. F. K.) on the adsorption at the surface of a solution, 907.
X-ray examination of electroplated chromium coatings, 853.
—— investigation of some copper-aluminium alloys, 980.
—— —— of some tin-antimony alloys, 441.
Zinc, fine structure of the spectrum lines of, and the energy levels of, 726.

END OF THE TWELFTH VOLUME.

Printed by Taylor and Francis, Red Lion Court, Fleet Street.

FIG. 1 (*a*).

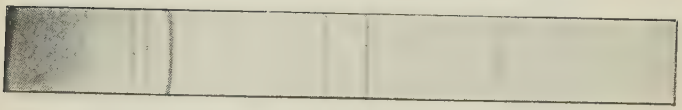

$Fe_3O_4$.

FIG. 1 (*b*).

$Fe_2O_3$.

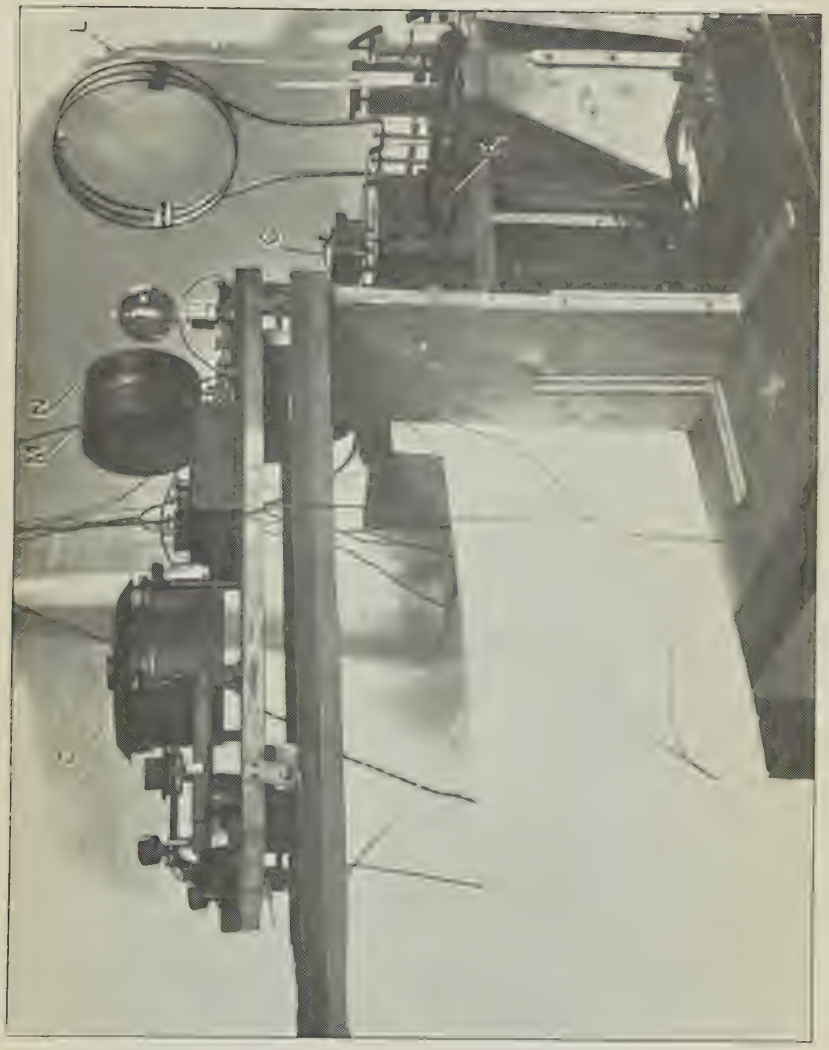

Fig. 3.

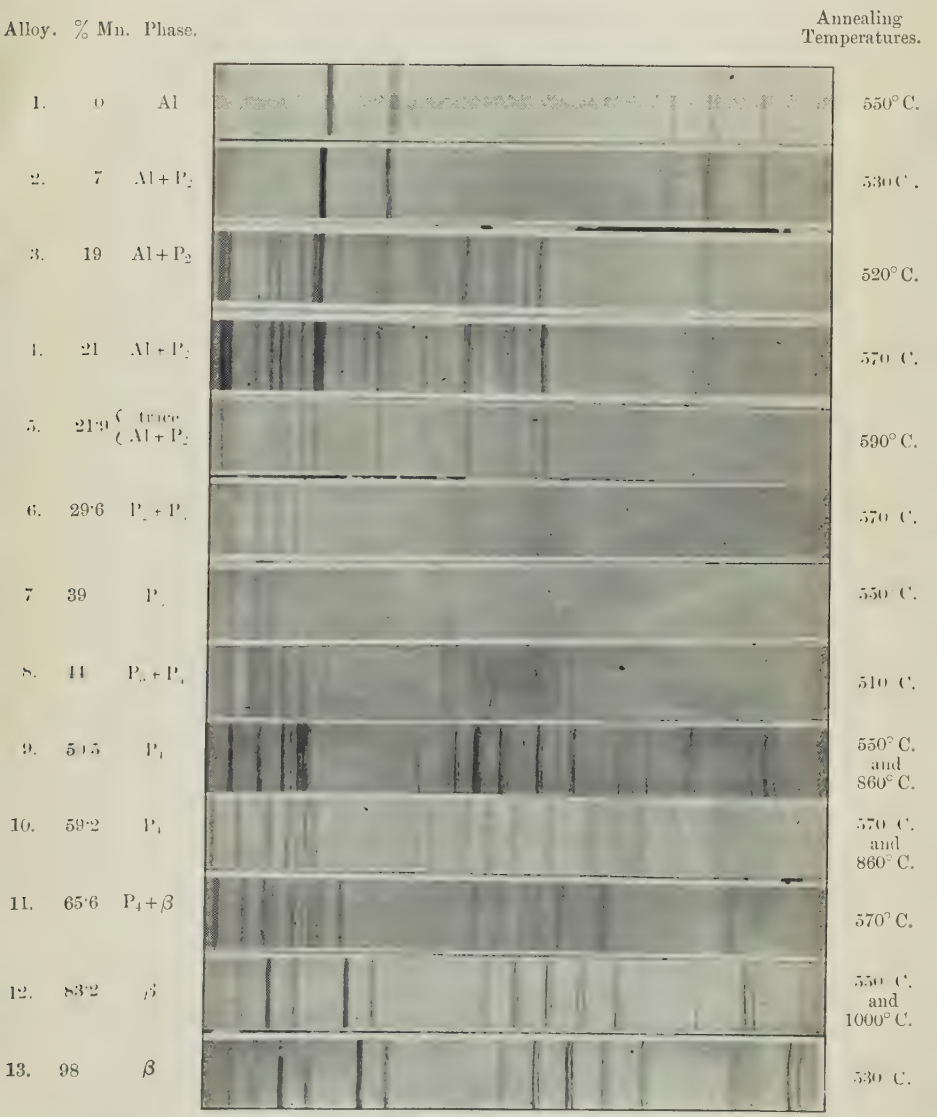
Alloy.
% Mn.
Phase.
Annealing Temperatures.
1. 0 Al 550° C.
2. 7 Al + P2 530° C.
3. 19 Al + P2 520° C.
4. 21 Al + P2 570° C.
5. 21·9 (twice) Al + P2 590° C.
6. 29·6 P2 + P1 570° C.
7 39 P1 550° C.
8. 44 P3 + P4 510° C.
9. 50·5 P4 550° C. and 860° C.
10. 59·2 P4 570° C. and 860° C.
11. 65·6 P4 + β 570° C.
12. 83·2 β 550° C. and 1000° C.
13. 98 β 530° C.

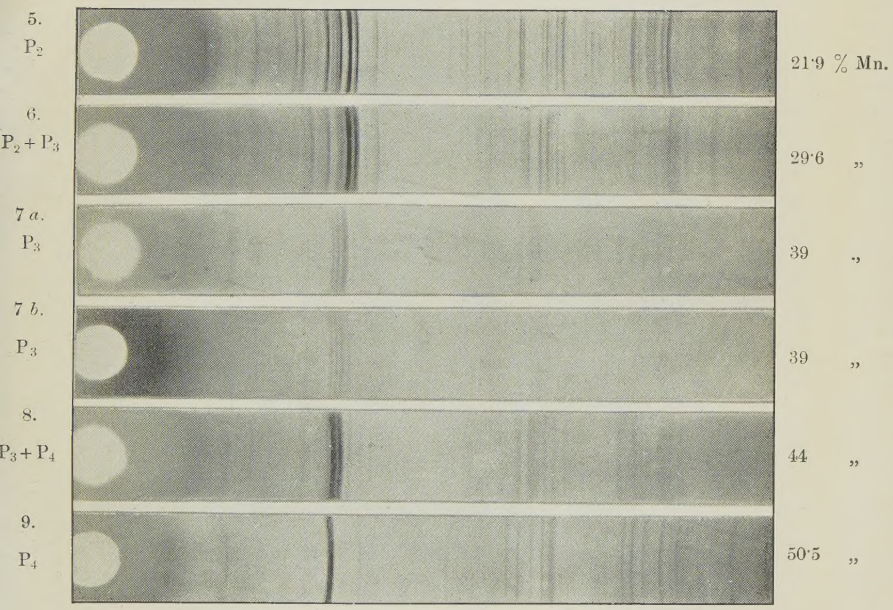
Composition.
5.
P2
21·9 % Mn.
6.
P2 + P3
29·6 „
7 a.
P3
39 „
7 b.
P3
39 „
8.
P3 + P4
44 „
9.
P4
50·5 „

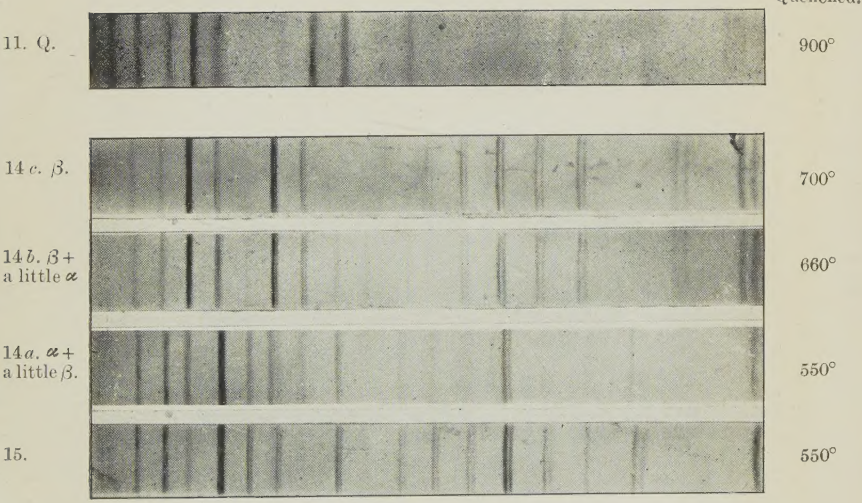
Quenched.
11. Q.
900°
14 c. β.
700°
14 b. β + a little α
660°
14 a. α + a little β.
550°
15.
550°